# Excitation and Control of a High-Speed Induction Generator

by

Steven Carl Englebretson

S.B., Colorado School of Mines (Dec 2002)

Submitted to the Department of Electrical Engineering and Computer Science
in partial fulfillment of the requirements for the degree of

Master of Science

at the

MASSACHUSETTS INSTITUTE OF TECHNOLOGY

September 2005



Author .....
Department of Electrical Engineering and Computer Science
August 26, 2005

Certified by .....
James L. Kirtley Jr.
Professor of Electrical Engineering
Thesis Supervisor

Accepted by .....
Arthur C. Smith
Chairman, Department Committee on Graduate Students

# Excitation and Control of a High-Speed Induction Generator

by
Steven Carl Englebretson

Submitted to the Department of Electrical Engineering and Computer Science
on August 26, 2005, in partial fulfillment of the
requirements for the degree of
Master of Science

## Abstract

This project investigates the use of a high speed, squirrel cage induction generator and power converter for producing DC electrical power onboard ships and submarines. Potential advantages of high speed induction generators include smaller size and weight, increased durability, and decreased cost and maintenance. Unfortunately, induction generators require a "supply of reactive power" to run and suffer from variation in output voltage and frequency with any changes to the input reactive power excitation, mechanical drive speed, and load. A power converter can resolve some of these issues by circulating the changing reactive power demanded by the generator while simultaneously controlling the stator frequency to adjust the machine slip and manage the real output power. This combination of real and reactive power control will ensure a constant voltage DC bus over the full load range. Tests were performed on a three horsepower motor to help validate models and simulations at both the two kilowatt and 5 megawatt level. After determining the equivalent circuit of the demonstration motor, it was tested as a generator under grid connected and capacitor excited conditions. A stand-alone five megawatt, 12,000 RPM generator designed specifically to operate at high efficiency and power factor over the full load rang was used to design converter parameters. A variety of reactive power excitation strategies were briefly examined before the flow of reactive currents through a converter was explained using a six step inverter with two different switching schemes. Steady state and transient simulations matched the measured machine performance and illustrated the performance of the control strategy as the load changes.

Keywords: induction generator, self-excitation, reactive power, power converter, rectifier.

Thesis Supervisor: James L. Kirtley Jr.
Title: Professor of Electrical Engineering

# Acknowledgments

Many thanks to Professor James Kirtley for excellent ideas and the freedom to learn at my own slow pace. Thanks are also due to Research Specialist Wayne Ryan for support with hardware and Professor Steven Leeb for generous loan of equipment.

This investigation began as part of the Naval Research and Education Consortium's Electric Ship Project which was supported by the United States Office of Naval Research.

Steven Englebretson

# Contents

# List of Figures

# *Chapter 1*
# *Introduction*

With the expansion of technology, modern ships and submarines require increasing amounts of power to meet the demands of electrical loads. This project investigates the use of high speed, squirrel cage induction generators in place of traditional synchronous generators for electrical power onboard ships and submarines. Potential advantages of high speed induction generators include smaller size and weight, increased durability, and decreased cost and maintenance. Naval initiatives examining the use of direct current (DC) voltage buses for distributed electrical systems, for more efficient use of DC loads, or for use with alternative power generation open the door for a combined induction generator and power converter used for primary or emergency power generation. For this DC application, the power electronics required to rectify the AC power can also be used to overcome the excitation and control complications of induction generators. The induction generator with integrated power conversion controller could be an attractive alternative to rectified synchronous or permanent magnet generators.

Most (around 85%) industrial motors are squirrel cage induction machines because they are relatively simple and inexpensive to build, operate, and maintain [23]. Potential advantages of the induction generator over synchronous or permanent magnet generators include a simple and robust construction, low cost, low maintenance, inherent overload protection, and no required external active power source [22]. Induction machines lack the separate DC voltage source and commutation issues of synchronous generators as well as the expense and material considerations of permanent magnet generators. Because of these features, induction generators are popular choices for grid-connected power generation applications with wind turbines and small hydroelectric facilities [24]. Unfortunately, the advantages of the induction machine come at the price of poor voltage and frequency regulation.

Induction motors are inductive loads that operate at a poor power factor unless capacitors or another form of power factor correction are connected to the motor input. The machine windings require a "supply of reactive power" to run. Apart from the real power that is burned up as loss inside of the machine, reactive power in Volt-Amperes-Reactive (VARs), with a current waveform 90° out of phase with the voltage, continually oscillates between the inductance of each phase of the machine and the capacitors or connected power system. This power is not used or lost (though the higher current does increase conductor losses) but must be present to energize the windings, generating the magnetic fields that couple the

electrical and mechanical parts of the machine.

Unfortunately, using fixed capacitors alone for excitation will result in unacceptable behavior for most applications because the equivalent inductance of the machine varies with the mechanical drive speed, voltage, frequency, and load. With fixed capacitor excitation, if the drive speed or load change, the output voltage and frequency will adjust to find a new reactive power balance. The poor voltage and frequency regulation of induction generators has led to their "under utilization" and suggested use only for frequency insensitive loads [21];[18]. Changes in rotor speed or load combine with the non-linear magnetic characteristics of the machine to complicate both the real power output and the required reactive power excitation. Maintaining a constant voltage and frequency for changing loads requires a continuously variable drive speed and excitation capacitance. To overcome this challenge, a DC power converter can manipulate the output frequency to control the generated power while supplying the machine with the required varying reactive excitation, maintaining a constant voltage output over the full range of load.

## 1.1 Thesis Scope

Focusing on induction generator control from a machine stand point, this work seeks to develop an understanding of the excitation process, requirements, and factors influencing generator output through design, testing, and simulation.

A variety of motor and generator tests and simulations examine induction machine behavior under changing conditions of load, speed, excitation, and voltage. Unfortunately, the frequency dependence of machine parameters is not included in this study.

A survey of common reactive power support strategies is provided, along with an in-depth examination of the reactive power circulation in a six-step converter.

Various attempts to implement thyristor controlled reactors and six-step converters have not met with success and are not included here.

Fundamental induction generator design considerations are discussed, and a preliminary design for a five megawatt induction generator is presented. The design criteria include small size and weight along with high efficiency and high power factor at 10%, 25% and 100% loads. Additional optimization and modification to meet more specific performance requirements have not been undertaken here. Preliminary work has been completed and important considerations are discussed.

The prime mover was not considered. The mechanical properties of the turbine will influence the total system behavior, but for now, a constant or near constant drive speed has

been assumed. More accurate modelling of turbine torque speed characteristics, limits to isochronous operation, and how these impact generator control are left for future work.

## 1.2 Thesis Organization

The two induction generators central to this investigation are a three horsepower commercial motor and a five megawatt generator design. Working first with the concrete, small scale machine, the behavior and operation of the induction generator is examined in detail. The collected generator data determines the circuit parameters for the small scale generator and controller and is used to verify models and simulations of both the small and large scale generators and controllers.

Equipped with a better understanding of induction generators, a design for the five megawatt machine is developed using software previously developed by Professor James L. Kirtley. The goal is to successfully control both generators, maintaining a constant DC output voltage while supplying a variable load. The combination power converter and generator controller will help to accomplish this by simultaneously providing the generator with reactive power to maintain excitation at a constant voltage while rectifying the generator output. A variety of possible reactive power compensators are evaluated, and the full bridge, six switch converter is selected. Using a six-step switching scheme, the converter can circulate reactive power among the three phases of the generator while rectifying the generator output. Controlling the stator electrical frequency will increase the machine slip with load to boost output power at a constant voltage. Simulations are run to first verify generator models. The simulated initial generator voltage build up is also examined, and the validity of the control strategy, using the converter frequency to maintain a constant voltage as the load changes, is confirmed.

Chapter 2 describes the experimental demonstration platform consisting of a variable speed drive connected to a 3 horsepower (HP) induction motor, coupled to a second, identical 3 HP induction motor driven as a generator. Using a 60 Hz, 0 to 130 V (when connected to the lab supply) variable transformer (variac) or fixed capacitors to excite the generator, extensive tests compared constant frequency, constant voltage operation to constant frequency with variable voltage operation to stand alone operation at variable frequency and variable voltage. These tests provided insight into generator behavior as well as experimental results for validation of the mathematical models and simulations of Chapters 5 and 6.

The third chapter focuses on induction generator design. To gain a better understanding of the capabilities of self-excited induction generators and to attempt to move toward optimizing their performance, a generator is specifically designed for stand-alone, self-excited operation. The generator is designed to operate around 12,000 RPM (400 Hz stator output frequency

for the four pole machine). Additional design considerations include determining real and reactive power losses in the steel laminations, minimizing the rotor resistance, and managing flux densities to deliver the desired power while limiting magnetic saturation. The design and analysis programs used in developing the five megawatt generator are discussed, the results are presented, and the generator's performance is examined. The generator design provides specific reactive power demands, voltage and current levels, and control requirements of the five megawatt generator for determining specifications of the large scale power converter.

Next, an introduction to induction generator control as well as an overview of common VAR support schemes for stand-alone induction generators are provided in Chapter 4. A brief operational explanation and evaluation for this application is given for switched capacitors, variable inductors, phase controlled/force commutated rectifiers, thyristor controlled reactors, and six-switch converters. Reactive power circulation in the six-step converter and a comparison of two possible switching patterns is also presented as part of the chosen control strategy.

Chapter 5 includes steady state and transient simulations of the two kilowatt and five megawatt machines. Steady state, single phase mathematical models and simulations based off of the single phase equivalent circuit are presented first. Computer predictions are compared to experimental measurements for grid connected and stand alone operation. Simulations illustrate how, with reactive power circulation to maintain excitation, adjusting the stator frequency can control power output at a constant voltage. Three phase, transient models and simulations of both the small and large scale machines start with the initial resonant voltage buildup and stabilization of the unloaded generators are illustrated. Then, displaying a roughly constant output voltage while adjusting the stator frequency as the load and/or drive speed change verifies the principle of the control scheme.

Finally, the results, conclusions, and possibilities for future work are discussed in Chapter 6.

The appendices include selected tables of the machine test data as well as the complete generator design and simulation scripts.

*Chapter 2*

# *Demonstration Hardware*

The goal of this project is to investigate the use of a high speed, five megawatt induction generator and controlled power converter as a source of DC electrical power for naval applications. Lacking the means to build or test a machine of this size, general induction generator characteristics and operation of the specific power converter/controller can still be examined in the laboratory on a much smaller scale. A two kilowatt test platform has been constructed to aid in the development of the large scale design. Developing a better understanding of how induction machines operate, measuring changes in reactive power input, and observing the generator voltage and frequency response to changes in drive speed, excitation, and load are all possible on the small scale test bench.

## 2.1 Test Platform Overview

In order to collect real machine data to verify simulation results and to evaluate control methods on a real induction machine, the demonstration platform shown in Figure 2.1 has been built. The small scale test platform includes dual three HP inverter duty induction motors and a Boston Gear VCX variable speed drive. To keep the machines light enough to move by hand the maximum size for a four pole induction machine was limited to about 3 HP (2.24 kW). With the improved insulation of the inverter duty machines, the increased current harmonics and wire temperatures from driving the motor with the variable speed drive and controlling the generator with the converter should not overheat the machine under reasonable load currents. The drive and first motor will act as the turbine. A variable speed and variable voltage can be delivered to the first motor to control the shaft speed of the second motor, running as the generator. Three 52.5 $\Omega$, 5 A variable resistors are used for loads. Six 80 $\mu$F and three 5 $\mu$F ac capacitors can be used to excite the generator.

The 3 HP demonstration induction generator has been tested under constant frequency and voltage operation, fixed 60 Hz variable voltage operation, and stand-alone capacitor-excited operation. First, the equivalent circuit of the machine was found using IEEE 112 test procedures. Before coupling the two machines together, resistance measurements, no load tests, and locked rotor tests were completed using the IEEE guidelines to determine the machine equivalent circuit, shown in Figure 2.2. This common induction machine model can be used

Figure 2.1: 2kW Test and Demonstration Platform

to determine steady state performance. After obtaining the single-phase equivalent circuit parameters for use in simulations, additional tests were performed to further investigate the generator behavior and to provide test data for comparison to the simulations.

Using a 60 Hz, 0-130 V variable three-phase transformer, the generator was tested under variable speed with constant voltage, and variable speed with variable voltage. The generator was also examined under stand-alone, capacitor excited operation with varying drive speed and several values of excitation capacitance and load resistance. Much of the literature on induction generators became clearer after running tests on the small scale motor. Results from the motor and generator tests are discussed in the remainder of this chapter.

## 2.2 Motor Testing

Before any models or simulations could be attempted, the single-phase equivalent circuit components had to be determined through winding resistance measurements with the machine at running temperature and the traditional no load and locked rotor tests.

### 2.2.1 No Load Test

During the no load test, the machine is connected as a motor and provided with electrical input, in this case by a 60 Hz three-phase variable transformer. The voltage is initially increased to 120% of the rated voltage and then gradually decreased until the motor stalls. Measurements of voltage, current, power (real or imaginary) or power factor angle, and speed are made at regular intervals after the machine has stabilized. The three-phase variable transformer could supply a maximum stator input voltage of only about 130 V RMS line-neutral when connected to the lab three phase 208/120 V power. The inability to increase the voltage above the 230 V machine rating resulted in failure to completely saturate the machine. Without the complete saturation data, extrapolation had to be used when modelling the mutual inductance at high voltage or current levels.

With no load torque, the stator input and the induced rotor fields rotate at nearly identical speed. The per unit slip, $\frac{\omega_s - \omega_r}{\omega_s}$, is a small negative value, and the equivalent rotor resistance, $R_r/s$, can be in the megohm range or larger. Typically, the rotor resistance is assumed to approach an open circuit; the rotor branch of the single phase equivalent circuit can be neglected; and the no-load current, the stator current, and the magnetizing current are identical around the single loop. This assumption greatly simplifies analysis of the no load test results and was found to introduce little error under normal operating conditions. Calculations with and without the simplification gave indistinguishable results at the larger voltage levels but showed greater discrepancy at the lowest levels of voltage and current. These start-up conditions are particularly important for modelling the generator initial excitation and voltage buildup. Measurements of rotor speed, not typically required for no load motor tests, are vital for calculating the slip when the rotor branch is included under low voltage and current input.

At a low enough input voltage, the measured current starts to increase. Most motor tests are concluded at this point as the motors should never have to operate under such low voltage input. Continuing measurements until the machine stalls is important for generator testing because the zero-voltage values of the mutual and leakage inductances will determine the initial excitation and voltage buildup of the generator. As the voltage decreases, the slip gradually increases from immeasurably small (less than $10^{-4}$) at maximum voltage to as much as about 0.31. With the increased slip, the no load approximation of infinite rotor resistance breaks down, and significant current flows through the rotor branch. The full circuit model, including the rotor branch, should be used for accurate determination of the machine mutual inductance at low voltage and current input. Results from the no load test are included in Appendix A.

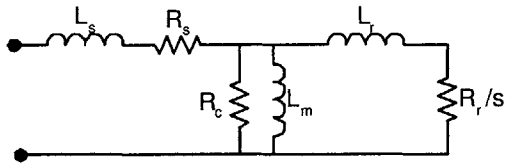


Figure 2.2: Induction machine single phase equivalent circuit model

### 2.2.2 Locked Rotor Test

For the locked rotor test, the rotor is secured so that it cannot rotate. Starting from the rated current, voltage is incrementally decreased, again with measurements of voltage, current, and the angle between them at each step. This test can be problematic because temperature increase from the large currents influences the circuit parameters. Also, with the rotor fixed at zero rotational frequency, the slip remains constant at 1, and the rotor branch consists of the rotor resistance, $R_r$, in series with the rotor leakage inductance, $L_r$. The rotor voltage and current are 60 Hz sine waves for the test while under normal operating conditions they oscillate at much lower slip frequencies on the order of a few Hz. The frequency dependence of these rotor variables can add significant error to calculations from the locked rotor test.

Not having a variable frequency source to investigate the frequency dependence of the machine parameters is a significant limitation of the machine testing. Control of the induction generator uses a decreasing stator output frequency to regulate the output voltage. Based around 60 Hz, the frequency will not vary by more than about $\pm 5$ Hz, so the 60 Hz values will function as rough approximations. Still, more precise modelling and realistic operating limits of the control system could be possible knowing the variation of the machine parameters, particularly the mutual inductance, as the electrical output frequency varies.

An interesting observation from the locked rotor test data is that the leakage inductance appears to increase as the voltage and current drop. The measured real input power approaches zero faster than the reactive power, and a few VARs are still measurable after the real power has gone to zero. Normally, the ratio of reactive to real power is in the neighborhood of 2.5 for an input current of about 3 A and above. Below 2 A, the ratio increases as the input voltage and current decrease, reaching 6 before the real power goes to zero. The operating 60 Hz leakage reactance was calculated to be about 1.885 $\Omega$. Ignoring the magnetizing branch and assuming the stator and rotor leakage reactances are equal, the total reactance at 3.77 $\Omega$ is about 2.77 times the 1.36 $\Omega$ total resistance at unity per unit slip. The temperature dependence of the stator and rotor resistance may be partly responsible for increasing the resistance with current. Still, the measured values for real and reactive power fit if the leakage reactance is a non-linear function that increases for low voltage and current.

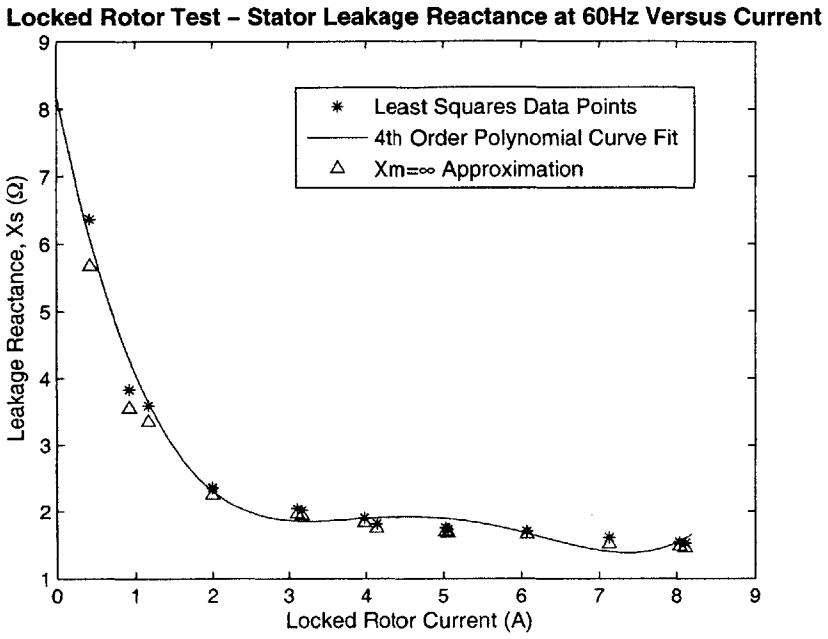


Figure 2.3: Non-Linear Stator Leakage Reactance - Calculation Comparisons

Induction machines do not experience such small values of input voltage and current during typical running conditions, so approximating the leakage inductance as a constant value adds very little error under normal operation. However, for the initial motor starting from zero voltage or generator voltage buildup, the increased leakage values could have a significant impact on machine performance. At no load, neglecting the rotor branch and stator resistance, the excitation capacitor is equal to $\frac{1}{\omega_e^2(L_m+L_s)}$. For a given output frequency and mutual inductance, the larger initial leakage inductance decreases the capacitance required to excite the machine.

Figure 2.3 compares the values for leakage reactance using the full equivalent circuit and the approximation neglecting the magnetizing branch and core resistance. The two methods give nearly identical results except at extremely low voltage and current, where the approximation appears to slightly underestimate the leakage reactance. This could be significant for determining the capacitance for initial excitation and voltage build up of the generator. A fourth order curve fit for the data points using the entire circuit is also shown. The no load current at running voltage from the no load tests is greater than 2 A, so the leakage reactance can be assumed constant for all cases except the initial voltage buildup.

## 2.3 Machine Characteristics

The results from the no load and locked rotor tests were analyzed to determine approximate equivalent circuit values of the small scale induction generator. In addition to gaining a better understanding of induction generators, the circuit parameters are vital for generator simulations. The test results give only approximations, and values for the leakage and mutual inductance are based on fourth order polynomial curve fits that apply only over a specific range of voltage and current, about 0-140 V and 0-9 A rms. Nevertheless, the parameters can now be used in models and simulations to predict the machine behavior. The single phase equivalent circuit for the tested 3 HP induction machine is shown in Figure 2.2 and the parameters are listed below.

The circuit parameters are:
$R_s = 1.03\ \Omega$
$R_r = 0.33\ \Omega$
$R_{core} = 800\ \Omega$
$L_s = 5$ mH
$L_r = 5$ mH
$L_m = 0.1$ H (Peak Value)

The stator and rotor leakage inductance, $L_s$ and $L_r$, are assumed to be identical. They may also be assumed constant under normal operating conditions, but as discussed in the previous section, the leakage inductance can increase substantially, more than doubling, under start-up conditions. Full curves for the nonlinear mutual inductance, $L_m$, as a function of air gap voltage and magnetizing current are shown in Figures 2.6 and 2.7.

Starting from simplifying assumptions, neglecting the rotor branch for the no load tests and the magnetizing/core path for the locked rotor tests, the equivalent circuit is straightforward to analyze. Stator resistance is measured directly and the rotor resistance is found using the input power of the locked rotor test, initially ignoring the core/magnetizing branch but later checked with the complete circuit. The core resistance is determined from the no load test data, initially using the circuit approximation neglecting the rotor branch and assuming a fixed 10 W friction and windage loss. The core resistance seems to vary significantly, but the value is large enough that the variation does not appear to impact circuit calculations.

The mutual inductance depends on the air gap voltage and current, but the voltage and current through the mutual inductance also depend on the value of that inductor. When the full circuit is included, circuit analysis techniques are insufficient. The final curves for both the mutual and leakage inductances are calculated using Matlab's `lsqnonlin` least squares fitting function with power balance and impedance matching equations.

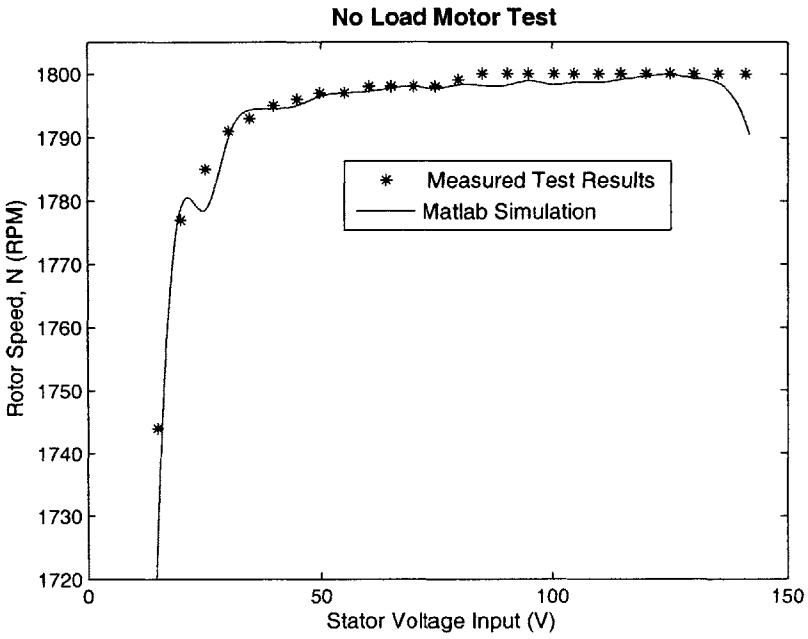


Figure 2.4: Comparison of motor model to measured results of no load test

The resistance values are assumed constant. The stator and rotor leakage inductance are assumed to be identical for the calculations. This is likely a source of some error, but it should be a reasonable approximation for a machine of this size. Regardless, both leakage values are small and of the same magnitude, and there is no convenient way to differentiate between the two. The measured input real and reactive power are used to determine the mutual and leakage inductances, completing the equivalent circuit. Several iterations are performed, checking each inductance value and the original resistance values in the full circuit with the new parameters, slightly modifying values until everything appears fairly constant.

As a quick check to verify that the determined parameters are reasonably accurate, a comparison is made between the measured results for the voltage versus speed during the no load test and calculations of the expected rotor speed given the input voltage, current, and circuit parameters. The results of this comparison can be seen in Figure 2.4 and demonstrate that the machine behavior can be modelled using the derived circuit parameters.

At realistic running voltages, around 100-130 V, the no load circuit approximations neglecting the rotor branch and treating the leakage reactance as a constant, provide nearly identical results with significantly less effort than using the full circuit model. Figure 2.5 shows the slight changes in calculated mutual reactance at lower voltages. The plot over the full range

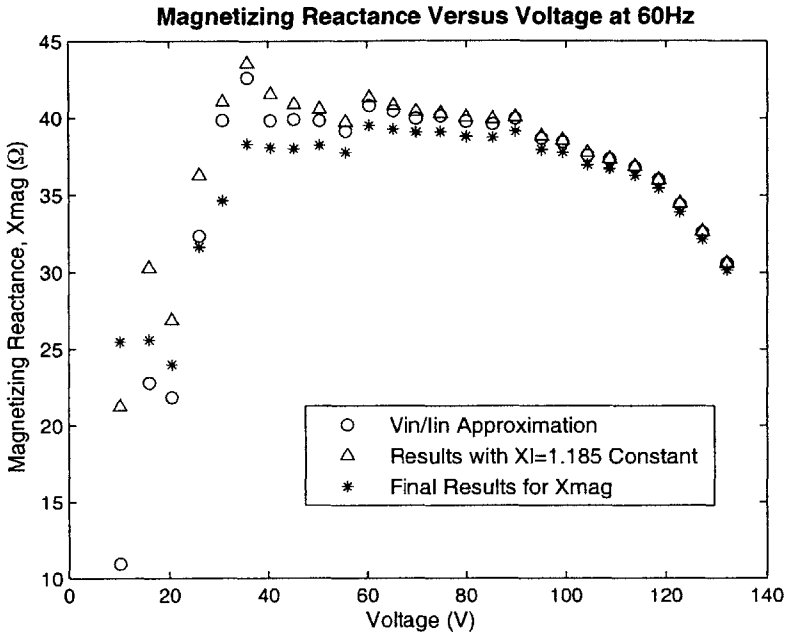


Figure 2.5: Various calculations of the mutual reactance at 60 Hz

of no load stator output voltage shows the s<<1 approximation neglecting the rotor branch, results assuming both stator and rotor leakage reactances are constant and equal to 1.885 H, and the final results using the varying values of slip and leakage reactance. For modelling this machine as a grid-connected motor, running with a nearly constant input voltage, the variable leakage reactance and mutual reactance at low voltage and current would not be an issue. However, when looking at the initial excitation of the induction generator, these factors have a significant impact on the excitation capacitance required for voltage buildup.

A plot of the calculated mutual inductance versus air gap voltage along with a fourth order curve fit is shown in Figure 2.6. The mutual inductance, $L_m$ peaks and falls off as the flux paths within the machine saturate with increased output voltage or current. The fourth order equation for mutual inductance as a function of air gap voltage from Figure 2.6 is sufficient for determining the start up and no load behavior of the machine. Unfortunately, for constant voltage operation, after establishing a stable operating voltage, the output voltage will be held constant and the air gap voltage will not change significantly as the load increases. The output power will increase with the output current as the load rises. The further saturation of the machine with load as the output current increases is not considered in the Figure 2.6 mutual inductance plot. Figure 2.7 displays the same no load data for the mutual inductance, now as a function of the magnetizing current, and another fourth order

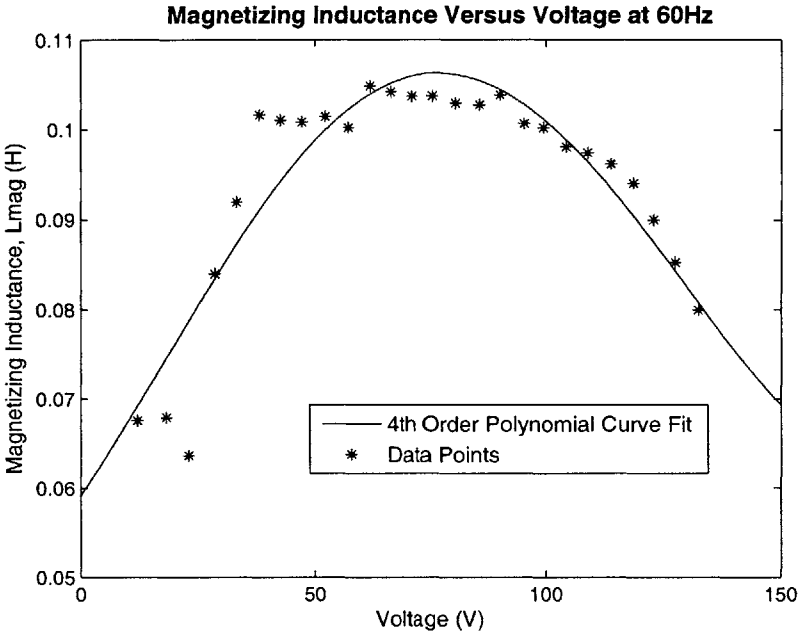


Figure 2.6: Mutual inductance at 60 Hz over the full range of no load stator voltage

polynomial curve fit, extrapolated to approach rated current. This equation for the mutual inductance considers machine saturation with output current and is included in machine simulations.

Due to the voltage limit of the 60 Hz variac used for the no load test, the current during testing only reached about 4.5 A. Beyond this value reasonable approximations for $L_m$ are given assuming a continued linear decrease of the inductance with increased current and magnetic saturation. The accuracy of the mutual inductance plots could be improved by running the no load test over a wider voltage range, but the plots generally match the expected appearance [17];[13];[18].

## 2.4 Steady State Capacitance

Squeezing the last bit of information from this set of tests before moving on to generator tests and control possibilities, the no load motor test data can also be used to find approximate capacitance values for generation at a steady state voltage.

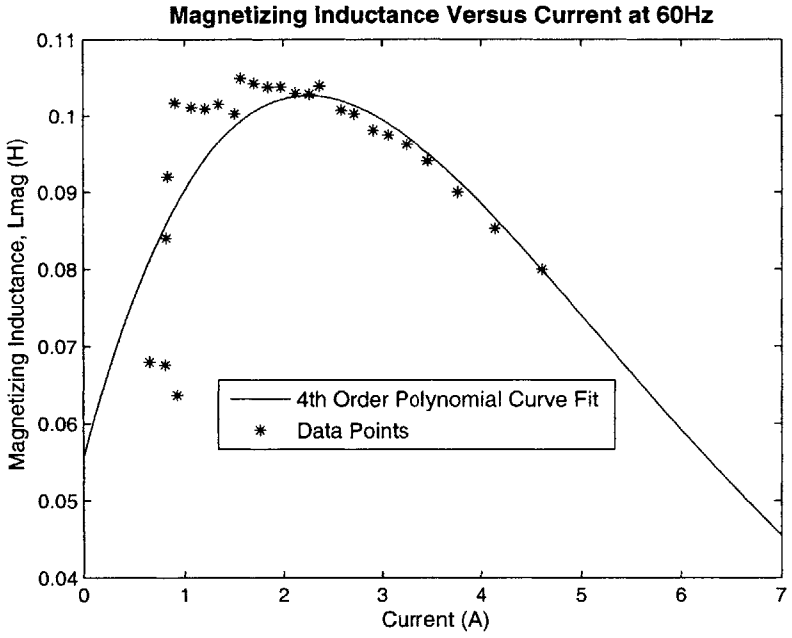


Figure 2.7: Magnetizing inductance at 60 Hz versus no load stator current

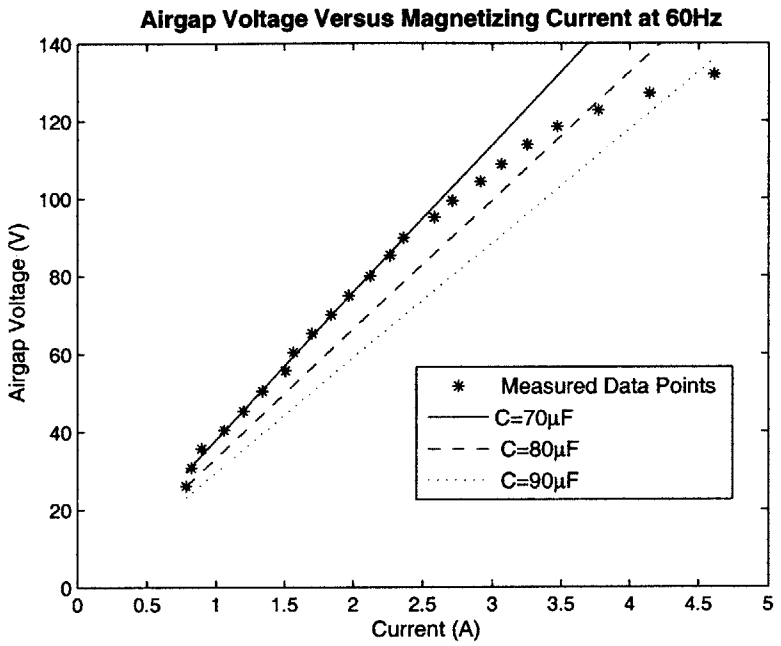


Figure 2.8: 60 Hz magnetizing current versus air gap voltage with 70, 80, and 90 $\mu$F capacitor slopes

One way to determine the capacitance necessary to excite an induction generator at rated speed is to use a plot of the air gap current plotted against the air gap voltage as shown in Figure 2.8. At no load, this is roughly equivalent to the expected no load current versus the air gap voltage [17]. The slope of this curve gives the mutual inductance at each operating point. The capacitance required to excite the machine can be found by adding the capacitor's voltage, which will be a straight line of slope $\frac{1}{\omega_s C}$, to the same graph. The stable operating points are where the linear capacitor impedance lines intersect the mutual inductance curve.

In measuring values for plotting the air gap voltage versus the magnetizing current, the machine is slowly saturating. Unfortunately, the maximum terminal voltage the variac could apply to to the motor while connected to the lab power was about 130 V. Greater voltages would have shown increased saturation of the machine with voltage and would have intersected impedance lines of larger capacitors at greater voltages.

The no load plot of the magnetizing current versus the air gap voltage of Figure 2.8 should show a finite residual voltage value at i = 0 representing remanent magnetism from orientation of magnetic domains in the iron of the machine, as if the machine contained extremely poor permanent magnets. Unfortunately, no voltage measurements were taken after the machine lost excitation at about 0.5 A, so the remanent magnetism cannot be seen in Figure 2.8. Still, these small stored fields allow the initial excitation of the machine without any initial capacitor voltage or additional voltage source, building exponentially as the machine inductance rings with the excitation capacitor and the negative rotor resistance adds current to the system.

Considering Figures 2.7 and 2.6, a slight disturbance in voltage is stable on the negative, decreasing slope of the mutual reactance but unstable in the initial rising slope. Assuming the current to be constant, if the air gap voltage on the negative slope increases, the mutual reactance will oppositely decrease, and with roughly constant current, the reduced reactance will tend to reduce the voltage back toward the original value. Likewise a disturbance decreasing the voltage on the saturated part of the curve will tend to restore the stable voltage by increasing the reactance and decreasing the voltage of a roughly constant current. Alternatively, on the initial positive slope, a decreasing voltage will cause a lower mutual reactance, that will further reduce the voltage, and the cycle will continue until the voltage has completely collapsed. Similarly a slight increase in the unstable region will set the voltage growing until it builds up past the peak into the saturation region.

The straight line plots for the impedance of 70 $\mu$F, 80 $\mu$F, and 90 $\mu$F capacitors are show in Figure 2.8. When intersecting the machine V-i curve, these values represent the capacitance required to maintain excitation at no load for a given speed, frequency, and running voltage. According to Figure 2.8, a 70 $\mu$F capacitor would not result in a stable output voltage at no load, but any larger capacitor should result in a stable output voltage up to the rated voltage limit. These are steady state values, and additional capacitance or increased drive

speed is required for initial voltage buildup at the decreased, zero voltage mutual reactance.

One of the data points from the stand alone, capacitor excited machine tests discussed below shows a nearly identical stable, steady state operating point. With the unloaded generator excited by 80 $\mu$F capacitors, values of terminal voltage and current are measured for different drive speeds. The generator voltage builds up to around 75 V at a drive speed of about 1700 RPM. Once running, a voltage as low as about 57 V can be maintained at 1682 RPM. During this no load generator test, the machine appears to be under-damped, with the measured values slowly oscillating between upper and lower bounds, over a range as big as 0.1 A and 5 V. As the voltage increases, the magnitude of the oscillations decreases.

At nearly the rated speed, 1799 RPM, and frequency, 59.9Hz, RMS terminal voltage and current measurements of about 129 V and 3.67 A were recorded. Using these values and assuming, at this voltage, that the approximation of neglecting the rotor branch because of small slip is accurate, the calculated air gap voltage is about 122 V using Equation 2.4. The current leads the voltage by nearly 90° because there is no real load, only reactive power circulating between the machine and excitation capacitor.

$$V_{airgap} = V + i(Rs + jXs) = 129 + j3.67(1.03 + j1.885) \approx 122V \tag{2.1}$$

Examining Figure 2.8, the 80 $\mu$F capacitance line intersects the no load generator data near 3.65 A and 121 V. These predicted steady state values are remarkably consistent with the measured 122 V and 3.67 A.

### 2.4.1 Machine Operation

The single phase equivalent circuit of Figure 2.2 offers the most straightforward explanation of induction machine behavior. For motors, a voltage and current input are provided at the stator terminals. The sinusoidal, rotating stator currents produce magnetic fields that induce voltages and currents in the rotor conductor bars. Fields from both the stator and induced rotor currents exert a force on the other current carrying conductor, rotating the freely turning rotor. The input current is proportional to the output torque and the input voltage to the rotor speed.

The equivalent rotor resistance from Figure 2.2 is given as $\frac{R_r}{s}$ where $R_r$ is the fixed rotor resistance and the per unit machine slip, $s$, is the difference in the stator and rotor electrical frequencies, compared to the stator frequency, $s = \frac{\omega_s - omega_r}{\Omega_s}$. This resistance represents the energy transferred to the mechanical load. As the mechanical load increases, more power is transferred to the rotor, or "burned" in the $\frac{R_r}{s}$ resistor of the equivalent circuit. Increased

power can be delivered by increasing the applied stator voltage, and with it the magnitude of the machine currents and fields. Alternatively, the equivalent resistance can be reduced by increasing the slip, raising the rotor current and power for a given voltage. To increase the slip, either the input stator electrical frequency must be increased or the output rotor speed must be reduced.

For generator operation, the machine slip must be negative. Now, mechanical power is converted from the rotor and flows out of the stator terminals. For grid connected, constant frequency and voltage generation, the drive speed is the only available control for the generator power output while the grid supplies the varying "input" reactive power to maintain the fields within the machine. With a constant stator frequency, the machine slip and power output can be adjusted by changing the drive speed. For stand alone operation the output voltage and frequency are no longer fixed. Feeding a DC voltage bus, a constant voltage must still be maintained, and reactive excitation power still must be provided at the stator terminals. However, now the electrical output frequency can also be used as a control variable.

Having developed a working equivalent circuit of the induction machine through the no load and locked rotor motor tests, additional generator tests were run to observe reactive power demand, investigate behavior, and gather data to verify generator simulations.

## 2.5 Generator Testing

After characterizing the induction machine, the two motors are coupled together and two main types of tests are conducted. First, simulated grid connected tests are performed at fixed 60 Hz frequency and a variety of constant voltage levels. The generator output was connected to the fixed 60 Hz, variable voltage source of the three phase variable transformer, and input VARs and output power were measured as the drive speed varied at a number of different voltage levels. The second group of tests involved running the machine in stand alone operation excited by fixed capacitors connected across each phase of the machine. In addition to gaining a better understanding of the machine behavior as a generator, the results from these tests are used check the accuracy of the computer models and simulations using the derived machine parameters. Representative test data is included in Appendix A.

### 2.5.1 Grid Connected Generator Tests

For the first set of tests, constant voltage levels of 60 V, 80 V, 100 V, and 120 V were applied to the generator output by the three phase variable transformer. The variable speed drive was used to adjust the rotor shaft speed to control the machine slip and vary the generator

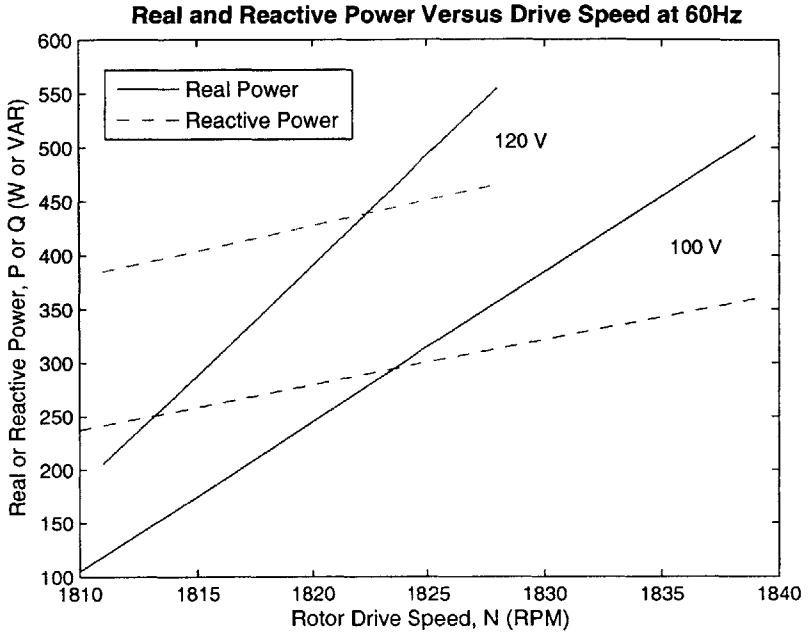


Figure 2.9: Real and reactive power versus drive speed

output power. Variable reactive power was supplied to the machine by the grid through the transformer.

With constant output voltage and frequency maintained by the connection to the power grid, control of the drive speed of the generator is the only adjustable variable to control the output power. In this case the grid connection must provide an adequate, varying supply of reactive power at the machine output terminals, which may or may not be possible while maintaining a constant voltage. The machine operates at a very poor power factor (less than 0.50 for the test 3 HP machine) at low loads. Ideally, generators with high mutual inductance could run at higher power factor by operating only when wind or water flow conditions are sufficient for the turbine to drive the rotor near the maximum speed for full load output.

As shown in Figure 2.9, both real and reactive power increase linearly with the load. At higher voltage levels, the reactive power varying over a smaller range will aid the VAR supply, but starting at a larger initial value reduces the machine's light load power factor, requiring additional excitation capacitance. At increased voltage levels, the machine reaches maximum current and power output at lower drive speed.

The reactive power drawn from the grid to maintain excitation increases with the delivered

power and can be significantly greater than the output power at low speeds.

The generator tests at fixed frequency and variable voltage also show how the machine output (and with it reactive input power) can be increased by raising the operating voltage. Naturally, the machine runs more efficiently and at a higher power factor closer to the rated voltage. The range of possible operating speed narrows as the voltage level increases, since the output current increases with voltage, reaching the rated limit at a lower speed. The minimum speed is still set by the fixed electrical frequency.

These grid connected tests are similar to the planned control strategy in that both have unregulated, automatic reactive power compensation, and use control of the machine slip to vary output power at a constant voltage. However, in stand alone operation, there will not be a fixed voltage maintained by the power grid, and a decreasing stator frequency will be used to increase the slip in place of the increasing drive speed.

### 2.5.2 Capacitor Excited Generator Tests

Initial experiments are run to see what conditions are necessary to excite the stand alone generator. Excitation capacitors are limited to only three 5 $\mu$F and six 80 $\mu$F, 270 V AC capacitors, so 5 $\mu$F, 40 $\mu$F, 80 $\mu$F, 85 $\mu$F, and 160 $\mu$F are the only equivalent per phase values used for testing. Using 40 $\mu$F, the generator will not excite running the machine up to speeds near 2000 RPM. Theoretically, any capacitance can excite induction machines, but the unreasonably high speeds may destroy the machine before the voltage builds up.

The difference between steady state operation and the initial transient voltage buildup is noticeable in these tests. Using drive speeds up to about 2000 RPM, the machine will not excite with the maximum available 52.2 $\Omega$ per phase load connected, even with 160 $\mu$F per phase. The smaller the load resistance, the greater the load current and power output at a given voltage. The load resistance over damps the LC resonant circuit made up of the machine and excitation capacitors, preventing the voltage from building up. For initial excitation, the greater the drive speed, the less the required capacitance.

Three separate five A, variable zero to 52.5 $\Omega$ resistors are used for the AC load. The nonuniform wearing and contact pressure of the resistors' sliding carbon contacts creates significant variation between the resistors. Each phase must be separately adjusted while measuring the resistance, so no changes can be made to the load while the machine is running. Even though tests are conducted at a variety of loads (52.5 $\Omega$, 39 $\Omega$, and 30 $\Omega$) the most reliable load is the 52.5 $\Omega$ test across the full length of the resistor, without the carbon contacts. Not only does this case eliminate any uncertainty in the resistance settings, together with the 80 $\mu$F excitation capacitance, the full 52.5 $\Omega$ load also results in the output frequency closest to 60 Hz, for minimal variation from the measured 60 Hz

machine parameters.

With 80 $\mu$F of excitation capacitance, a small steady state voltage of 1.1 V at 49.6 Hz was measured at a drive speed of about 1488 RPM. The voltage and frequency crept up as the drive speed increased, from 1.7 V and 53.8 Hz at 1613 RPM, to 2.6 V and 56.2 Hz at 1684, and finally 3.7 V and 57.4 Hz at 1720 RPM just before the voltage built up. Once the voltage begins to visibly build up, the drive speed is reduced to limit the steady state value. Once excited, stable output voltages can be maintained at speeds below what is required for the initial excitation.

With no load (infinite load resistance), around 80 $\mu$F on each phase, and sufficient drive speed (greater than about 1700 RPM), the voltage quickly builds up. Once the voltage approaches 100 V, the load can be switched in and the drive speed increased to achieve a steady state. After the machine is running at a stable voltage, the speed is varied and measurements of the drive speed, output stator voltage, stator frequency, and capacitor current are taken incrementally over the widest possible range of voltage output. At a low enough drive speed, the capacitor can not supply sufficient reactive power to maintain the machine fields and the output voltage collapses. At high drive speeds, the test setup ran extremely loud from increased harmonic currents in the drive motor. The upper limit was set by the current ratings off the generator and the motor drive. These tests provided a better understanding of induction generator operation and test data to verify generator models. Data from illustrative generator tests is included in Appendix A.

## 2.6 Sources of Error

The test setup incudes two identical 3 HP induction machines. The no load and blocked rotor motor tests were performed on the first machine, running as the drive motor. The calculated machine parameters from these tests were assumed to be roughly true for the second machine, set up to run as a generator. The generator tests were performed on the second machine, but the simulation models that will be compared to the generator results use the parameters calculated from the first motor tests. The same machine should have been used for both cases. As first order approximations, simulations using the measured motor circuit parameters seem to match the measured generator data. Any discrepancies between the two should not interfere with the goal of validating the general control process so that it can be used with greater confidence on the 5 MW scale. Still, running all of the tests on the same machine would have eliminated any chance of unexpected manufactured differences between the machines.

There is also some obvious error in the measured test data in that the voltage and current data does not perfectly match the real and reactive power data. All of these values shown in

Appendix A were taken directly from a digital, power multimeter. The variations might be caused in part by constant machine fluctuations during measurements, but the discrepancies are small and should not impact the circuit parameter approximations.

For a more accurate representation of the induction machine, the core loss resistance, $R_C$, should also vary with saturation. The core loss is often neglected entirely for approximate solutions, and a simplified model is preferred for easier analysis and quicker calculations at this stage of understanding and verifications of the general control scheme.

*Chapter 3*

# *Generator Design and Optimization*

---

High speed induction generators with cage rotors can offer increased power output at a reduced overall size and weight. The simple, sturdy construction can also be manufactured and maintained at less cost than synchronous or permanent magnet machines. With a control system to maintain a constant output voltage, an induction generator is an appealing option for DC power generation.

The reactive power requirements of the machine are fundamental in determining an acceptable control solution. Capacitance values and voltage and current ratings for all components are dictated by the generator. Before delving too deeply into the specific control and power conversion possibilities, the machine characteristics must be determined. To some extent, the parameters of the induction generator can be designed to aid initial self-excitation and generator operation by reducing the machine's required reactive power, optimizing voltage and frequency regulation, and improving the magnetic saturation characteristic of the generator [19]. The following machine is designed to obtain example values for determining the generator controller.

## 3.1 Induction Generator Design Considerations

Any induction motor can, in theory, run as a generator when the rotor shaft is driven at a drive speed, $N_r$, resulting in a rotor electrical frequency, $\omega_r$, greater than the stator electrical frequency, $\omega_s$. This gives the machine a negative per unit slip, $s$, and a negative rotor resistance in the single phase equivalent circuit (Figure 2.2) that generates real power when a voltage is present.

$$\omega_r = \frac{2\pi N_r p}{60} \tag{3.1}$$

$$s = \frac{\omega_s - \omega_r}{\omega_s} \tag{3.2}$$

Even though any motor should be able to generate power, the machine may be far from optimized when running as a generator. Often, motors run at a specific operating point or

over a restricted range. Motor design emphasizes starting torque and current and running torque-speed characteristics. Provided that the torque can be achieved by the drive turbine, these criteria become less important for a large generator. For induction generators, change in torque from no load to full load as well as the operating efficiency and power factor over the full load range become more significant.

The fundamental parameters in determining the power factor of induction machines are the mutual and leakage inductance terms. The space fundamental mutual inductance, $L_M$, for induction machines can be calculated as

$$L_M = \frac{4\mu_o r l N_s N_r k_a k_s}{\pi g p^2} \tag{3.3}$$

where $g$ is the effective air gap, $p$ is the number of pole pairs, $r$ is the rotor radius, the $k$ are the winding and skew factors dependent on the geometry of the stator windings and angle of the rotor bars, $\mu_o$ is the permeability of free space, $N_s$ is the total number of turns of the stator, and $l$ is the rotor length [12]. The fundamental mutual inductance of the machine should be designed large to reduce the magnetizing current and required reactive power excitation, maximizing the power factor. Additionally, a soft saturation characteristic that slowly decays as the current increases offers a wider generator operating range.

The leakage inductance under normal operating conditions should be as small as possible. As the rotor and stator currents increase with load, the leakage reactance contributes additional inductive VARs that must be cancelled out by increased capacitance or increased VAR circulation through the output inverter. If a machine could be designed with a leakage inductance that decreased as a function of the current squared, a fixed excitation capacitance could possibly maintain a constant voltage and frequency output over a limited load range. The leakage inductance is so small, only around 0.005 H for the tested 3 Hp motor, that sufficiently decreasing leakage inductance would be difficult to achieve.

The effects of the mutual and leakage inductances can be seen in the plot of real and reactive power from the grid connected test shown in Chapter 2, Figure 2.9. With a constant output voltage, the air gap voltage remains roughly constant and so do the magnetizing current and mutual reactance. Operating under nearly constant flux conditions, the initial reactive power for zero real power output is primarily due to the mutual inductance. Decreasing the mutual inductance reduces the capacitance required to initially excite the generator. As the power output increases, the rotor and stator currents through the leakage inductances increase. This can be seen by the increasing slope of the reactive power as the real power output increases. Minimizing the leakage inductance limits the increase in capacitance or otherwise supplied leading VARs over the full range of load.

## 3.2 Iron Loss Models

Another benefit of not being tied to the grid is flexibility in the output frequency. One of the more unusual aspects of this machine design is the roughly 400 Hz stator frequency. For DC power production, the stator AC frequency can be varied for greater design flexibility. Taking advantage of the high speed, the goal is to design a higher power density machine. The 400 Hz frequency also reduces the size of excitation capacitors and any filtering components. Disadvantages of the increased speed include increased magnetic saturation, increased real and reactive core losses, and an increase of the required switching frequency of the power converter. Iron loss models for both real and reactive power loss densities in the generator design script were modified in an effort to better model 400 Hz machine losses at a 5 MVA scale. The existing loss models have been compared and show reasonable agreement with manufacturer data. However, the loss models in the original program were intended for 60 Hz operation. The loss equation coefficients and exponents have been adapted for use over the full frequency range from 60 Hz to 400 Hz.

Though approximate equations exist, loss mechanics in rotating machines are still not completely understood and cannot be exactly predicted or modelled [6]. Involved geometries with nonuniform flux densities and the varying amplitude and frequencies of harmonic components complicate loss calculations. Often, machine core loss is broken up into three separate terms: hysteresis loss, eddy current loss, and "excess" loss [30]. Functions of lamination thickness, conductivity, mass density, and grain size, these equations are not included in the current analysis program. Core loss estimation is far from perfected and predictions according to these or similar equations often fall 50% or more short of measured machine losses [3]. Instead, the analysis program uses an alternative loss estimation with the following two equations modelling the real and reactive power loss densities in the machine steel laminations [12]. The losses densities in W/kg or VAR/kg are determined for a given frequency, $\omega$, and magnetic flux density, B. Different flux and loss densities are calculated for the rotor teeth, stator teeth, and back iron.

$$p = a\left|\frac{B}{B_o}\right|^b \left|\frac{\omega}{\omega_o}\right|^c \qquad \left[\frac{W}{kg}\right] \tag{3.4}$$

$$q = \left(d\left|\frac{B}{B_o}\right|^e + f\left|\frac{B}{B_o}\right|^g\right)\left|\frac{\omega}{\omega_o}\right|^h \qquad \left[\frac{VAR}{kg}\right] \tag{3.5}$$

The coefficients and exponents are a, b, c, d, e, and f. The baseline frequency and magnetic flux density for the loss calculations are $\omega_o$ and $B_o$.

Determining the coefficients and exponents of these equations so that they mirror Epstein

test data for laminations of reasonably high quality steel should provide a good model to estimate generator iron losses. The equations might underestimate actual machine losses since any effects of the rotating magnetic fields are not considered in the alternating field measurements of the Epstein loss data.

Manufacturer loss data in both W/lb and VA/kg at 50 Hz and 400 Hz from Cogent Power Ltd for non-oriented NO 07 (.007" thick) steel sheets was used to determine the high frequency loss equations. These sheets of 3% Si, 0.4% Al typically have a density of 7.65 g/cm3 (0.276lbs/in3), and a yield strength of 599,000 psi. The W/kg, and VAR/kg loss equations from the machine analysis script were plotted alongside manufacturer loss data, and the equation coefficients and exponents were varied until both curves roughly matched, with slight priority given to the high frequency curve. The final loss approximations are given in the following two equations and the comparisons at 60 Hz and 400 Hz are displayed in Figure 3.1.

$$p = 1.30 \left| \frac{B}{B_o} \right|^{1.85} \left| \frac{\omega}{\omega_o} \right|^{1.15} \qquad \left[ \frac{W}{kg} \right] \tag{3.6}$$

$$q = \left( 1.58 \left| \frac{B}{B_o} \right|^{1.37} + 0.04 \left| \frac{B}{B_o} \right|^{15.4} \right) \left| \frac{\omega}{\omega_o} \right|^{1} \qquad \left[ \frac{VAR}{kg} \right] \tag{3.7}$$

The final loss models try to err on the high side, slightly overestimating the machine losses. The reactive power losses, plotted with a logarithmic VAR/kg y-axis scale in Figure 3.1 increase rapidly as the flux density increases and the machine saturates. Operating at 400 Hz, the iron saturates at significantly lower flux densities than conventional 60 Hz machines, limiting realistic magnetic flux densities to around 1.0 Tesla (T) in the machine iron.

## 3.3 Five Megawatt Induction Generator Design

The optimized design and evaluation of a high speed induction generator could easily fill an entire thesis. An initial design has been completed using design synthesis and analysis programs previously developed by Professor James L. Kirtley. Professor Kirtley's Monte-Carlo based design program, the "Novice Design Assistant" generates random values within specified ranges for selected design variables. Literally millions of randomly generated designs are evaluated by the program, and the best designs based on on preset criteria are stored and displayed. Designs are evaluated by another induction motor analysis program, also developed by Professor Kirtley. The evaluation program was compared with actual test data for several small (several kW) motors, and predicted values agreed reasonably well with the

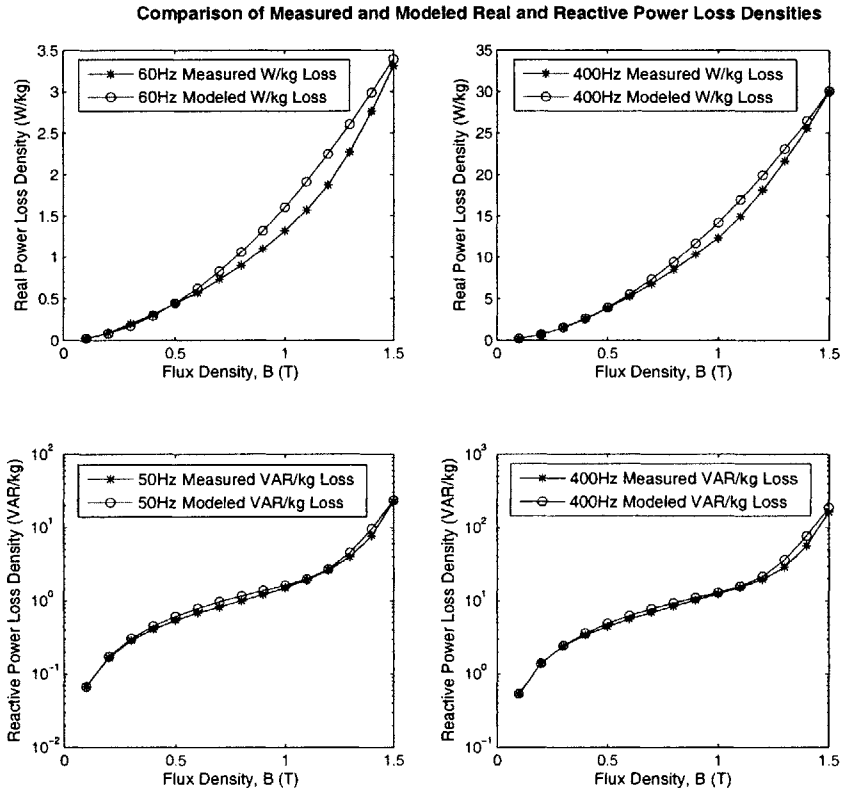


Figure 3.1: Comparison of data and models for losses in non-oriented .007 Inch Steel Laminations

actual measured results. Following extensive review, the motor program has been adapted for generator operation. The program appears to be functioning correctly, but doubtless, bugs still remain as the machine efficiency appears unrealistically high and the designed air gap is probably too small. The fundamental design equation used in this program is the magnetic flux density in the air gap:

$$B_{gap} = \frac{Vp}{2N_s\omega_s rlk} \tag{3.8}$$

where $V$ is the air gap voltage, $p$ is the number of pole pairs, $N$ is the number of stator turns, $\omega_s$ is the stator electrical frequency, $r$ is the rotor radius, $l$ is the active length, and $k$ is a winding factor. This equation can be derived either from

$$V = vBl \tag{3.9}$$

for the voltage, $V$, induced across a conductor (the rotor bars here) of length $l$ moving at a velocity $v$ through a magnetic flux density, $B$, (cutting magnetic field lines) or by

$$V = -N\frac{d\Psi}{dt} \tag{3.10}$$

where a changing magnetic flux, $\Psi$, linked by a conducting coil of $N$ turns, generates a voltage $V$, directed to induce a current that opposes the change in flux.

Based on classical machine analysis, the complete program is extremely detailed, including equations for the effects of lower order harmonics. An initial design, detailed in the next section, has been selected after running a two and a half million iteration design search, but additional work remains to further refine the analysis program and to optimize the final design.

The generator design and analysis programs examine the machine's performance when running at full load, one-quarter load, and ten percent load. The design with the consistently highest efficiency and power factor after the 2.5 million iteration design search is selected. The generator voltage, drive speed, rotor radius, length, air gap, the ratio of both the rotor and the stator surfaces that are used for slots (or bars), rotor bar depth, stator slot depth, number of rotor bars, and the number of stator slots were all used as design variables. Adjustments remain to be made, but this design seems to behave extremely well, outperforming the other evaluated designs.

A dimensioned sketch of the generator design shows some of the main features of the machine in Figure 3.2. The complete design specifications can be found in Appendix B. Again, this design is not ready for manufacture but evaluation suggests it has properties meriting further investigation.

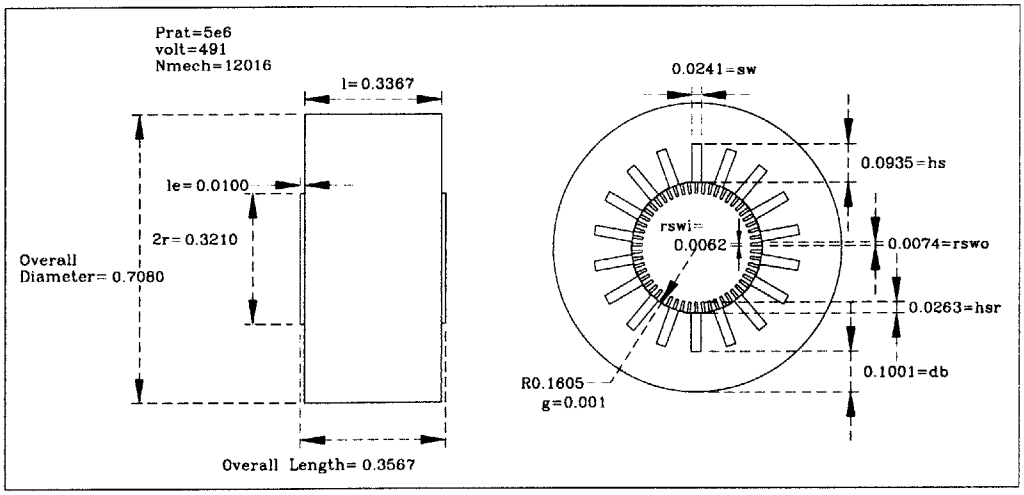


Figure 3.2: Dimensioned sketch of 5 MW generator design

## 3.4 Generator Performance

This design was selected because of the favorable, probably unrealistically optimistic, initial analysis.

| Initial Generator Performance Results | | | |
|---|---|---|---|
| | Full Load | 25% Load | 10% Load |
| Efficiency | 95.4 | 98.4 | 97.9 |
| Power Factor | 87.2 | 88.4 | 66.6 |

The equivalent circuit (Figure 2.2) parameters of the five MW machine are:

The full load per unit slip: $s \approx -0.011583$

$R_s = 0.74\ m\Omega$
$R_r = 11.33\ m\Omega$
$R_{core} = 160.4\ \Omega$
$X_s = 39.02\ m\Omega$
$X_r = 12.45\ m\Omega$
$X_m = 1.29\ \Omega$ (at full load)

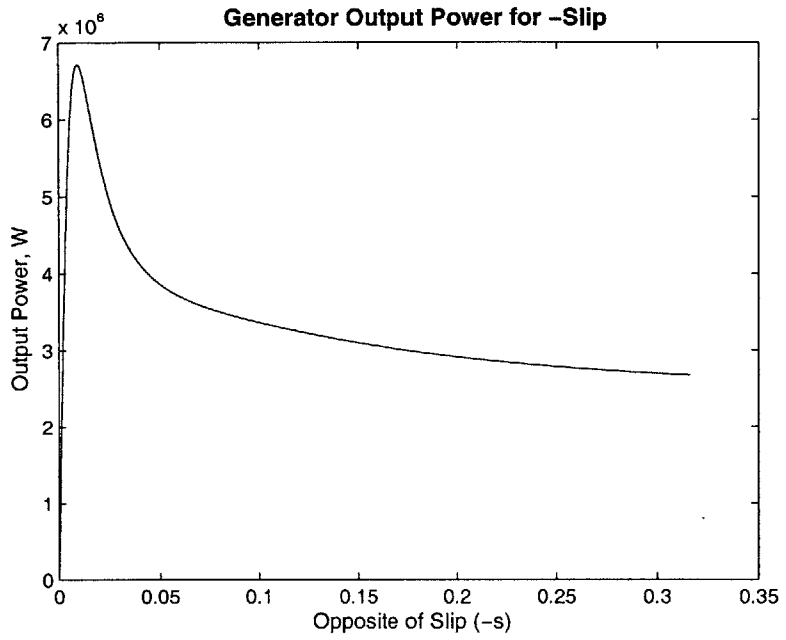


Figure 3.3: Change in generated power with machine slip for 5 MW design

A plot of the generator power output as the machine per unit slip varies is shown in Figure 3.3. The generator slip is negative, so the opposite of the slip is plotted to make the graph more readable.

## 3.5 Design Improvements

The Matlab random number generator used with the design program is not completely random in that consecutive trials give repeated results. The only way to obtain new designs is to change which parameters are variables, change the values of the parameters' mean or standard deviation, or increase the number of iterations. After searching for any remaining bugs or adjustments that can be made to the program, the attributes from the initial design can be used as center points for additional random searches with smaller variations to attempt to further optimize the design.

Additionally, the majority of machine characteristics have not been fully evaluated. The impact of different rotor bar geometries, rotor skew, and stator winding arrangements could also be investigated. It would also be extremely interesting to design a six or more phase

stator, potentially improving the quality of DC output at the cost of additional converter components.

With a working induction generator design, the general requirements of the controlled power converter are known and specific component values can be determined. The next chapter examines a variety of possible methods to provide the generator with varying reactive power and maintain a constant DC voltage as the power demand changes.

*Chapter 4*

# *VAR Support Schemes*

Robust, low cost, low maintenance induction generators are attractive for off grid applications and can operate in the self excited mode using only the input mechanical power from the rotating prime mover and a source of reactive power. This reactive power can be supplied by a variety of methods, from simple capacitors to complex power conversion systems. This section briefly introduces the main induction generator control issues and covers the wide variety of possible excitation and control methods for stand-alone, self excited induction generators. After examining the general purpose of each scheme, possible advantages, disadvantages, and issues to consider for each strategy are discussed. It should be stressed that all of these methods can operate in stand alone systems, where a fixed grid reference voltage or frequency is not required. Each scheme is evaluated for use with a 12,000 RPM, 5 MVA induction generator to supply a 700 V DC bus. Selected references are also given for each excitation method.

## 4.1 Induction Generator Control

In an attempt to better understand how to control induction generators, it helps to start with a brief look at the more common induction motor. Induction motors are inductive loads that operate at a poor power factor unless capacitors or another source of leading reactive power is connected to the motor input. The machine inductive windings require this "supply of reactive power" for the motor to run. In addition to the real power that is burned up as loss inside of the machine, reactive power, with a current waveform 90° behind the voltage, oscillates in and out to energize each phase, drawing VARs from the capacitors or connected power system. Similarly, an induction generator will not operate without sufficient capacitance to maintain the voltage and flux within the machine by "sloshing" power in and out of each phase.

Reactive power can be a confusing topic, but examining the basic behavior of inductors and capacitors helps explain some of the requirements for induction generator control. Inductors resist change in current according to the equation for voltage across an inductor, $V = L\frac{di}{dt}$. When the voltage across an inductor changes suddenly, the current through the inductor is slower to respond, and the current waveform lags the voltage. More specifically, a changing

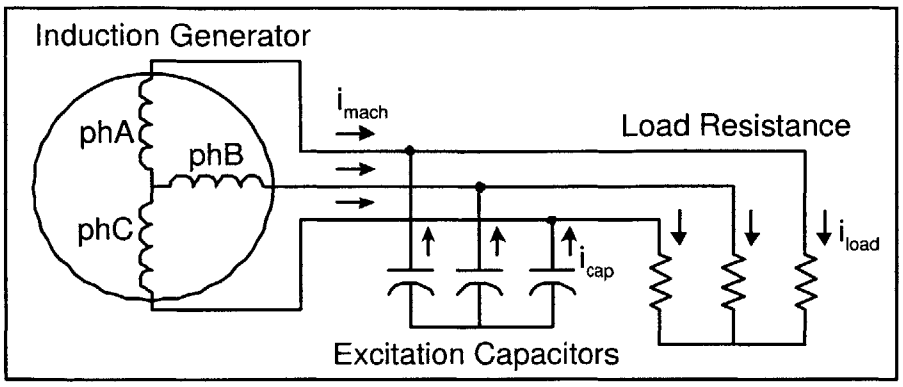


Figure 4.1: Currents of basic capacitor excited induction generator system

current in a coil generates a magnetic field through the coil. The changing magnetic field through the coil induces a second voltage across the coil that opposes the original change in current, delaying the change in current after an outside change in voltage.

Capacitors, on the other hand, try to maintain a constant voltage. The current through a capacitor can change immediately, but the voltage will be delayed according to $i = C\frac{dv}{dt}$ with the current waveform leading the voltage wave form. Conceptually, with stored charge on opposite plates of the capacitor, if the current suddenly reverses direction, the voltage across the plates will gradually decrease as the built up charge is bled off. In a system including either capacitors or inductors, the power will be distorted away from unity power factor, and the voltage and current will be out of phase. However, with ideally balanced inductive and capacitive elements, the current contributions 90° ahead and behind the voltage add to zero, leaving only the unity power factor real power with voltage and current exactly in phase. One of the challenges in induction generator control is to maintain the balance between the inductive and capacitive elements, in effect "supplying reactive power" to keep the machine energized.

The impact of the inductive and capacitive elements can be observed by looking at different currents within the system with respect to the stator terminal voltage. Measured data from a grid connected generator test analogous to the generator system of Figure 4.1 is used to produce the currents displayed in Figure 4.2. The stator voltage at one-tenth scale is included in each plot for reference. The multiple current waveforms in each plot show the change in each particular current as the input drive speed and the output power increase.

Current out of the inductive windings at the machine terminals, in the upper plot, lags the voltage by a variable amount depending on the machine equivalent inductance and the load. The capacitor current in the middle plot leads the voltage by 90°. The final load current of the bottom plot is in phase with the voltage, for the unity power factor resistive load.

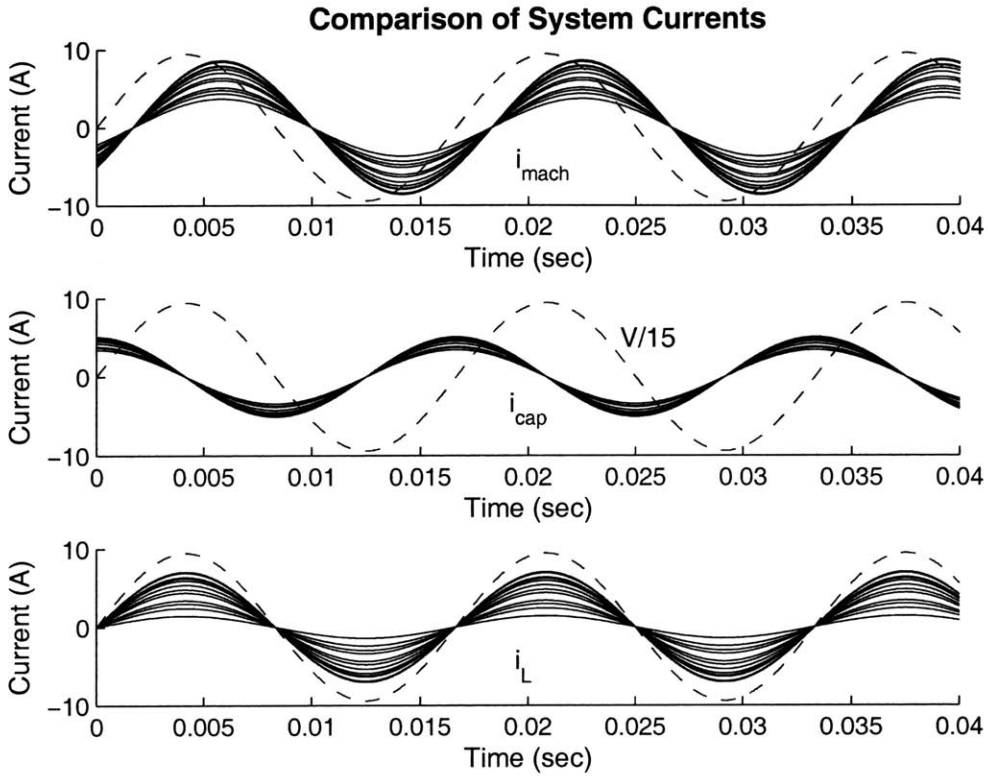


Figure 4.2: System current comparison with voltage reference

The sum of the load and capacitor currents in the lower two plots equals the total machine terminal current in the upper plot.

Notice how the capacitor current varies over a narrower range of values. Under constant voltage operation, the machine operates under nearly constant flux, with the magnetizing current and inductance roughly constant. A relatively large initial capacitance is required to cancel out the reactive power of the mutual inductance, but the smaller change in reactive capacitor current is caused by increasing currents through the leakage reactances. As the output power increases, the rotor and stator currents rise, increasing the reactive power $I_s^2 X_s$ and $I_r^2 X_r$ in the stator and rotor leakage reactances. The initial no load power factor is poor as the excitation capacitance must cancel out the mutual reactance, but the power factor measured at the machine terminals improves with increasing load as the real output power increases much faster than the increasing reactive power from the leakage terms.

In addition to the individual inductances from the rotor and stator sets of conducting coils, induction machines also include an equivalent mutual inductance, or magnetizing inductance, resulting from interaction between the rotor and stator sets of coils. Changing currents in the stator or rotor coils generate changing magnetic fields that induce voltages on the opposite coil. From a design standpoint, the mutual inductance depends on electrical and mechanical characteristics of the machine including the air gap width, winding scheme, slot geometry, characteristics of the iron laminations, and machine dimensions. In terms of operation, the mutual inductance is a nonlinear function varying with the machine output frequency, voltage, and current. As shown in Figure 2.6, the mutual inductance increases roughly linearly up to a point before gradually peaking and decreasing after the machine paths become saturated with magnetic flux.

To fully control an induction generator, an equivalent variable capacitance must be provided to match the machine's changing inductance, providing the reactive power required to keep the machine energized. Both the real power output and the reactive power input to the generator must be simultaneously managed, in this case to supply the fixed 700 V DC bus with the variable load up to 5 MW. The machine drive speed, electrical output frequency, and supplied capacitance are the available control parameters that can be manipulated to provide this control. A wide variety of strategies can be used to control the capacitance applied at the machine terminals.

## 4.2 Capacitor Schemes

First of all, a single capacitor or bank of capacitors in parallel with the generator output terminals is the simplest means of self-excitation. There are hundreds of published papers examining the capacitance requirements and performance of self-excited induction machines.

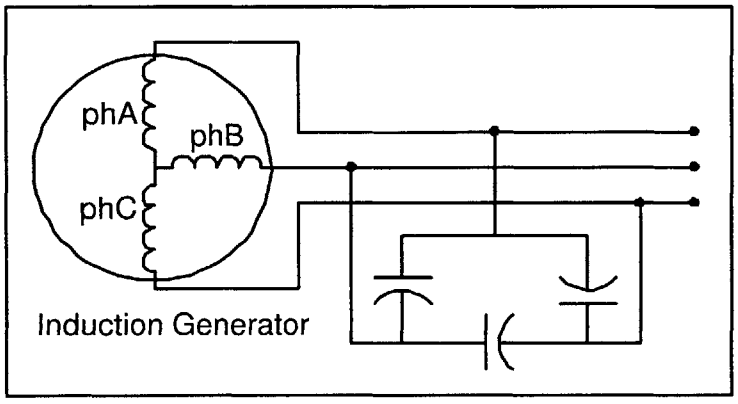


Figure 4.3: Capacitor excited induction generator

Most of these use the basic model of a single parallel capacitor for each phase of the machine as shown in Figure 4.3. The parallel capacitance requirements for voltage buildup over the full range of loads are given by Seyoum, Grantham, and Rahman [18]. Wang and Su present the dynamic response of an isolated induction generator to changes in load and excitation capacitance [26].

The excitation capacitance serves a dual purpose for stand alone induction generators: first ringing with the machine inductance in a negatively damped, resonant circuit to build up the terminal voltage from zero using only the remanent magnetism of the machine, and then correcting the power factor of the machine by "supplying" the generator with reactive power. An example of the exponential voltage buildup is shown in Figure 4.5. During the voltage build up, the machine and capacitors act as a negatively damped RLC circuit, similar to Figure 4.4. The machine has a variable equivalent inductance and variable negative equivalent resistance in series with the excitation capacitor. After the machine starts to saturate, the equivalent inductance drops, a stable voltage is reached, and the capacitor corrects the output power factor. For grid connected generators, the capacitors can still provide power factor correction, but VARs can also be drawn from the grid. The voltage is also supplied by the grid and need not build up. Current still oscillates between the machine inductance and excitation capacitor or other source of leading current, but with the grid connection, that source can be down the street or miles away.

The voltage would continue to grow as shown in Figure 4.5 until something melts or explodes except that the machine starts to saturate. The magnetic flux approaches a maximum and any increase in magnetic field only generates more loss and heat in the machine. Once the increasing losses are large enough to cancel out the negative rotor resistance, the circuit stabilizes at a particular voltage. The equivalent inductance of the machine also reaches a

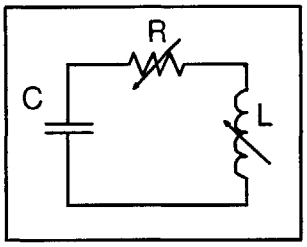


Figure 4.4: Series RLC circuit

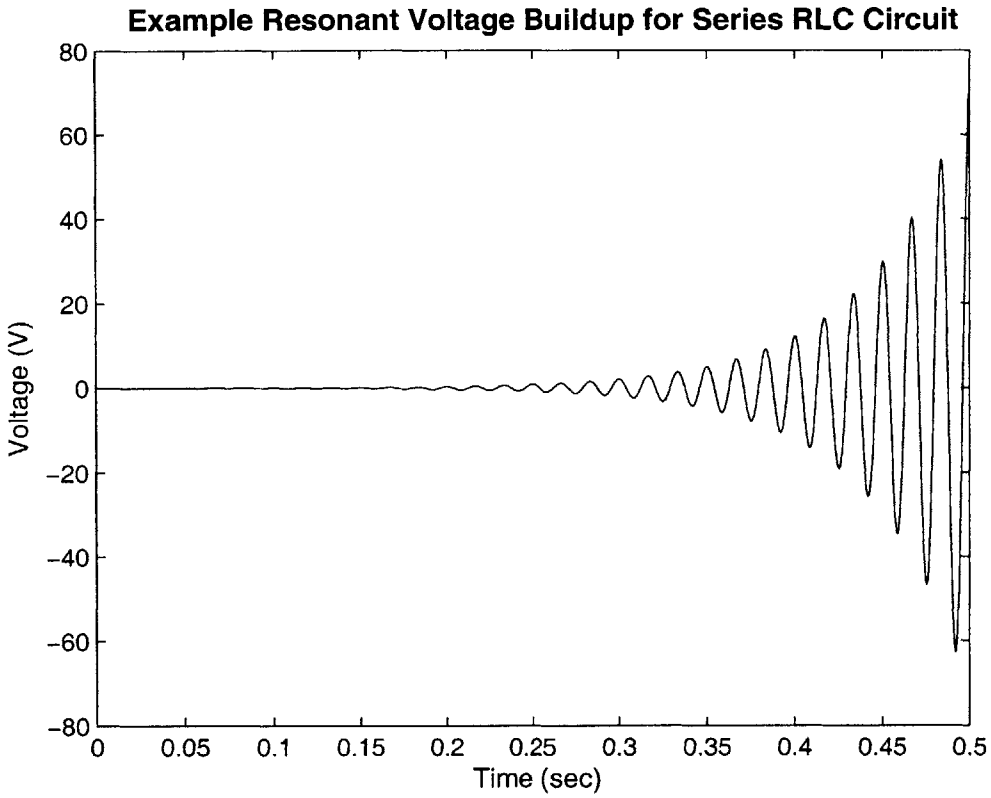


Figure 4.5: Voltage buildup in an RLC circuit with R=-2.5 $\Omega$, C=100 $\mu$F, and L=70.36 mH

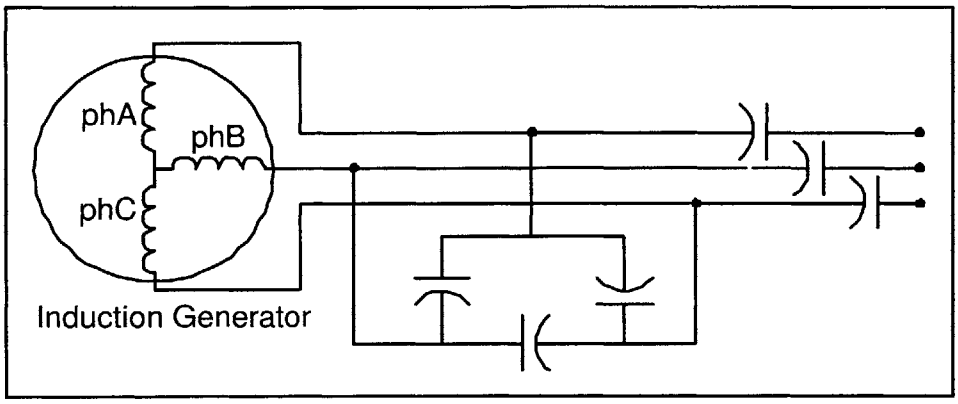


Figure 4.6: Series capacitor excited induction generator

peak and then declines as the machine saturates, so the equilibrium voltage depends on that inductance as well as the excitation capacitance, electrical frequency, and mechanical drive speed (together with the electrical frequency sets the slip and negative rotor resistance).

The single capacitor is ideal to provide the reactive power required for self-excitation when the generator supplies a constant AC load and is driven at a fixed mechanical shaft speed. Also, the single capacitor bank is the best choice when supplying a load insensitive to variations in voltage and frequency. Without any additional components (active or passive) and no required controls, only the capacitor is needed for this simple case. However, any changes in load or rotor speed will result in fluctuating output voltage and frequency unless a more elaborate excitation and control strategy is used [24]. For the 5 MW generator, additional electronics will be required for the AC to DC conversion as well as to insure a stable voltage over the entire load range.

### 4.2.1 Series Capacitor

A slightly more complex variation includes an additional series capacitor on the machine output, as in Figure 4.6. This added series capacitor helps maintain the output voltage for variations in load, but causes significant voltage droop at low loads when using large series capacitors and may interact with inductive or dynamic loads as shown in [16]. For frequency regulation, the readings suggest that the series capacitor helps to maintain output frequency with varying rotor speed to a limited extent. For a 5 MVA system, the significant cost and weight of the additional capacitor, combined with the inherent voltage regulation from the power conversion process, will make the series capacitor unnecessary.

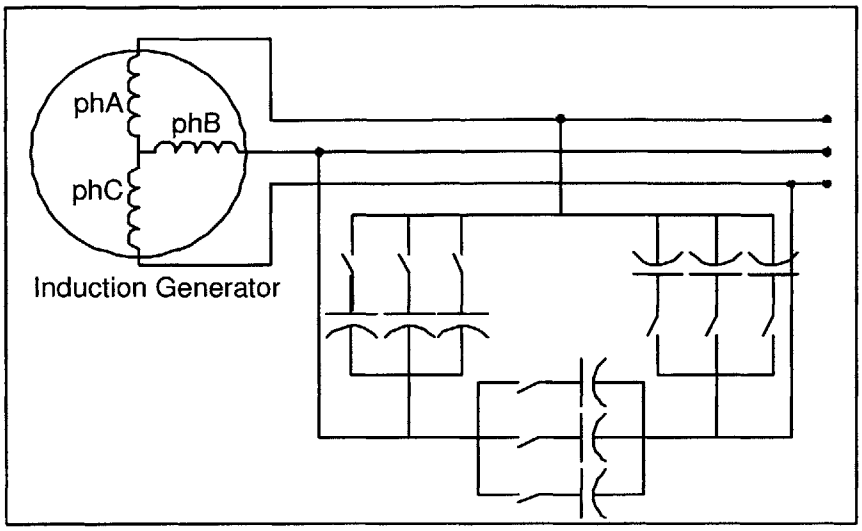


Figure 4.7: Switched capacitors

### 4.2.2 Switched Capacitors

There are a variety of ways to vary the amount of capacitance connected to the generator output. First, discrete blocks of capacitance can be added or removed in different combinations using contactors while voltage sensors monitor when the output voltage exceeds preset limits. The number of switching steps would be determined by the allowable ripple in voltage output, but nine different capacitors were required to maintain a 10% variation in voltage on a three-phase 415 V, 3.7 kW squirrel cage induction machine in [22]. The number of capacitors and contactors needed, in addition to the switching noise, are serious drawbacks to this strategy.

Similarly, IGBTs, GTOs, or other modified thyristor in series with each of the capacitors can be actively switched on and off to vary the total system capacitance. These solid state switches allow for much faster response times than the relays, reducing losses and transients provided that the switches are turned on at peak voltage with negligible current [8]. These schemes still require multiple capacitors per phase, at least one switch per capacitor, and coordinated controls. As before, the number of steps can quickly become unreasonable for stringent output voltage requirements, and there is an inefficient use of the total available capacitance unless running at full load.

An interesting possible alternative uses an adjustable, "controlled" capacitor. This scheme includes switches now in parallel with three wye or delta connected capacitors (Figure 4.8) so that the apparent capacitance seen by the generator can be varied with control of the

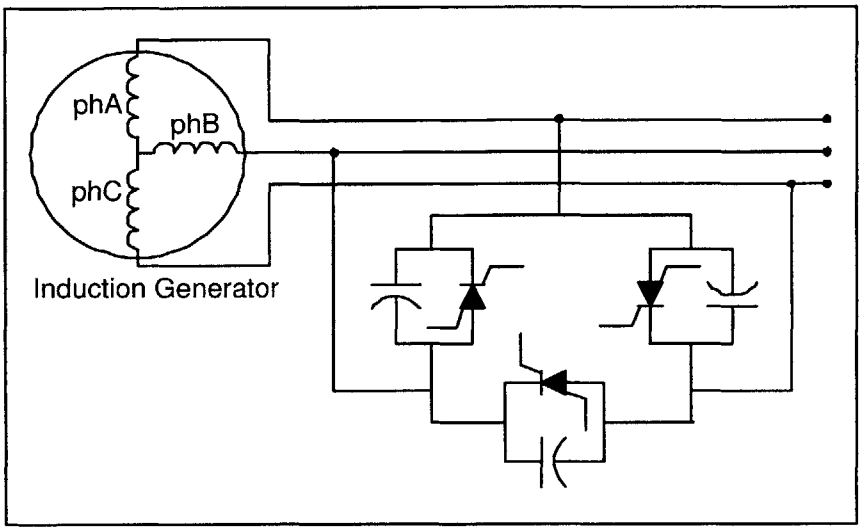


Figure 4.8: Controlled capacitors

switches [2]. Theoretically, the apparent capacitance can be varied from a minimum value of the actual capacitance, when the switches are kept open, up to infinite capacitance with the switches shorted. This strategy will also require careful control of the switches to achieve zero current switching, and the apparent capacitance values will be limited by the frequency in activating the switches only at half-cycle intervals. With sufficiently large AC capacitors rated to withstand the large voltage changes when switching and suitably robust switches, only three capacitors of reduced size would be required to excite the generator. Though a potentially attractive excitation scheme, the generator output will still have to be converted to DC. Unless the capacitor savings overcome the cost of the additional switches and control complexity, combined excitation and power rectification in a single step is preferred.

## 4.3 Inductor Schemes

Another major category of excitation methods involves connecting sufficient capacitance to maintain output voltage at full load and then varying inductive elements to counteract part of the capacitance as necessary for lighter loads or higher speeds. All of these methods have the inherent disadvantage of the added inductor. The simplest case involves a saturable reactor in series with the capacitor at the generator output as shown in Figure 4.9. An inductor built as a wound core with a stepped or sloped air gap gradually saturates as the current increases, decreasing the inductance value with load, and increasing the equivalent

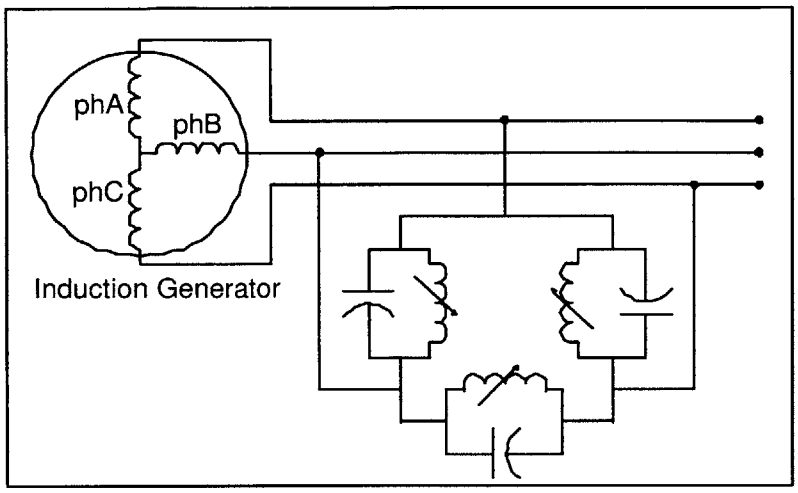


Figure 4.9: Saturable inductors

capacitance per phase [29]. This simple scheme requires no switches or controls, but full load capacitance is still required, and the custom reactor adds design complexity and expense. The AC output from this scheme would also still require rectification.

### 4.3.1 Thyristor Controlled Reactor

A thyristor controlled reactor (or thyristor controlled inductor) is another solution that can offer continuous or nearly continuous variation in reactive power with fewer capacitors and switches than the switched capacitor scheme. The more general term "static VAR compensator," or SVC, is often used to refer specifically to the thyristor controlled reactor [15]. Gyugyi gives a solid overview of the full range of static VAR compensators, including the thyristor-controlled inductor [9]. Shown in Figure 4.10 and analogous to the switched capacitor, the maximum capacitance to supply full load VARs is connected to each phase of the machine, and a series inductor and thyristor switch are connected in parallel to the excitation capacitance. Controlling the switches, naturally commutated for zero current switching, allows for adjusting the inductor current to balance the total reactive power in the system [5]. Sufficient capacitance must be connected to the machine terminals to supply the maximum VARs at full load. At any other load, the switches in series with the inductors on each phase of the machine output are fired at a variable delay angle to increase the fundamental inductor current, feeding lagging VARs to the generator, and reducing the effective capacitance seen by the machine. Figure 4.11 illustrates an arbitrary voltage and decreasing inductive current as the phase angle increases. For a phase delay greater than a

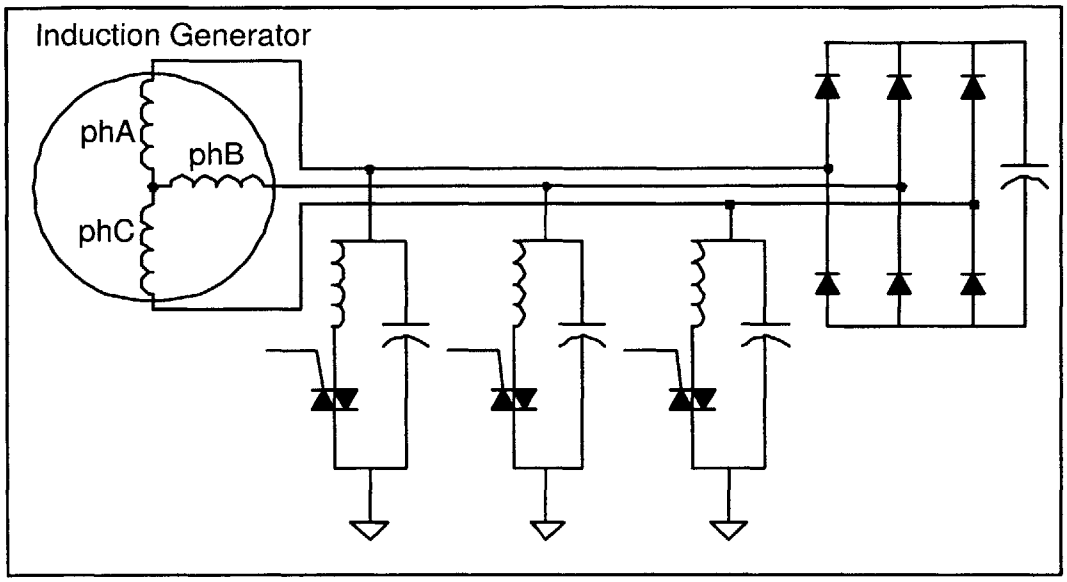


Figure 4.10: Thyristor-switched reactor circuit schematic

quarter of a cycle, the inductor is completely removed from the circuit.

The naturally commutated, zero current switching thyristor is controlled so that the inductor is completely removed from the circuit at full load when the full capacitance is needed. The inductor is gradually switched in at decreasing phase delays to increase the current through the inductor as the load decreases. As the current in the inductor increases, the parallel L-C combination results in a smaller equivalent capacitance to reduce the supplied VARs at lower loads. At no load there is zero switching delay. The thyristor acts as a short circuit, and the inductor must be sized correctly so that the parallel combination of the capacitor and full inductance gives the equivalent no load capacitance to maintain excitation at the desired frequency.

The 400 Hz frequency of the 5 MW machine will help reduce the size of the inductors and capacitors of any VAR support scheme. The advantages of the thyristor-controlled reactor include relatively simple operation and controls, at the cost of capacitance equivalent to maximum VARs on each phase as well as the weight and expense of the three large inductors. Again, an additional rectifier will also be required for the DC output voltage.

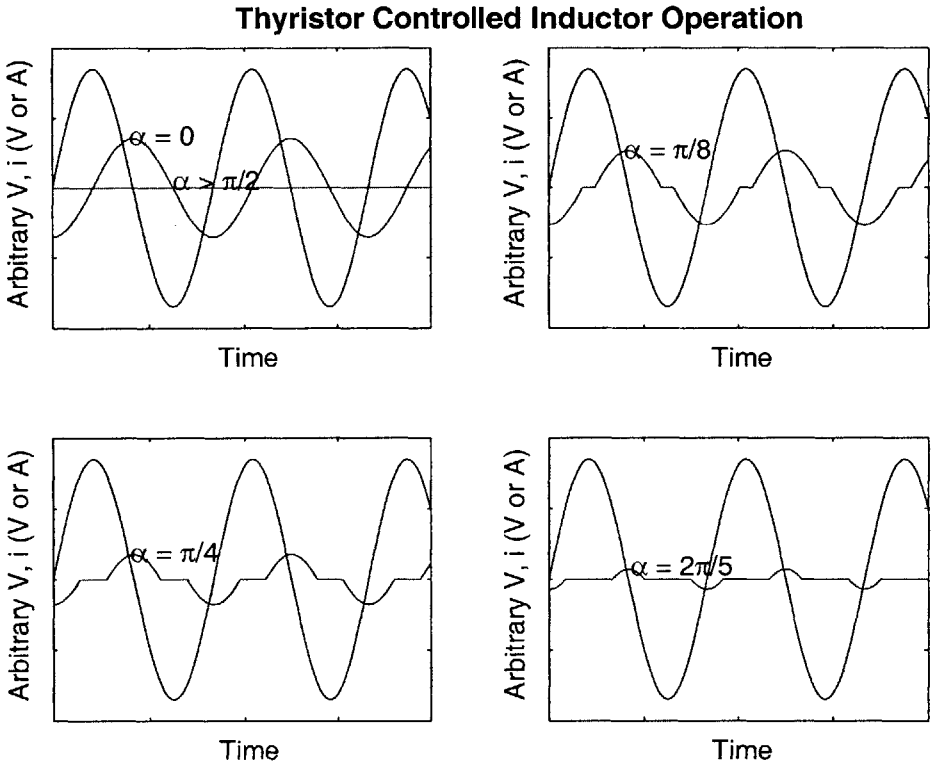


Figure 4.11: Thyristor-switched reactor voltage and currents with increasing delay angle

## 4.4 Force Commutated Rectifiers

Uncontrolled diode rectifiers are the simplest and least expensive power rectifier, but they are only capable of delivering power in one direction. An additional source of reactive power is required. A promising controlled rectifier scheme is the force commutated rectifier. This is the first solution that offers both VAR support and rectification in a single step. The force commutated rectifier will be set up similarly to the three phase diode bridge but with controlled switches as in Figure 4.12. To avoid using extra commutation circuits, the switches should be fully controllable for both turn on and turn off and must be able to block both forward and reverse voltages. Gate-Turn-Off thyristors, "GTOs," or symmetrical, "non-punch-through," IGBTs would work for this application. The switches are fired early compared to the diode rectifier, resulting in the fundamental sine wave of the rectifier input current leading the voltage. Figure 4.13 illustrates an arbitrary phase A voltage and the voltage output from both an uncontrolled diode rectifier ($\alpha = 0$) and a force commutated rectifier. The fundamental of the quasi-square wave current of phase A resulting from the controlled rectifier with firing delay can be seen to lead the phase A voltage. Watanabe and Barreto use this operation of force commutated rectifiers to excite an induction generator [27]. At the expense of increased harmonics and a reduced voltage, reduced current, and reduced power output compared to the diode rectifier, the controlled rectifier can be a variable capacitive load to help excite the induction generator. Figure 4.13 shows a phase angle delay of roughly $\alpha = 0.09\pi$ or 0.283 radians or about 0.75 ms for the 60 Hz waves. The output voltage decreases quickly when $\alpha > \frac{\pi}{6}$ with the switches firing before the peak voltage is reached. As the voltage and current are reduced by a factor of $\cos\alpha$, the output power decreases as $\cos^2\alpha$, limiting the useful range of the controlled rectifier. The induction machine requires more Q at higher outputs, so as $\alpha$ increases, the machine terminal voltage must increase to maintain a constant DC voltage. This strategy will not provide enough reactive power to maintain excitation of the generator under the full range of load but could be used to support another controller.

## 4.5 Power Converters

Finally, the most elaborate excitation schemes involve power electronic converters to sink or source the required reactive power to excite the generator and maintain voltage and frequency for a range of load and speed. The converters are typically used in addition to parallel excitation capacitance, but the converter can significantly reduce or eliminate the AC excitation capacitance given sufficient DC capacitance, switch ratings, and an initial source of voltage.

Historically, utility scale VAR supplies of this type were known as static condensers [7], or

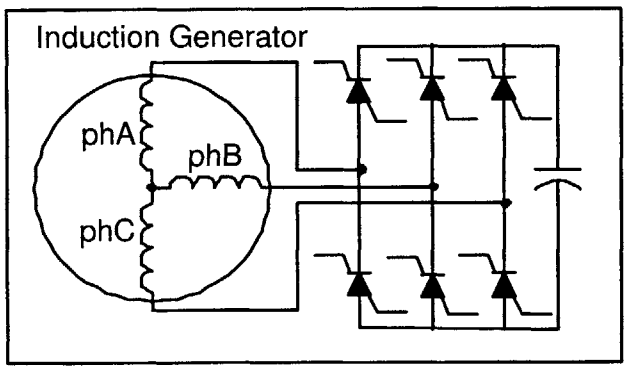


Figure 4.12: Force commutated rectifier circuit schematic

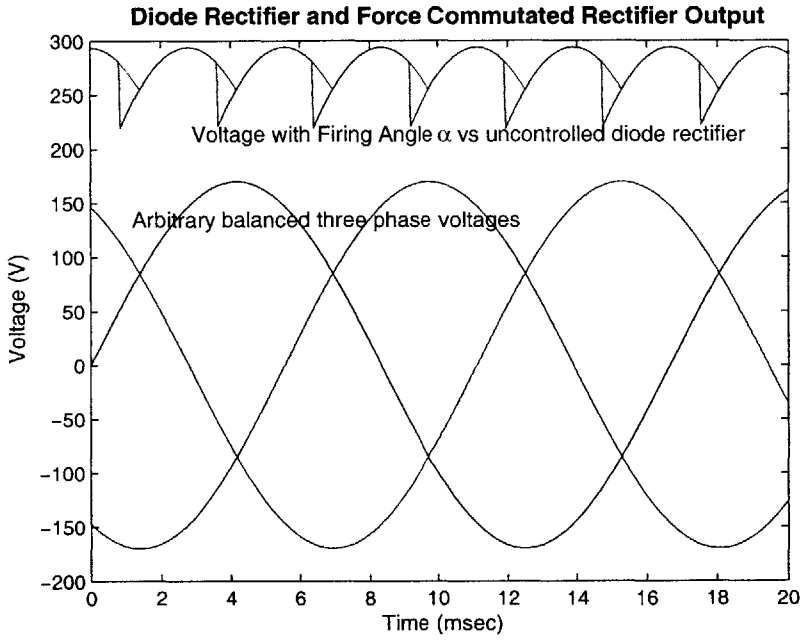


Figure 4.13: Force commutated rectifier output waveforms

"STATCONs", as opposed to synchronous condensers, which are overexcited, unloaded synchronous motors that supply varying reactive power by controlling the applied DC voltage and field. Currently, IEEE designates these static VAR compensators as "STATCOMs." Without the inertia of synchronous condensers, STATCOMs offer faster reaction times and are typically constructed with multi-level topologies to reduce harmonics and switching stresses. Grid connected STATCOMs can take advantage of the voltage reference provided by the power grid to vary the real and reactive power by controlling the magnitude and phase of the converter voltage [15]. The solid state switches can synthesize voltages above or below the grid reference or can generate a current waveform with a fundamental component leading or lagging the grid voltage. This strategy is unavailable in stand alone operation, where the converter is the only connection to the machine terminals. On the other hand, grid connected generators also have their output frequency fixed at the grid frequency. In this case, the only way to increase the machine slip and power output is to increase the drive speed. Stand-alone inverters can use the output frequency as a control variable.

The voltage source inverter (or current source rectifier) with a single DC capacitor voltage source, optional capacitor bank at the machine terminals, and internal machine inductance acting as the current source as shown in Figure 4.15 seems to be the most widely used circuit [4];[21];[14]. Alternatively, the voltage source rectifier/current source inverter topology, as in Figure 4.14, with AC capacitors and an inductor on the rectifier output, can also be used. The voltage source inverter/current source rectifier appears superior in this application for two reasons. First, depending on the switching scheme, the reverse diodes can be used for circulating reactive current and for switching transitions. Also, the fixed voltage DC bus requires a constant voltage output with variable load, similar to the voltage source setup. Though requiring active switches, filtering inductors and capacitors, and elaborate controls, these schemes offer the most flexible operation for supplying both the reactive power required by the induction generator and the varied load of the DC system.

Most converters use Pulse Width Modulation (PWM) control schemes to increase harmonic frequencies, shrinking filtering components. For PWM operation, the switching frequency should be greater than about ten times the stator output frequency. For 60 Hz grid connected machines this would be less of an issue, but for this higher speed, 400 Hz machine, 4 kHz at megawatt power levels approaches the upper limits for ratings of commercially available switches. In practice, multi-level topologies reduce the switching currents and also eliminate selected harmonics. This could be the most practical control strategy. Still, with PWM, switching losses increase, driver complexity increases, the output voltage drops, and the benefit in reduced passive component sizes is reduced at the 400 Hz frequency. These drawbacks, in addition to the aid in understanding inverter operation, seem to favor the simpler six step switching strategy for this initial investigation.

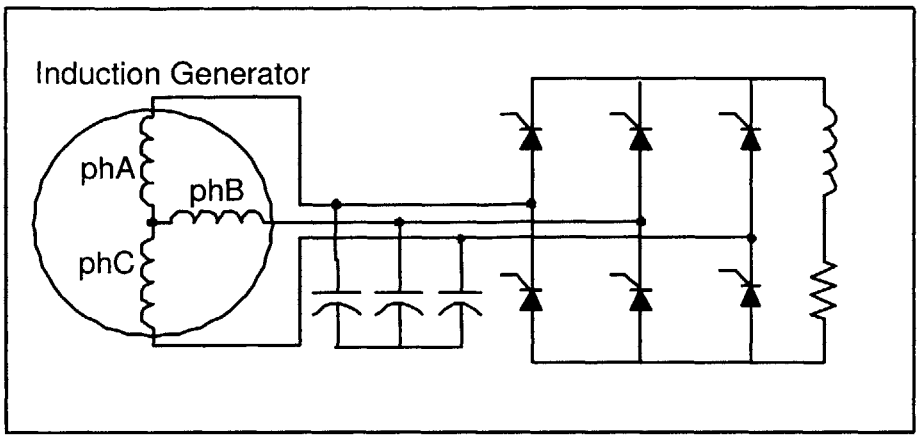


Figure 4.14: Current source rectifier/voltage source inverter circuit schematic

## 4.6 Six Step Converter

A six step inverter could be used either for single stage AC to DC rectification with simultaneous VAR support or purely as a reactive power supply with a diode rectifier or other converter managing the real power rectification. For the simpler case of a single stage handling both real and reactive power, a three phase bridge of six switches in antiparallel with diodes is connected between the machine terminals on the AC side and a single DC capacitor on the DC side as shown in Figure 4.15.

Initial excitation could be slightly more complicated with this strategy. If the single DC capacitor is not large enough or does not have a great enough initial charge to allow the generator voltage to build up with a reasonable drive speed, a battery on the DC side or a bank of AC capacitors could be added. The power factor measured at the stator output terminals will always decreases as the load decreases. The AC capacitors will also decrease the switching current by supplying much of the no load VARs at the machine terminals. Ideally, slightly less AC capacitance would be connected than is necessary to excite the generator at operating speeds. That way, the DC capacitance can aid in the excitation process and maintain control of the frequency from the start instead of synchronizing to an existing stator frequency. The switches are MOSFETs for the 2 kW prototype and could be the latest generation of thyristor hybrid with turn off control for the 5 MW design. A variety of switching schemes can be used to generate the three stepped-voltage waveforms with sine wave fundamental components, each 120° out of phase with the other two.

In the previous schemes, separate capacitors on each phase continually charged and discharged, sloshing back and forth all of the reactive power required by each single phase.

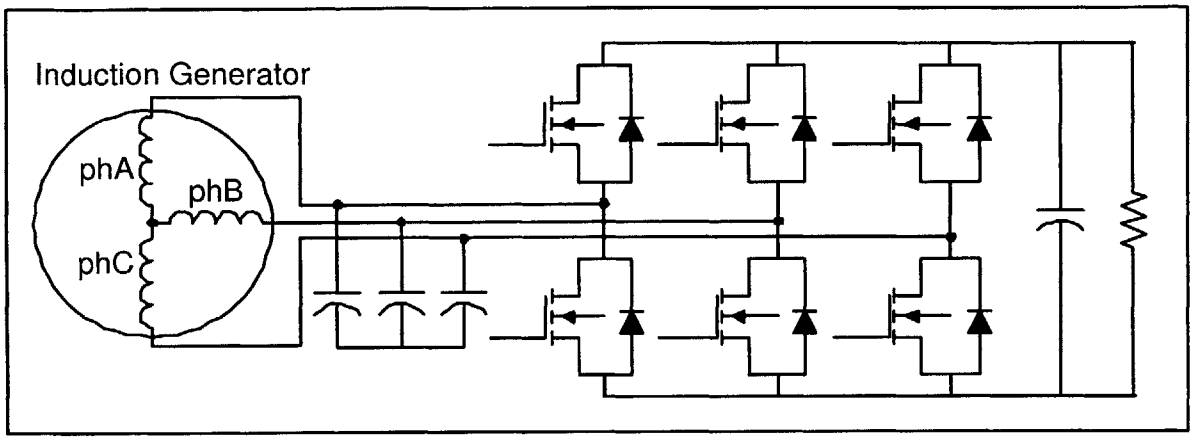


Figure 4.15: Six step converter circuit schematic

With the six step inverter, a single DC capacitor can supply power to one phase while charging from another, or current can flow directly from phase to phase. In a balanced three phase set, the instantaneous sum of the power from all three phases is always zero. Novotny, Gritter, and Studtman explain that by circulating power correctly among the three phases, individual energy storage for each phase is unnecessary [17]. In fact, currents can be circulated among the three phases of the machine, and capacitance for energy storage and VAR supply is unnecessary. The converter switches must be rated to withstand the additional current from the circulating reactive power that would not be present if variable capacitors or alternative AC VAR supply corrected the power factor before the generator output was delivered to the rectifier. The DC capacitor could be sized to handle any transient power changes and to minimize output voltage ripple.

Additionally, the DC voltage, using the peak machine line to line voltage, approaches 2.45 times the RMS phase voltage of the 3 individual phase AC capacitors. With capacitor energy storage a function of the voltage squared, the single higher voltage DC capacitor can store nearly six times the energy of each AC capacitor. Furthermore, DC electrolytic capacitors are available at significantly higher (20+ times) the rated capacitance at an equally small fraction of the cost, size, and weight of AC capacitors. Figure 4.16 illustrates the difference between a 80 $\mu$F, 270 V AC capacitor and a 1200 $\mu$F, 400 V DC electrolytic capacitor used with the 2 kW converter.


Figure 4.16: Comparison of 80 $\mu$F, 270 V AC and 1200 $\mu$F, 400 V DC capacitors

### 4.6.1 Converter Reactive Power Circulation

There appears to be a number of options for reactive power compensation using a six step inverter. First, the single DC capacitor can supply the reactive power for all three phases of the machine, charging from one phase before discharging to another. Voltage ripple in the DC capacitor could be a significant issue with this scheme. Alternatively, the converter can periodically short two alternating phases of the machine together, increasing voltage harmonics but circulating reactive power directly from phase to phase instead of between each phase and a capacitor. Additional AC capacitance on each phase or line to line can also be used with either of these strategies to aid in the initial voltage build up and to reduce the power flow through the inverter.

The addition of AC excitation capacitance will reduce the current circulating through the inverter, but as long as sufficient excitation is provided, will not impact the stator terminal current. Figure 4.2 illustrates generic stator terminal, capacitor, and resistive load currents for the capacitor excited case. Even though the delivered output power is unity power factor, the current out of the inductive machine must be lagging the voltage fundamental, with the difference supplied by the capacitor. Now, the difference can be supplied by a combination of AC capacitors, the single DC capacitor, and direct phase to phase currents.

## 4.7 Reactive Power Circulation

The idea of using a converter to circulate reactive power was developed in the seventies through several US patents including #3,829,758 and #4,006,398 by the Borg-Warner Corporation [17]. Novotny, Gritter, and Studtmann explain how "viewed as a whole, the air gap field is of constant amplitude and once established requires no net reactive power input." They built and tested a 1 HP induction generator controller that used the converter to transfer energy between the generator phases.

Operation here assumes that the DC output voltage is maintained roughly constant. Sufficient capacitance must be installed to limit the voltage ripple. If the converter acted merely as a diode converter, rectifying the generated real output power, there would still be voltage ripple, with no reactive power support from the DC capacitor. This results in the highest quality DC output voltage. If the DC capacitor is also used to sink/source reactive power with the three generator phases, the ripple on the DC output voltage will increase.

Additionally, the following analysis considers perfect sine wave currents. The actual machine currents will not be perfect sine waves, but should still be balanced with sinusoidal fundamental components. The magnitude and phase of the stator terminal current will depend on the load, varying from lagging the voltage by nearly 90° at no load up to a best case power factor in the range of 0.8 or 0.9, depending on the machine design. Assuming purely resistive loads and ignoring the AC excitation capacitance for now, the following plots show switched voltage waveforms and arbitrary stator current fundamental sine waves at varying power factors to illustrate the circulation of reactive power in the converter.

The power converter will operate as both an inverter, converting the DC bus voltage to AC while circulating reactive power, and as a rectifier transferring the real power from the machine to the DC loads. Looking at the converter as an inverter, a variety of different switching schemes can be used with a six step inverter to produce a sinusoidal fundamental from a DC voltage. Two different switching patterns, one with three switches conducting simultaneously that allows reactive power circulation and one two-switch scheme that does not, should demonstrate how the converter can satisfy the generator excitation requirements while maintaining a constant frequency and delivering a variable load.

The two switching patterns are shown in Figure 4.17. The conducting switches for each interval are shown along with the voltage waveforms. Depending on which switches conduct, a closed circuit is formed including the DC capacitor and different combinations of the machine phases. Both generate similar fundamental voltage sine waves. The magnitude of the three switch scheme is slightly higher, at $\frac{2}{\pi}V_{DC} \approx 0.637$, versus $\frac{\sqrt{3}}{\pi}V_{DC} \approx 0.551$ for the simpler two switch scheme. Figure 4.18 compares the switching waveforms along with the fundamental sine waves of the three and two switch patterns.

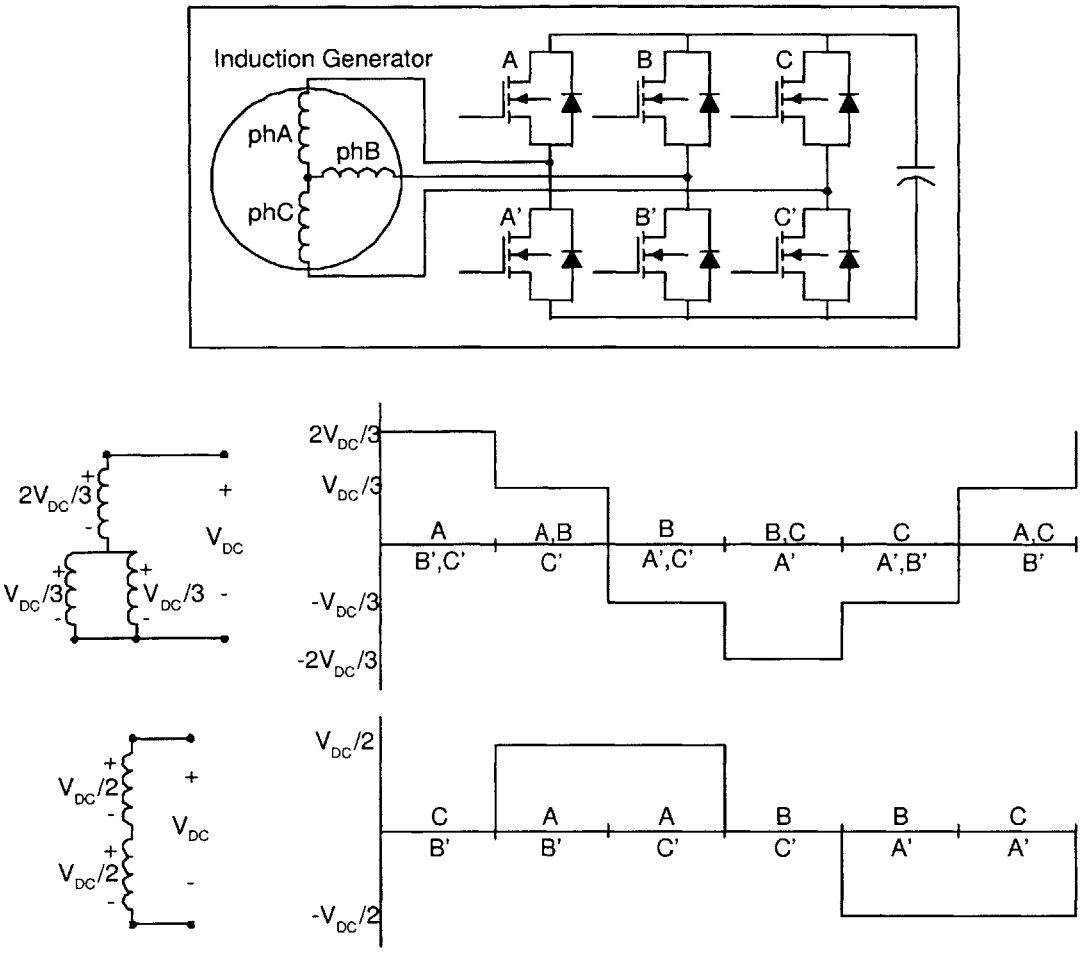


Figure 4.17: Comparison of two and three switch inverter patterns

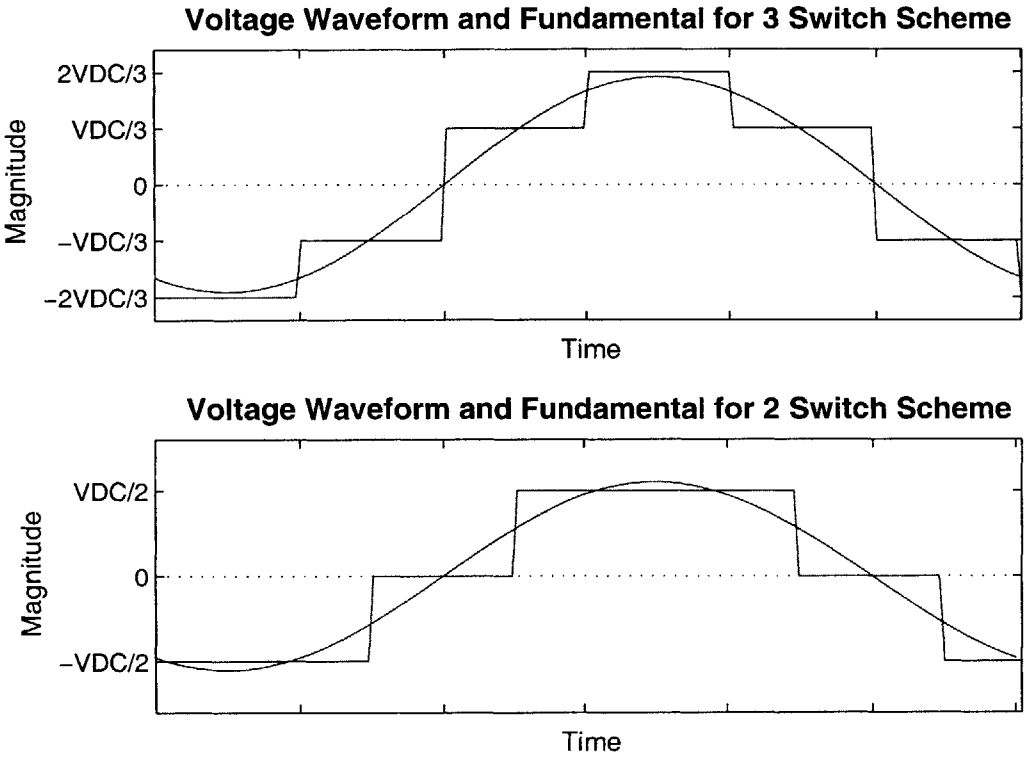


Figure 4.18: Comparison of voltage waveforms for the three and two switch patterns

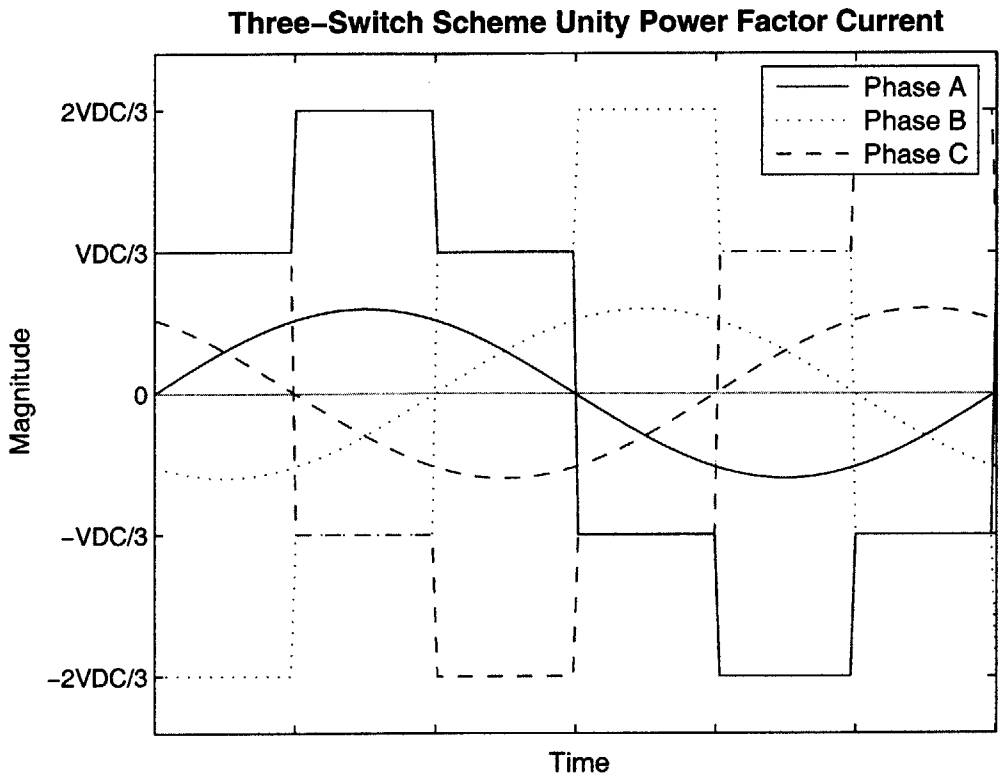


Figure 4.19: Stepped voltages and arbitrary unity power factor current for the three switch scheme

With three switches conducting at a time, two generator phases are shorted to the same voltage whenever two high side or two low side switches conduct simultaneously. During these switching intervals, a path exists for current to flow from one phase to the other. For comparison, the two switch scheme circulates reactive power among the three phases via the DC capacitor. The two switch scheme eliminates all danger of shoot-through currents. Now, each switch conducts for only one third of the cycle. The three switch scheme is examined in more detail first.

### 4.7.1 Three Switch Pattern

The six step converter switches the DC voltage source across the machine phases in patterns approximating ideal sinusoidal terminal voltages. In this manner, a charged DC capacitor

can place an AC voltage on all three phases of the machine, providing initial excitation to build up the fields within the machine. The three switch pattern connects the DC capacitor to all three machine phases as shown on the left side of Figure 4.17. At any time, either two low side switches or two high side switches conduct, shorting two phases together placing a voltage of $\frac{V_{DC}}{3}$ across both phases.

A current in phase with the voltage, though not possible with an induction machine, is shown in Figure 4.19. With the three switch pattern, current flows out of the single switch through the load and back to the machine through a changing combination of the other two switches. In this unity power factor case, there is no reactive power flow in the system. As the power factor decreases and the current lags the voltage by an increasing angle, increasing VARs circulate through the machine.

Figure 4.20 illustrates when these intervals occur for a variety of possible currents. The arrows highlight the sections when current, and reactive power, circulates between two of the phases. The duration increases as the power factor decreases and disappears altogether at unity power factor, when no VAR circulation is required. Arbitrary sine waves represent the fundamental components of the currents in each phase.

Taking positive current to be out of the machine terminals, at the beginning of each switching period there is a short interval where the currents of the two phases shorted together (the two phases with both high side or low side switches conducting simultaneously) are of opposite magnitude. In the unity power factor case, power flows out of the single switch, through the load, and back into the machine via the remaining pair of "same side (high or low)" switches. With a slightly lagging power factor, current still flows out of the single switch, but now, during a variable initial time period following a change in the state of the switches, current also flows from one of the shorted phases to the other.

Figures 4.20(d) illustrates the equal real and reactive power for the 0.5 power factor case. Past that, the real power decreases quickly to zero for 90° lagging current of Figure 4.21. The stator current will never reach this condition because of internal real power losses in the machine. However, at no load the current will approach this case (a small amount of real power must flow into the machine to account for the internal losses, but this power will be almost negligible compared to the reactive power excitation).

Figure 4.22 attempts to illustrate how the intervals of circulating current can act as capacitors, maintaining excitation of the generator. First, Figure 4.22(a) repeats the plot of the three switch voltage waveforms along with the fundamental sine components of arbitrary magnitude stator terminal currents that lag the voltage waveforms by 30°. The arrows show the segments where reactive power is circulating between two of the phases, through two conducting high side or low side switches. In the next subplot, Figure 4.22(b), the approximate fundamental sine wave of the reactive current flowing from phase C to phase B, the small triangular sections of the phase C current, is added as the dotted sine wave of smallest

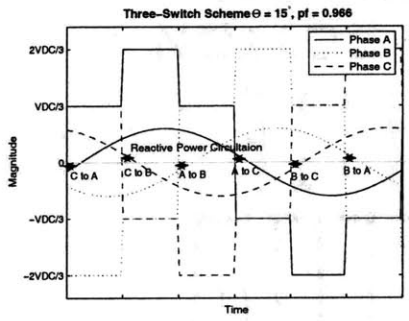


(a) $\theta = 15°$, Power Factor = 0.966

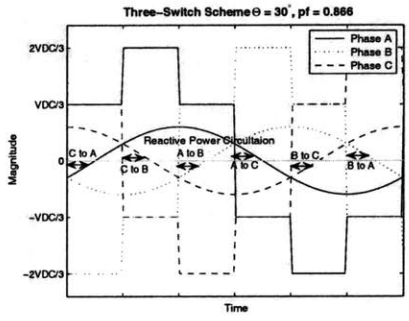


(b) $\theta = 30°$, Power Factor = 0.866

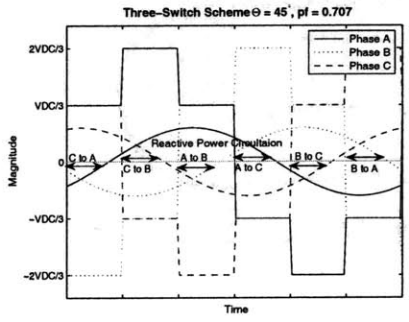


(c) $\theta = 45°$, Power Factor = 0.707

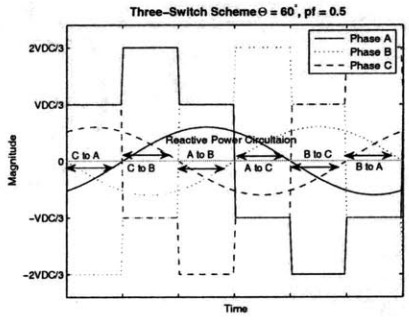


(d) $\theta = 60°$, Power Factor = 0.5

Figure 4.20: Increasing intervals of reactive power circulation for the three switch pattern with decreasing power factor

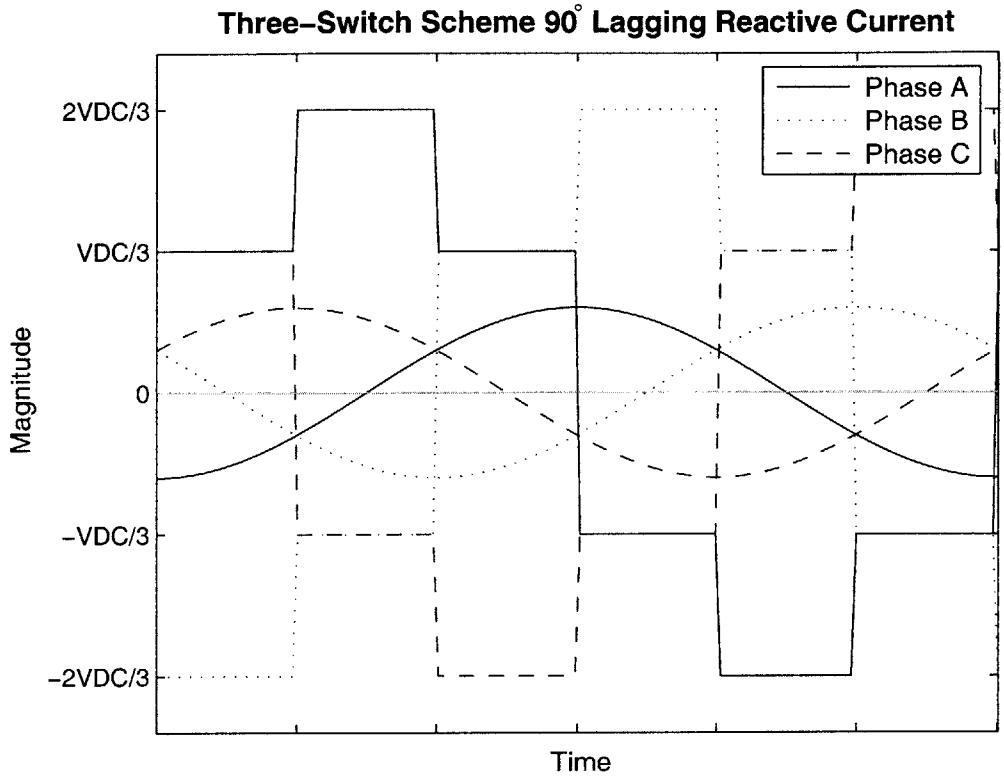


Figure 4.21: 90° lagging current with three switch scheme

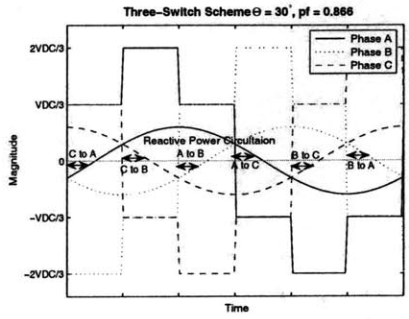


(a) $\theta = 30°$, Power Factor = 0.866

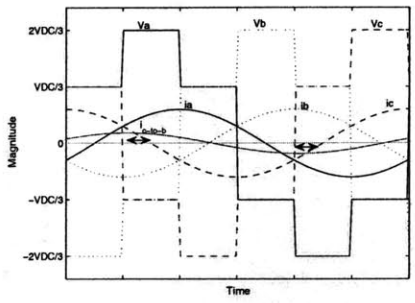


(b) Added rough sine fundamental C to B current

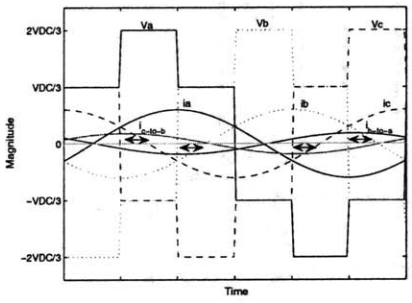


(c) Added rough sine fundamental B to A current

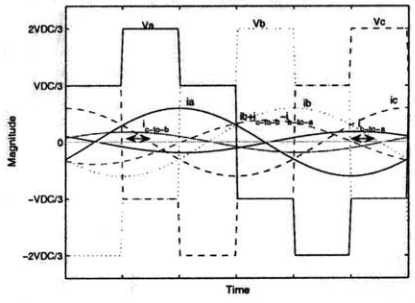


(d) Added sum Ib+Icb-Iba

Figure 4.22: Attempt to illustrate reactive power circulation by adding the fundamental of the reactive power segments to phase B current

amplitude. The peaks of this current are centered around the two reactive power regions, highlighted by the double sided arrows. This current flows through the short circuit of the two low side switches, B and C, while phase A is maximum at $2V_{DC}/3$.

The repeated triangular pattern of the reactive power sections form nearly an odd function. Approximating the reactive power currents as an odd function yields accurate enough results to demonstrate the converter operation. The magnitude of the fundamental of the Fourier sine series is calculated to be about 0.1629 and 0.3045 for $\theta = \frac{\pi}{12}$ and $\theta = \frac{\pi}{6}$. This fundamental sine wave will be of similar frequency to the original currents, with peaks centered over the larger ends of the reactive current segments.

Figure 4.22(c) includes another identical sine wave fundamental current, this time for reactive power flow from phase B to phase A. Finally, the last subplot, Figure 4.22(d), includes the addition of the sum of the phase B current with the C to B current and the opposite of the B to A current as the new dashed wave. Comparing the peak and zero crossings, this new total current is very nearly in phase with the phase B voltage. The reactive power required by phase B is supplied by phases C and A during the shorting periods.

Ignoring the voltage smoothing of the DC capacitor, the worst case converter output currents for unity, 0.866, and 0.5 lagging power factors are shown in Figure 4.23. The output current for this strategy is similar to the force commutated rectifier controller. However, the six step converter dictates the voltage frequency of the stator, controlling the slip and machine output. The controlled rectifier can only adjust the phase delay of the rectifier switches to generate a distorted, capacitive current.

If the unity power factor case of Figure 4.19 could exist, the diodes of Figure 4.17 would be unnecessary as the switches operate exactly under zero current conditions. This is not so for the real life cases of a lagging power factor. For all lagging current conditions, current will flow out of the diodes during the short dead time between switching intervals until the opposite switch is fully conducting. This time period is so brief that it should not significantly impact the overall power flow and is neglected for this analysis. Apart from the dead time between switching intervals, the three switch pattern does not utilize the diodes. The next section describes how the diodes are used in circulating the reactive power with the two switch strategy.

### 4.7.2 Two Switch Scheme

In contrast, the 2 switch method, without any shorting between machine phases, cannot circulate reactive power directly from phase to phase. The two switch method circulates reactive power to all three phases via the DC capacitor.

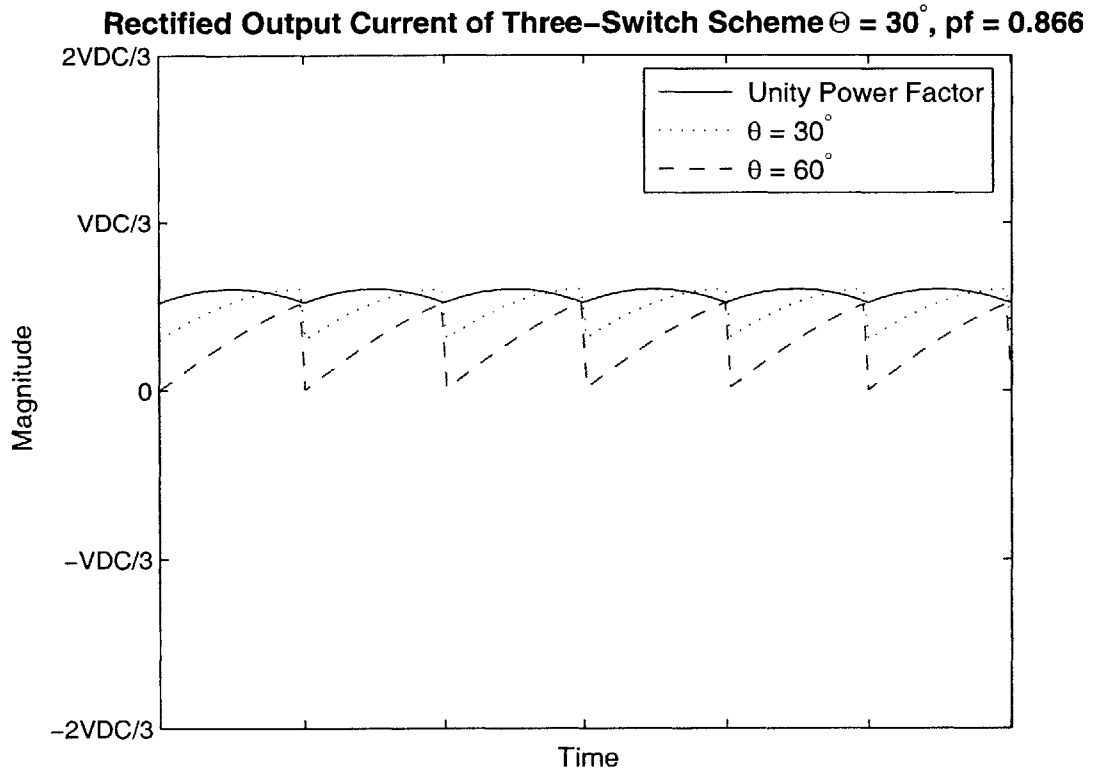


Figure 4.23: Rectified output current with the three switch scheme

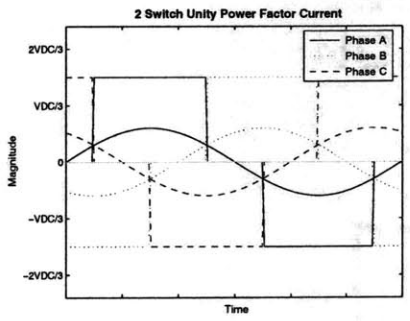


(a) Unity Power Factor

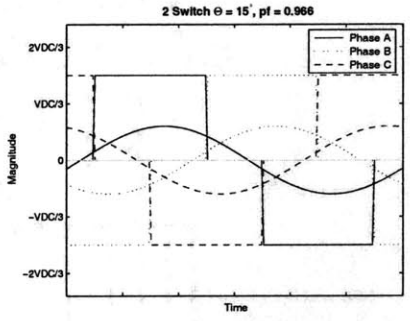


(b) $\theta = 15°$, Power Factor = 0.966

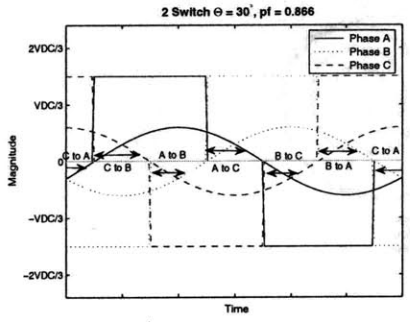


(c) $\theta = 30°$, Power Factor = 0.866

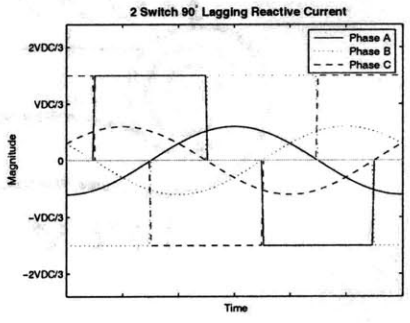


(d) $\theta = 90°$ Lagging

Figure 4.24: Increasing intervals of reactive power circulation through the DC capacitor for the two switch pattern from unity power factor to 90° lagging

The first plot, Figure 4.24(a), shows the impossible situation of unity power factor current to illustrate power flow in the converter with zero net reactive power circulation. Contrast this case with the final subplot, Figure 4.24(d), showing 90° lagging power factor and zero net real power output. The machine terminal currents exiting the machine equivalent inductance cannot change instantaneously. After a phase voltage switches to zero, the currents can flow to or from the DC capacitor via the diodes in anti-parallel with the switches. Figures 4.20(a) and 4.24(c) illustrate an increasing period of reactive power transfer with the DC capacitor.

# Chapter 5
# Modelling and Simulation

## 5.1 Steady State Analysis

The first computer model uses the single phase equivalent circuit values to simulate the behavior of the 3 HP machine operating as a motor under no load with the input voltage varying over the maximum range. This basic simulation verifies that the derived machine parameters are reasonably accurate. Armed with working estimations of the machine parameters, more complicated generator models and simulations are generated.

## 5.2 Grid Excited Steady State Behavior

First, examining the steady state behavior of the generator when connected to a constant 100 V, 60 Hz supply, the equivalent capacitance and load resistance of the absorbed reactive power and delivered real power are calculated for a given drive speed. Measured test results using the three phase variable transformer to maintain the fixed 60 Hz stator frequency and 100 V output voltage were used for comparison against the computer predictions. With the grid connection, no physical load resistance or excitation capacitance are present. However, equivalent values are calculated based on the constant terminal voltage, the measured "input" reactive power from the grid connected transformer, and the measured real output power to the grid. Variation of the machine single phase circuit parameters with frequency is not a consideration for this model since the frequency is fixed at 60 Hz. The leakage inductance varies with the stator current, and this appears to have a significant impact on initial excitation. However, under normal operating conditions, such as the fixed 100 V output in this case, the leakage inductance can be assumed constant with negligible effect to the results.

Steady state evaluation of the machine typically involves impedance analysis of the equivalent circuit, repeated here in Figure 5.1, by setting both the real and imaginary parts of the total system impedance equal to zero [22];[10];[16]. These two equations can then be solved for two unknowns, assuming all of the remaining potential variables ($\omega_s$, $N$ *or* $\omega_r$, $V$, $L_m$, $R_L$, $C$, and the assumed fixed circuit parameters $R_s$, $R_r$, $R_{core}$, $L_s$, and $L_r$) are known. If $\omega_s$,

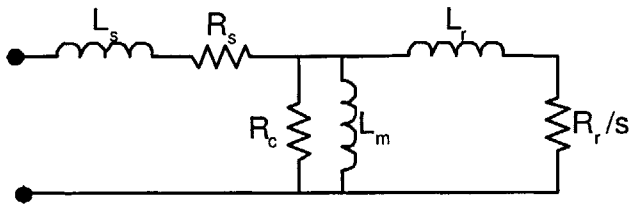


Figure 5.1: Induction machine single phase equivalent circuit model

N, V, fixed machine parameters ($R_s$, $R_r$, $R_{core}$, $L_s$, and $L_r$), and $R_L$ are all known, the two impedance equations can be solved for $L_m$ and C. Alternatively, since $L_m$ is a known non-linear function of the magnetizing current (from the motor tests), with the remainder of the circuit and the voltage known, $L_m$ can be expressed as a function of $R_L$ and C. This set of two non-linear equations has been solved using Matlab by two different numerical methods. First, the Matlab nonlinear least squares function is used in conjunction with real and reactive power balance equations (equivalent to the impedance equations, but simpler to separate the components). After giving the `lsqnonlin` function a likely starting point (the maximum $L_m$ and the corresponding $L_s$ were used), Matlab calculates the stator and magnetizing currents, minimizes power (or impedance) balance functions, and returns the results for $R_L$ and C. The results along with comparison to the measured equivalent values of $R_L$ and C from the first set of generator tests are shown in Figures 5.2 and 5.3.

Alternatively, and as a check because the results from this method showed significant, but not unrealistic, discrepancy with the measured data, another numerical strategy was tried. In the second case, random (and it turns out completely irrelevant, as long as they are in the range of possible values) initial values for $L_m$ and $L_s$ are selected and the now entirely known equivalent circuit, combined with the fixed output voltage are used to calculate values for the load resistance and excitation capacitance. These values of $R_L$ and C are then used with the fixed terminal voltage to calculate machine currents and new values of mutual and leakage reactance. The new reactance values are once again used to determine load and capacitor values, and the iterative cycle continues until it converges to specific values. The process terminates when any identified circuit parameter (the stator current in this case) differed by less than a preset value (1e-6 here) after one full cycle. Encouragingly, this method yields nearly identical results to Matlab's `lsqnonlin` function. The results of this process are again compared to the measured test results and are displayed now in Figures 5.4 and 5.5. The $R_L$ and C values are nearly indistinguishable from those shown in Figures 5.2 and 5.3, with this iterative approach yielding improved results for reactive power at high speeds.

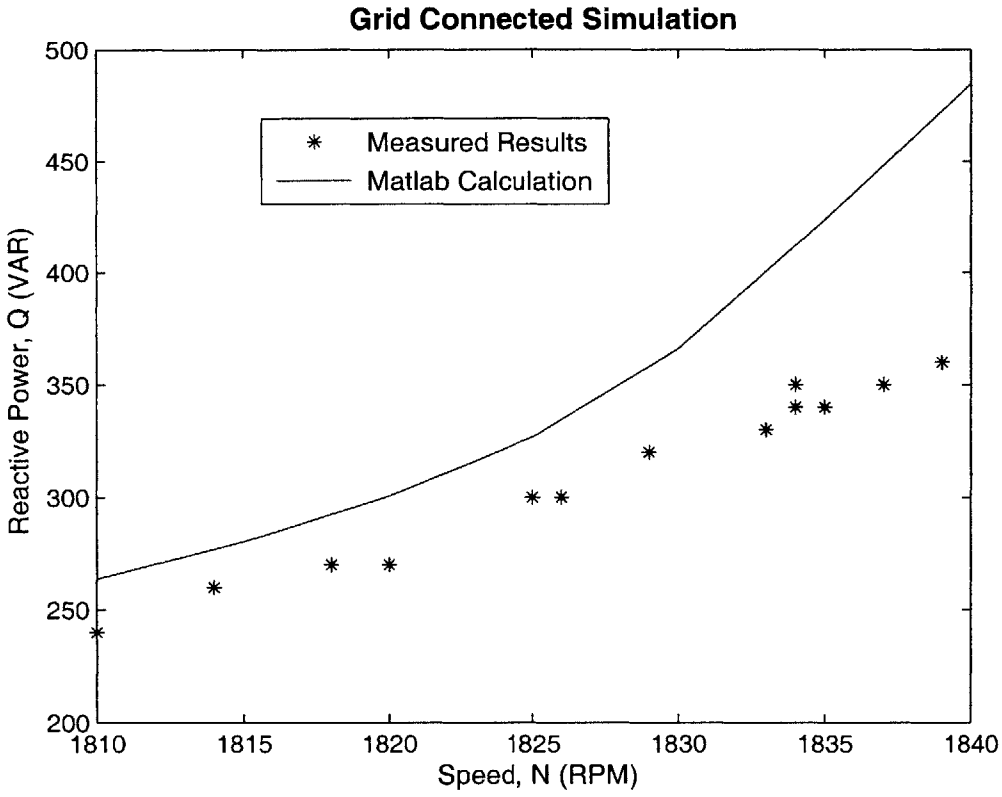


Figure 5.2: Comparison of Matlab least squares function to measured results of steady state reactive power for varying drive speeds at 100 V, 60 Hz

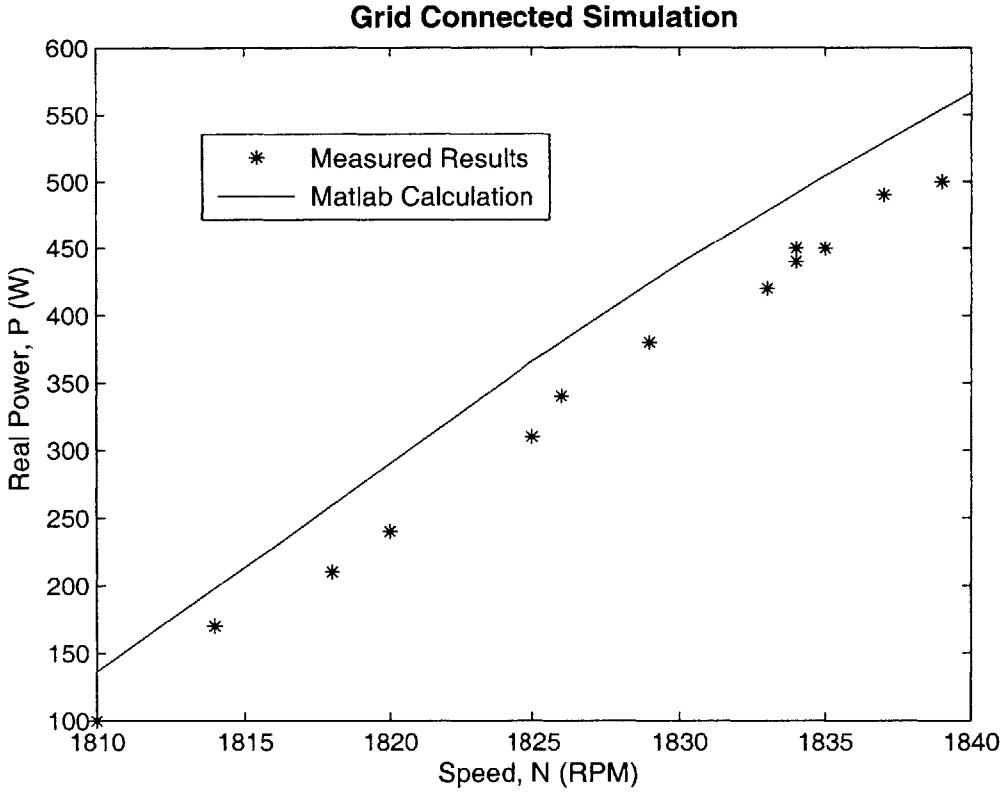


Figure 5.3: Comparison of Matlab least squares function to measured results of steady state real output power for varying drive speeds at 100 V, 60 Hz

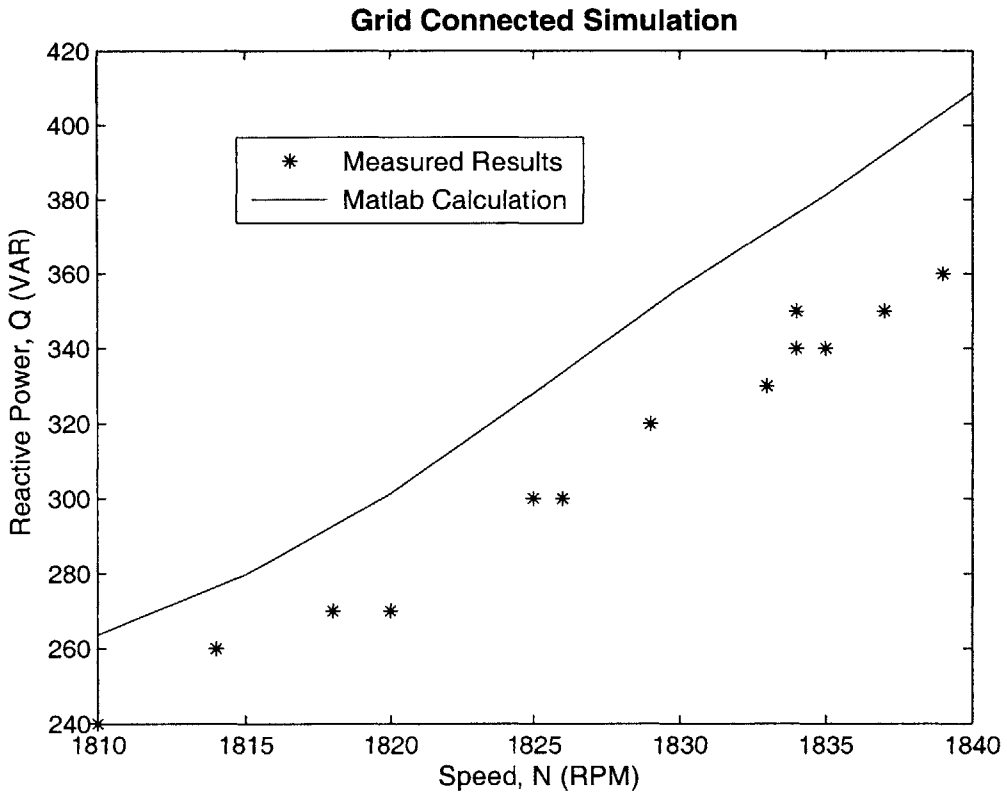


Figure 5.4: Comparison of iterative solution to measured results of steady state reactive power for varying drive speeds 100 V, 60 Hz

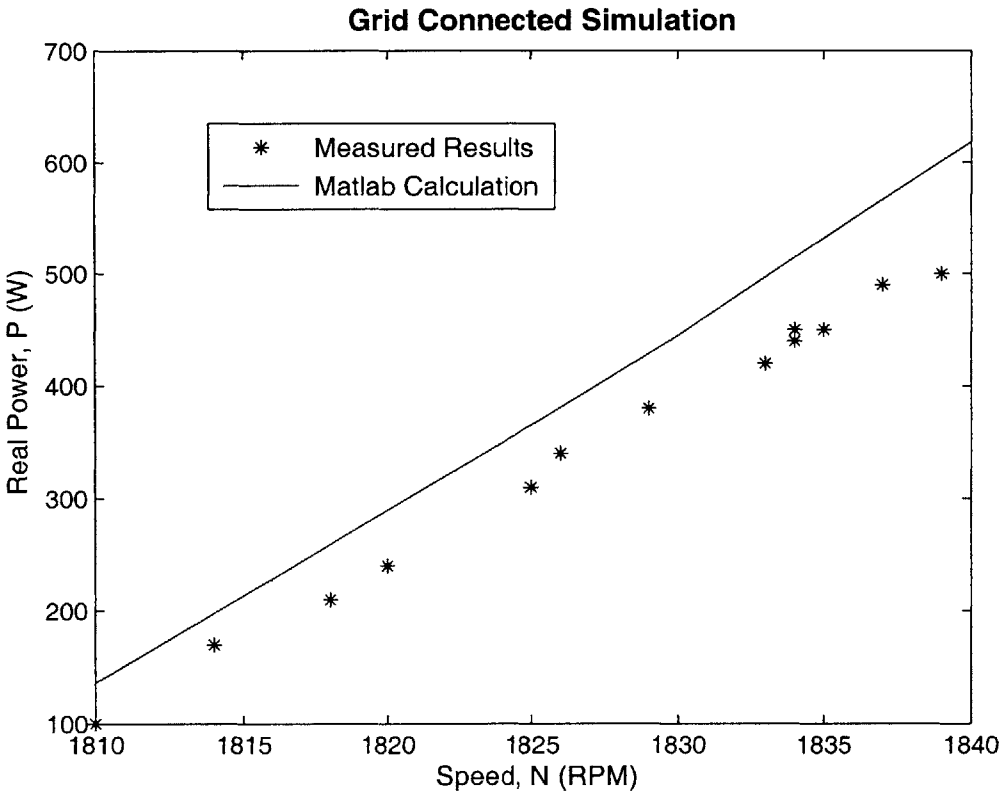


Figure 5.5: Comparison of iterative solution to measured results of steady state real output power for varying drive speeds at 100 V, 60 Hz

## 5.3 Variable Voltage Steady State Behavior Under Load

With grid connected induction generator operation at a fixed output voltage and frequency, the only available control variable is the drive speed. The machine slip can be adjusted by changing the speed, and this will determine the power output to the grid. The reactive power drawn from the grid to maintain excitation will increase with the delivered power and can be significantly greater than the output power at low speeds. For constant voltage operation, the output power varies with N (and the slip) and varying reactive power, Q, must be supplied by the grid. For stand alone operation, the output frequency is now a controllable variable and more sophisticated control becomes possible. Unfortunately, the stand alone machine tests were limited by available excitation capacitors and load resistors, and the induction machine has not been tested or modelled under variable frequency operation. Nevertheless, results near 60 Hz demonstrate the variation in output voltage and frequency as the drive speed changes for a particular excitation capacitance and load resistance. As will be shown, the results from the computer models correlate well with the measured stand alone generator test data.

The next batch of models examines the steady state generator performance in stand alone operation, excited by an 80 $\mu$F capacitor on each phase of the machine. Unlike the designed generator system, the voltage varies for the first few stand alone tests for easier comparison to the recorded test data. Later, the same process is used to calculate the required frequency at a constant output voltage. The results presented in this section are also valuable in demonstrating some of the potential difficulties of uncontrolled, capacitor excited induction generators.

Assuming known, fixed load resistance and excitation capacitance and a varying output voltage, the drive speed was treated as a controllable input parameter in calculating the only remaining unknown in the circuit, the stator output electrical frequency. Again, picturing the single-phase equivalent circuit from Figure 5.1, a variable frequency complicates the analysis as every impedance value except the stator and load resistance depends on the frequency. An iterative approach was used where an initial electrical frequency of 60 Hz was assumed. This initial value was used to evaluate an initial approximation for the reactance of the excitation capacitor. Then, together with the load resistance and output voltage, the complex stator current can be found.

$$I_s = \frac{V_{out}}{Z_{out}} \tag{5.1}$$

where

$$Z_{out} = \frac{\frac{-jR_L}{\omega_s C}}{R_L - \frac{j}{\omega_s C}} \tag{5.2}$$

Plugging the stator current into the polynomial curve fit yields the stator reactance and the assumed equal rotor reactance (although the assumed constant running value should work nearly as well). Next, the air-gap voltage could be found using the output voltage, stator current, and total stator impedance, and a real power balance equation could be used to equate the power in the rotor resistor to the load and machine losses.

$$V_{ag} = V_{out} - I_s(R_s + j\omega_s L_s) \tag{5.3}$$

Real Power Balance Equation:

$$\frac{V^2}{R_L} + I_s^2 R_s + \frac{V_{ag}^2}{R_{core}} - I_r^2 \frac{R_r}{s} = 0 \tag{5.4}$$

where

$$s = \frac{\omega_s - \omega_r}{\omega_s} \tag{5.5}$$

$$I_r = \frac{V_{ag}}{Z_r} \tag{5.6}$$

and

$$Z_r = R_r + j\omega_s L_r \tag{5.7}$$

The stator electrical frequency, $\omega_s$, is the only unknown parameter and can be quickly resolved using Matlab. This new frequency value is then used to calculate the capacitor reactance again and the cycle continued until the electrical frequency changed by less than a preset value (1e-6). The frequency value quickly converged in about five steps.

The input drive speed was swept over the full range found during the earlier generator test, with the above process winding the equilibrium stator frequency for each speed. The predicted values are compared to the actual measured results in the figures below. Both figures use the same calculation of stator frequency, showing the change in frequency as the output voltage or drive speed vary.

The results from these simulations appear almost too good to be true, and it seems likely that there is some kind of an error, if not here, then in the previous 60 Hz simulations that showed a consistent displacement between the measured and predicted values. However, there was only one unknown in solving for $\omega_s$, in place of both $R_L$ and C from the first grid connected simulation. Furthermore, the underlying real power balance equation used to solve for the stator frequency was completely independent of the magnetizing inductance. If the error from the earlier simulation was confined to the magnetizing inductance, then it should not appear here in the determination of $\omega_s$.

These simulations also illustrate the voltage and frequency regulation problems of standard capacitor excited stand-alone induction generators. As the drive speed is swept up over a

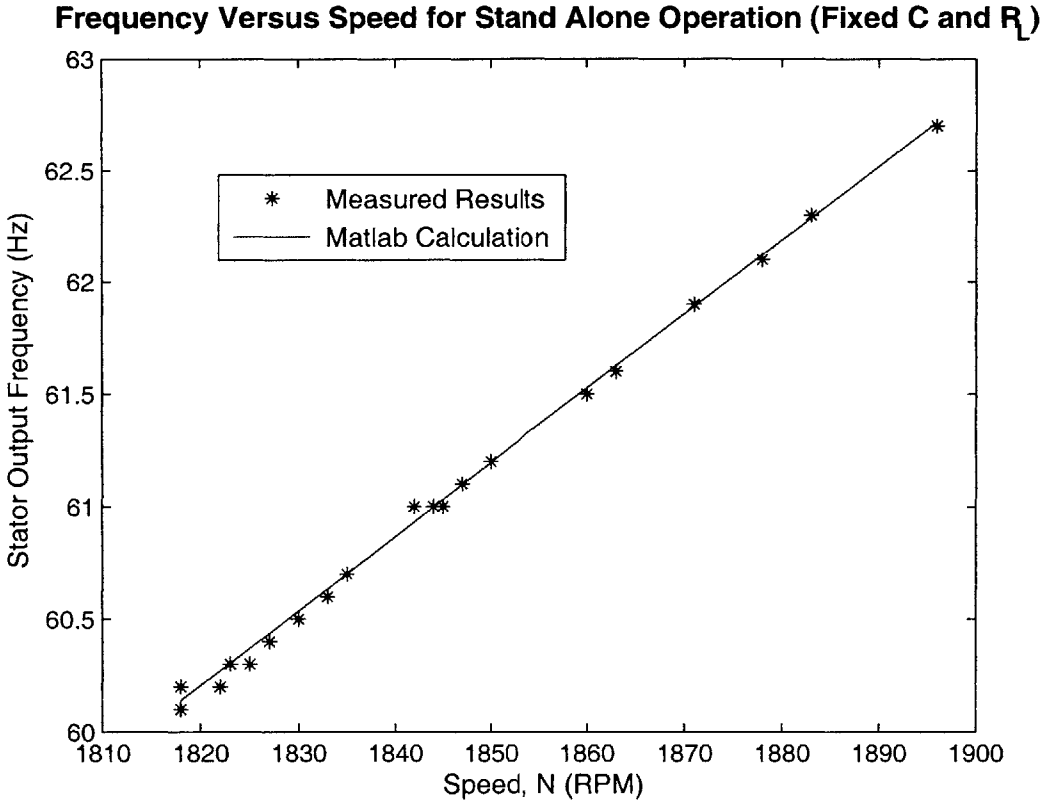


Figure 5.6: C=80$\mu$F, $R_L = 52.5\Omega$ stand alone operation showing stator frequency for varied drive speed

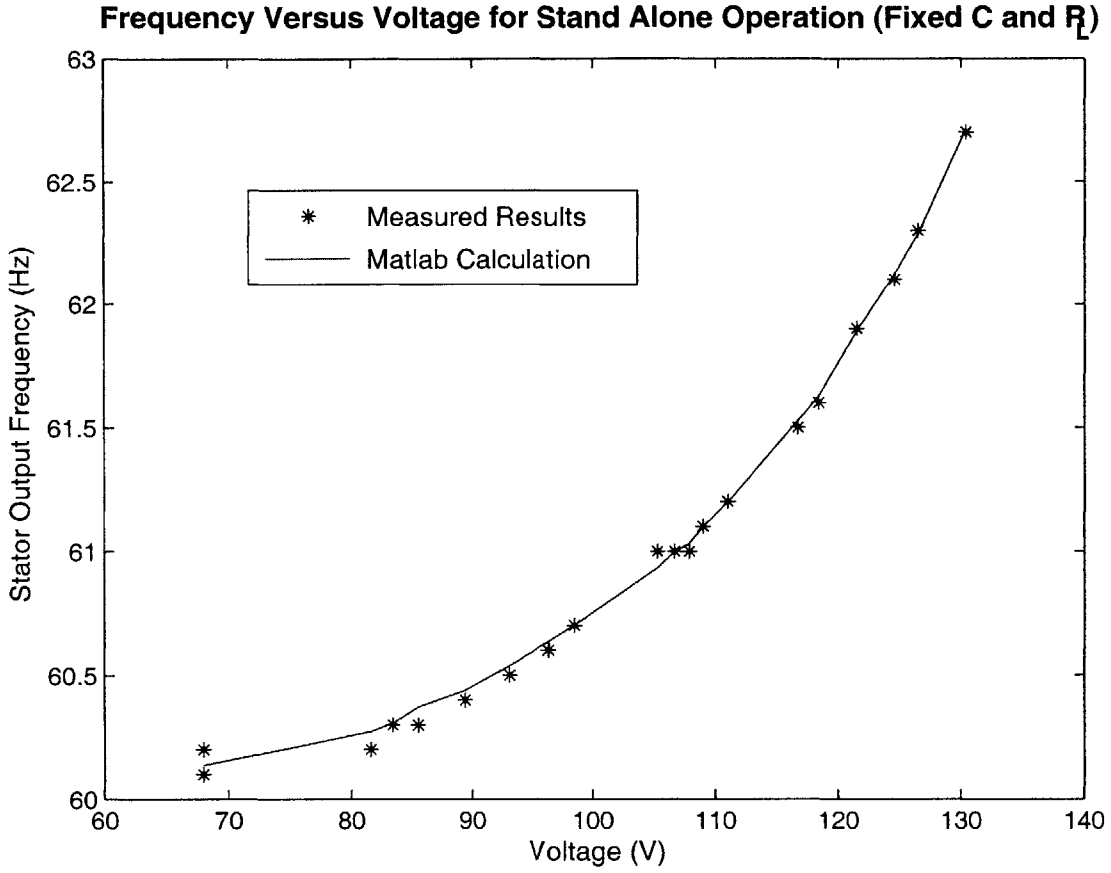


Figure 5.7: C=80$\mu$F, $R_L = 52.5\Omega$ stand alone operation showing stator frequency for varied stator voltage

range of less than 100 RPM, the output frequency increases by about 2 Hz (≈12.57 rad/sec). The more significant issue is the output voltage, nearly doubling from less than 70 V to almost 130 V. This dramatic swing in voltage is responsible for the "under-utilization" of induction generators [21]. The next set of simulations attempt to overcome this voltage regulation challenge, using the stator frequency to maintain a constant output voltage over the full range of load.

One final verification of the stand-alone models involved almost the reverse of the previous calculations. Now, the load resistance, $R_L$ and excitation capacitance, C, are calculated knowing everything else about the generator circuit. The tests were run with fixed 80 $\mu$F capacitance and 52.5 $\Omega$ resistance, so how well the results match these values will provide a straightforward check of the model. The results can be seen in 5.8. The resistance value is a little low, but at nearly 50 $\Omega$ appears close to the actual value. There is less variation in the excitation capacitance, but the calculated value falls short of the expected 80$\mu$F value.

It turns out that the equivalent capacitance seen by the machine terminals during testing as determined by $C = \frac{Q}{V^2\omega_e}$ was found to be about 73 $\mu$F rather than the nameplate 80$\mu$F. The lower value agrees quite closely with the simulations, and adding in only a 1.5 $\Omega$ equivalent series resistor to the 80$\mu$F capacitor reduces the equivalent capacitance by about 6 or 7$\mu$F. The simulations appear to be accurate.

## 5.4 Constant Voltage, Steady State Operation Under Load

With an accurate model, values of $R_L$ and C were now found for operation at a fixed 100 V output voltage and a drive speed of 1850 RPM.

Since the single-phase equivalent circuit elements in this model are (unlike real life) frequency independent, changing the drive speed merely shifts the operating frequency range so that the machine can maintain the same range of slip and exhibit the exact same performance at the increased or decreased frequency. In reality, magnetic saturation of the machine will increase and the magnetizing inductance $L_m$ will drop with frequency so that the machine power factor and output power will suffer if the generator operates at increased frequency.

Figure 5.9 shows the difference between the real and reactive power transferred to the grid during the fixed 60 Hz, 100 V tests where an increasing drive speed was used to increase the negative slip, the simulated real power output, and circulated reactive power as the stator frequency was decreased. The slope of the computer generated curves for both real and reactive power nearly match the experimental data. Possibly because of machine losses not included in the simplified equivalent circuit, the predicted power values are slightly higher.

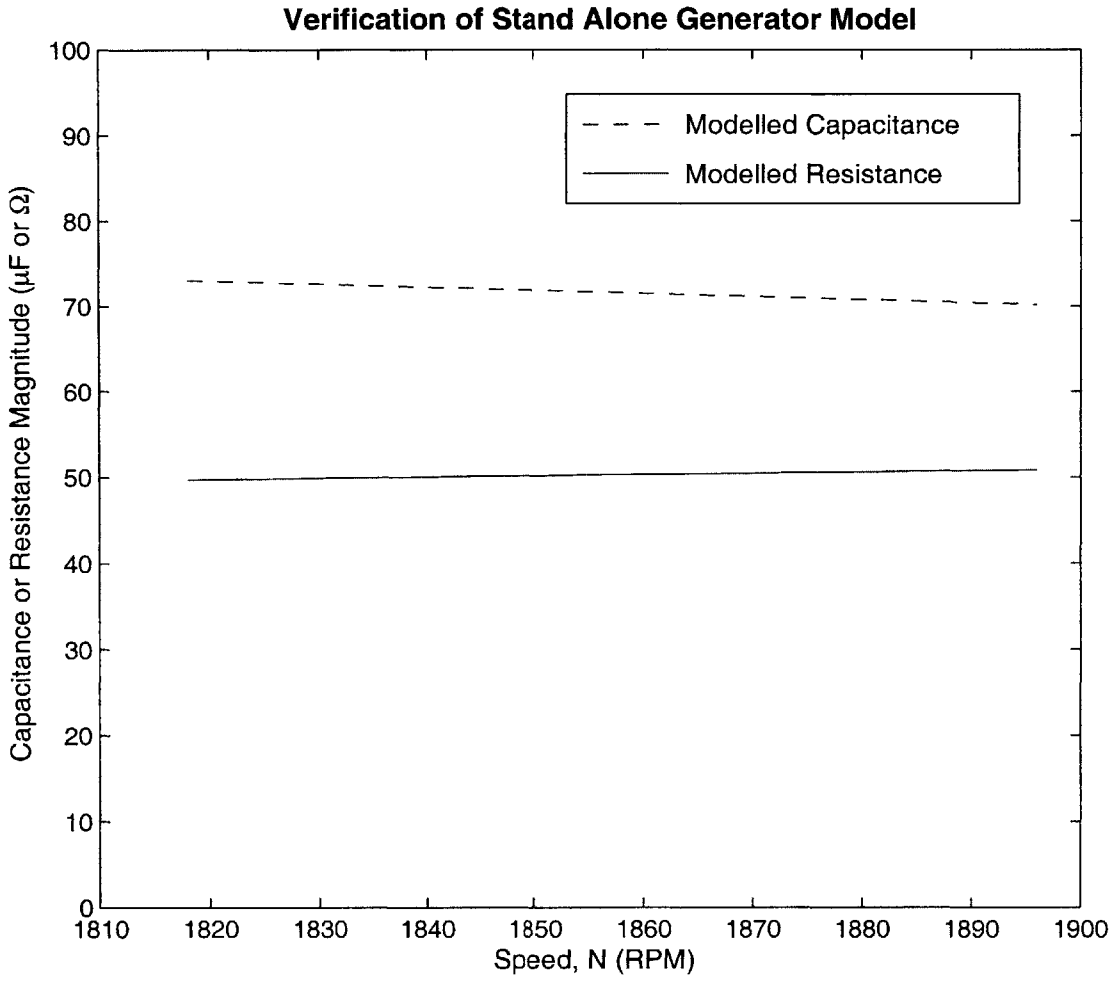


Figure 5.8: Verification of stand alone model - RL and C

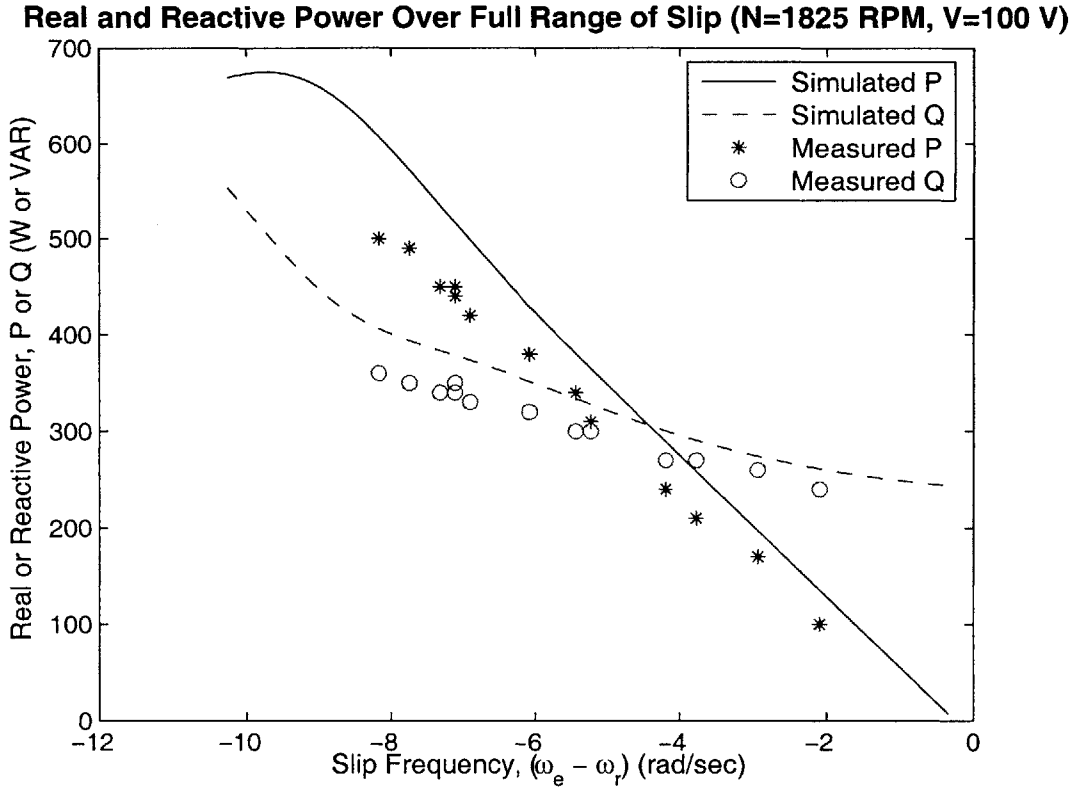


Figure 5.9: Simulated real and reactive power over the full frequency range, N=1825 RPM

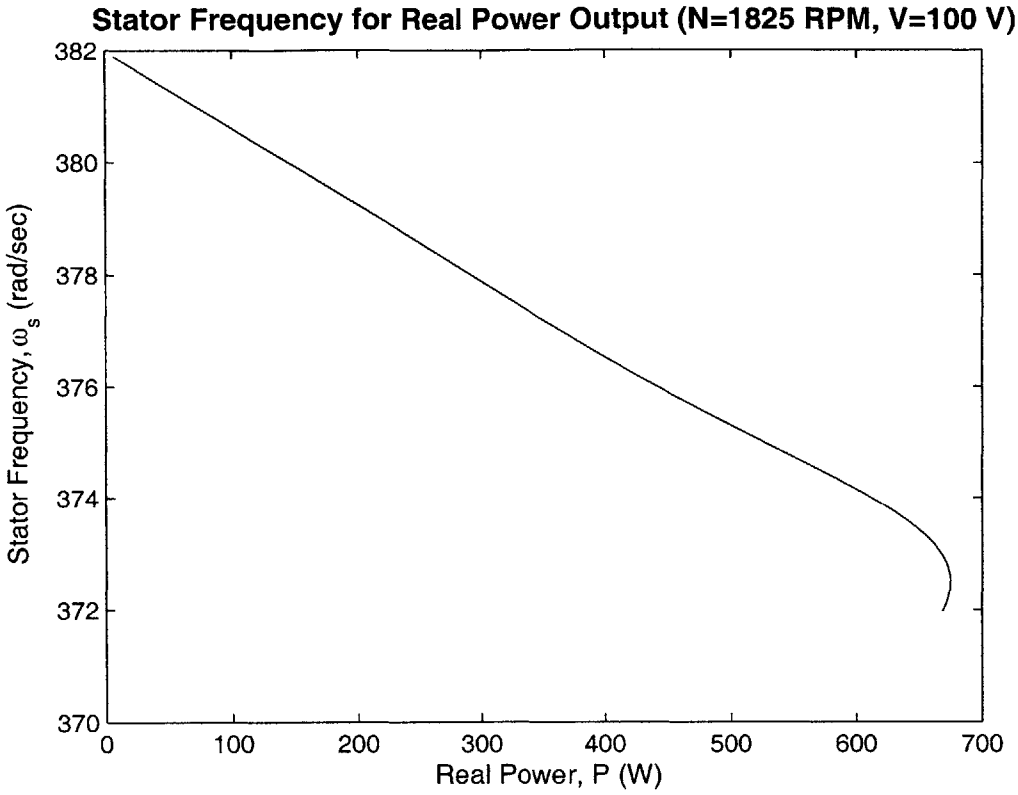


Figure 5.10: Simulated stator frequency required for varied real power Output, N=1825 RPM, V=100 V

The measured data stops at the likely maximum operating point, just before the power factor of the modelled machine starts to fall. The recorded data stops short of zero slip only because a higher than necessary drive speed was used to eliminate all possibility of generating with the grid connected drive motor and back-feeding the variable speed drive.

As Figure 5.11 shows, the required reactive power exceeds the output power at low loads (high speeds). The power factor of this generator will never be great, regardless of the operating conditions, with the best case roughly 0.85, with P $\approx$ 650 W and Q $\approx$ 400 VAR at a little less than 374 rad/sec (59.52 Hz). This is a standard, off the shelf, inverter duty induction motor that has been pressed into service as a generator and is operating at a low voltage. Performance could, no doubt, be improved if the design were optimized for generation.

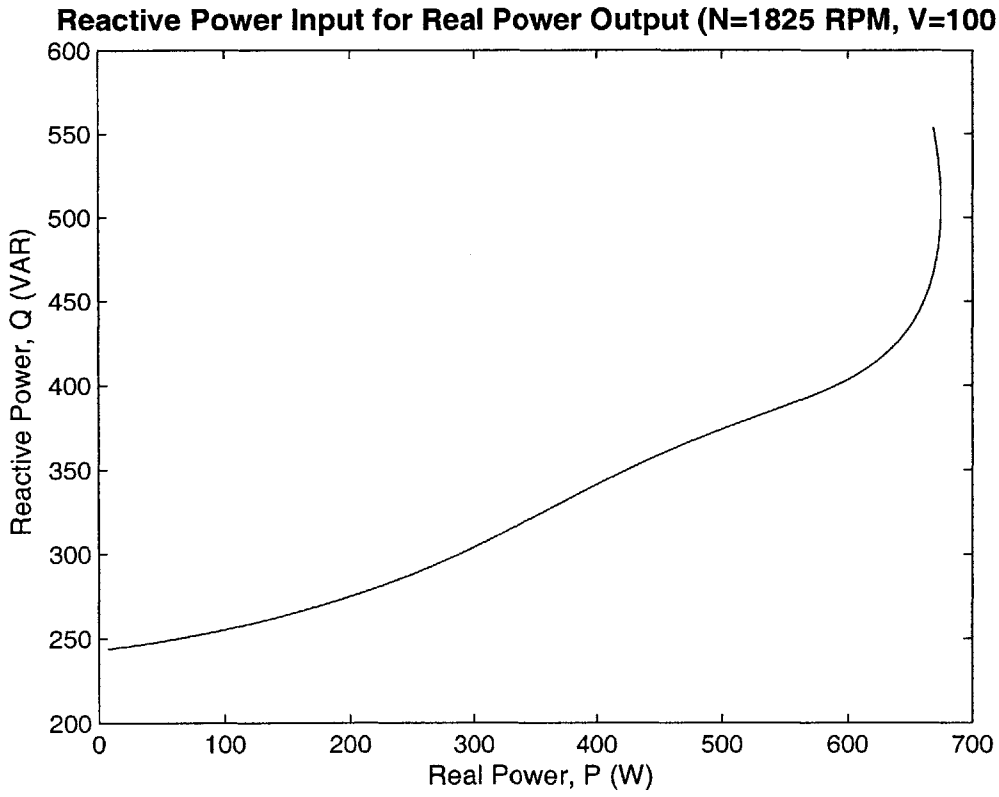


Figure 5.11: Simulated reactive power required for varied real power output, N=1825 RPM, V=100 V

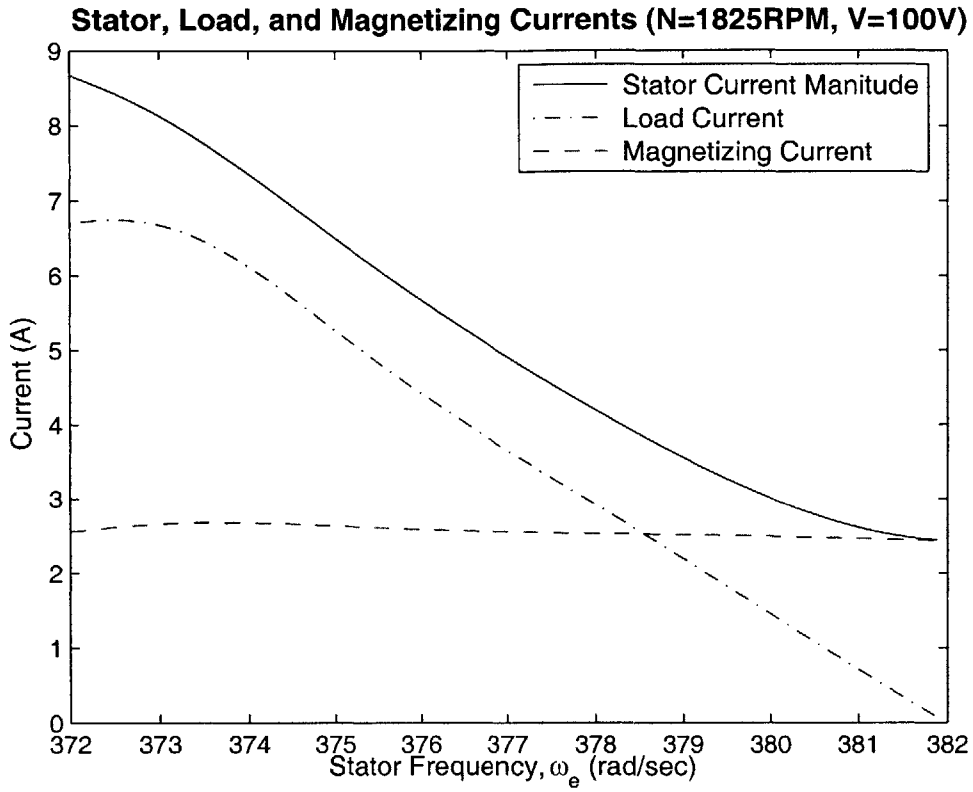


Figure 5.12: Simulated stator, load, and magnetizing currents over the full frequency range, N=1825 RPM, V = 100V

The rated machine current is 8 A, so with a load that can withstand the maximum output current (the 52.5 AC test resistors are only rated for 5 A, reached at about 375.3 rad/sec [59.73Hz]) the machine could operate over a stator frequency range from 381.98 rad/sec at no-load to 373.18 rad/sec at full-load 660 W output. Here the 3 HP motor could theoretically deliver up to about 1980 W over all three phases. This operation is shown in Figure 5.12. The frequency is adjusted to control the power output. The stator and rotor currents vary with the load requirements but the magnetizing inductance maintains a fairly constant value. With nearly constant magnetizing voltage and current, the magnetizing inductance is also a constant, and the machine is operating under constant flux, $\lambda = Li$.

The ideal excitation capacitance can be found by examining the required Q at no load. At $\omega_e \approx 381.884$, Q $\approx$ 243.886 and C $= \frac{Q}{\omega_e V^2} \approx 64\mu$F. In practice, the capacitor will need to be larger than this to account for ESR, but smaller, higher voltage capacitors could be

connected line-to-line. Also, if there is a known permanently connected minimum load, the capacitance can be further increased. This capacitance will allow for the initial excitation and voltage build up of the machine, and under load, will decrease the reactive current circulating through the power converter.

Steady state analysis of the machine behavior suggests that this basic control strategy can be used to maintain a constant output voltage over the full range of load by merely varying the stator output frequency as in Figure 5.10, provided that the increasing reactive power is supplied to the machine and the drive speed does not change so much with load that the machine cannot operate at the new frequency.

Ideally, for a megawatt scale machine, the torque-speed curve of the large steam turbine would be stiff enough that the speed drops little from no load to full load. In the worst case scenario, additional isochronous turbine controls could be required for constant speed operation. There will likely be some sort of steam regulation for efficient operation, regardless of the generator.

In the ideal case of a constant drive speed near the machine's rated operating point, the full load range of load can be met with only about a $\pm 8$ rad/sec $\approx 1.3$ Hz change in stator frequency. This investigation did not examine the variations in machine parameters with frequency, however Seyoum, Grantham and Rahman include a plot detailing the changes in mutual inductance of a 415 V, 50 Hz, 3.6 kW, four pole machine over a range from 35 Hz to 55 Hz [18]. As the frequency decreases, the peak of the curve shifts to a slightly (about 10%) lower voltage and the operating inductance decreases significantly, with a steeper slope over the 20 Hz drop. At lower frequencies, lower maximum output voltages are possible. A change in frequency of 5 Hz corresponds to about a 31.4 rad/sec or 150 RPM adjustment. While the magnetizing inductance is affected by the $\pm 5$ Hz change in frequency, the impact would not have a significant impact on this control scheme. Operation could break down if the frequency is reduced by a significant decrease in rotor speed with load. As long as the frequency dependence of the remaining machine parameters is similar or less pronounced, the controller for a small scale machine could probably be designed to operate according to this slip-frequency control scheme over a range of up to 300 RPM before the low frequency spoiled the operation.

# *Chapter 6*
# *Transient Analysis*

This section shows dynamic models of the initial excitation of the machine, and how the machine responds to changes in load. Transient analysis of induction machines typically takes advantage of the fact that most machines operate with roughly balanced three phase voltage and current to represent the three phase machine in an equivalent two-phase, d-q representation. Learning this strategy is complicated by the fact that two different representations are commonly used in the literature. Both lead to identical results but the variations can be confusing. Additionally, multiple frames of reference, attached to the stator, fixed to the rotor, or rotating at the electrical frequency can also be used.

### 6.0.1 No Load Initial Generator Excitation

When sufficient capacitance or an alternative source of leading reactive power is supplied to the machine terminals and the rotor is driven at a speed greater than the output electrical frequency, the generator output voltage will build up as the capacitor resonates with the machine inductance and the increasing voltage across the negative rotor resistance delivers current to the load.

The goal is to reach a stable operating point where the positive real power through the negative rotor resistor is burned up as loss in the internal resistance of the machine, and the excitation capacitor balances out the machine equivalent inductance, due largely to the magnetizing inductance. The real power balance will be highly dependent on the machine slip, since it directly impacts the value of the equivalent rotor resistance. Too small of a slip value, and the voltage might never build up. Excessively large slip could cause the steady state value to exceed the rated voltage, or, equivalently, for the mutual or leakage inductance parameters in the simulations to exceed the regions where the polynomial curve fits remain valid. Ideally, a value could be used where the slip required for initial excitation also results in steady state operation at a reasonable voltage. This is determined by the mutual inductance characteristics of the machine.

During the capacitor excitation tests, the machine voltage appears to build up at a constant frequency. It might be interesting to record and examine the voltage waveforms during the excitation process with a more sophisticated power analyzer. Since the power converter

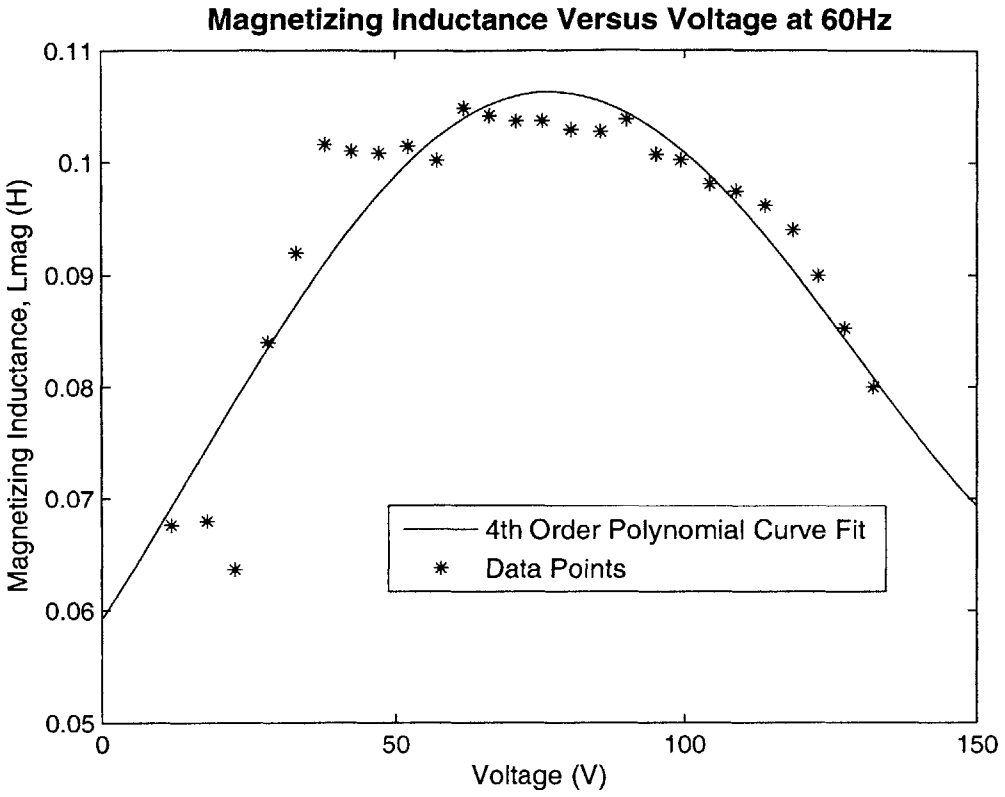


Figure 6.1: Mutual inductance at 60 Hz over the full range of no load stator voltage

dictates the stator output frequency, and for simplicity in the transient analysis, the stator frequency is assumed constant during the excitation process.

With the mechanical drive speed also assumed to be constant, the generator voltage does not build up under a constant frequency with fixed excitation capacitors. A steady state operating point is not reached. Either the voltage does not rise or the mutual or leakage inductance continues changing until leaving the region where the curve fit is a valid approximation, becoming negative or unreasonably large. Examining the magnetizing curve (plot of mutual inductance, $L_m$, against output voltage at no load) included again here as Figure 6.1 can provide an explanation for the lack of steady state operating point.

The initial inductance value of about 0.06 H is less than the inductance at the maximum voltage, 150 V, shown in Figure 6.1. Considering the total inductance to be the mutual inductance in series with the stator leakage inductance would increase the initial inductance

value. Still, the stable operating point required to initially excite the machine does not occur within the desired voltage operating range of about 100-130 V. The drive speed and frequency required to build up the voltage will not stop increasing the voltage until some point after 150 V. Designed to run at either 230 V or 460 V, the machine does not significantly saturate due to voltage at the levels tested or used in these models. This slightly complicates the dynamic simulations of the machine start up.

The curve fits for the magnetizing and leakage inductances are valid only over a restricted range of voltage or current. With the operating point of the machine outside of this working range, the inductance eventually increases rapidly, causing the output voltage to approach infinity. To avoid this problem, a higher initial starting speed is used to develop the stator voltage. Less than a second at a speed increased by 25 to 50 RPM is more than necessary to boost the initial voltage to a point where the lower speed can be switched in to settle the voltage at the desired steady state point. This also speeds up the excitation process and allows for reduced computation time and plots of reduced time spans, showing greater detail. Too great an initial speed for too long will also cause the voltage to blow up or the variable inductance models to break down. Plots of the voltage buildup for the capacitor excited induction generator are included in Figures 6.2 and 6.3. Both figures are nearly identical but are generated with different models, one using machine fluxes as state variables, the other using currents.

As the voltage increases, the rotor current will increase. Initially, the mutual reactance will also increase, slowing the rise in magnetizing current, and limiting the stator current. Eventually, the mutual inductance will reach a peak and begin to decrease. After that point, the magnetizing current will increase, with the increase in current flowing through the stator from the capacitor. Ideally, a slip value can be selected such that the increase in stator current at a particular output voltage and value of mutual inductance can create just enough loss in the machine to balance out the current flowing from the rotor.

There is a minimum slip (maximum stator frequency for a fixed drive speed) necessary to maintain voltage for a given capacitance and drive speed. Below this slip, the simulated voltage will fail to reach a steady value, decaying even if initially brought above the desired voltage by an increased starting speed.

If too large of a drive speed is used or the larger starting speed is held for too long, the voltage exceeds the machine rating and the simulation breaks down as the mutual inductance exceeds the range where the curve fit is valid. If too small of an initial drive speed is used, the voltage fails to build up to a stable value.

The initial flux, current, or voltage must be included in the machine models as initial conditions. These values, taken as initial rotor fluxes or currents, represent the remanent magnetism in the machine from aligned iron magnetic domains. These arbitrarily small (1e-6 or less) amounts of energy in the machine are essential to start the voltage buildup. Smaller

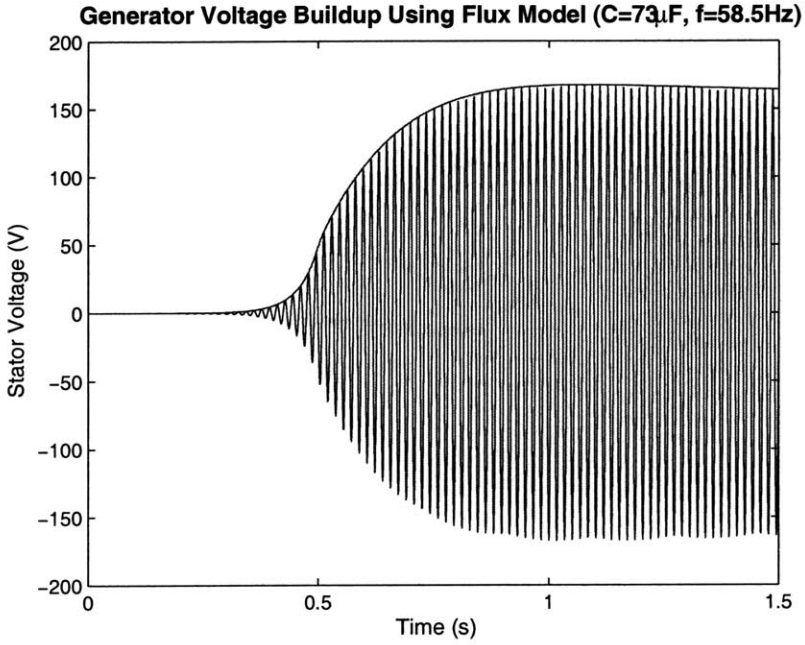


Figure 6.2: Induction generator voltage buildup from flux model

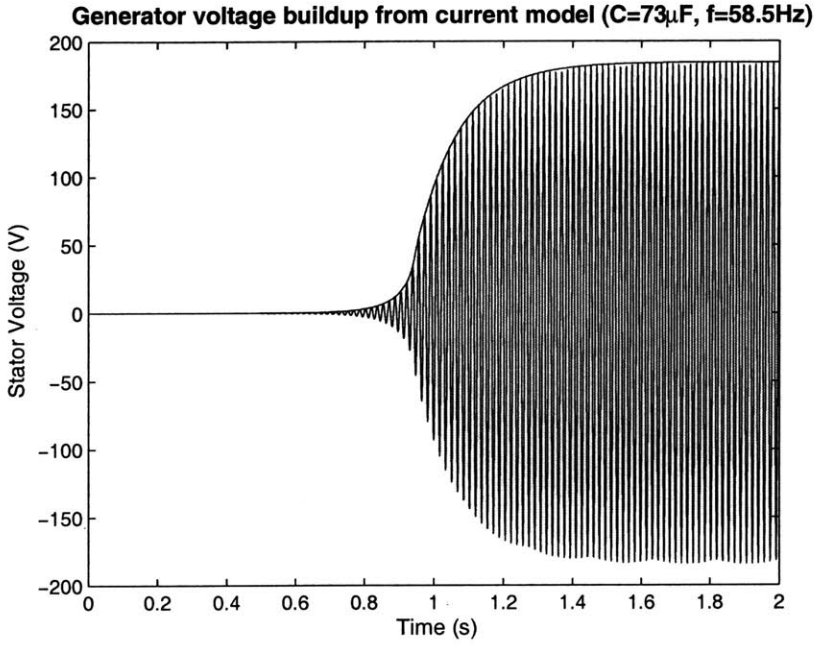


Figure 6.3: Induction generator voltage buildup from current model

values merely increase the time for the simulated voltage to rise to running levels. These values represent the initial energy that rings between the excitation capacitance and machine inductance, resulting in a minute current through the rotor negative resistor and building exponentially from there.

The characteristics of the voltage buildup are controlled by the starting speed, the duration of the starting speed, the running speed, the stator frequency, the excitation capacitance, and the initial flux, current, or voltage values. These parameters determine whether the voltage will successfully build up and stabilize, how long the buildup will take, and the magnitude of any voltage overshoot.

The d-q model neglects the core loss component of the single phase equivalent circuit. The real power produced in the rotor negative resistance must balance out with only the stator copper losses. This approximation should have a significant impact on the machine slip and output voltage at no load; where as, if the air gap voltage is roughly equal to the output voltage, both the stator copper losses, $P_s = I_s^2 R_s$, and the core losses, $P_{core} = \frac{V^2}{R_c}$, will be on the order of 10 W. Under load, the core loss becomes much less significant. The 10 W core loss is only about 2% of the about 500 W full load output, and $R_c$ can be neglected without significant error. Adding in the core loss should increase the slip of the machine, decreasing the stator operating frequency, $\omega_s$.

Expecting the slip to increase with the addition of the core losses, including $R_c$ in the simulations, actually increases the slip slightly (the stator frequency increases to about 58.486 Hz from 58.48575 HZ). This may have been partly due to a reduced mutual inductance and stator current. This adjustment brought the simulation results slightly closer to the measured output voltage and frequency, but it also shows why no one includes it in the simulations. Including $R_c$ did not significantly alter the no load generator behavior.

Using a recursive calculation of the mutual inductance from the machine currents, either calculated at each step from the flux variables or available directly if using the current state variables, resulted in steady state voltages similar to predicted values. However, the final voltage output levels are extremely sensitive to small changes in slip, from either the frequency or drive speed. At a drive speed of 1755 RPM, the peak steady state output voltage can range from below 134 V to over 205 V while decreasing the output frequency from only 58.486 Hz to 58.47 Hz. A change of only 0.016 Hz (0.10 rad/sec) results in a 70 V swing. If accurate, this could make precise voltage control extremely difficult. For the simulations, it means that small changes within the +/-.04 Hz and +/- 0.4 RPM error limits of the test equipment can give any desired output voltage, and it is difficult to determine the accuracy of the simulations. The limited precision of the test equipment measuring the stator frequency and shaft speed has a significant impact on these generator simulations.

The simulations seem reasonable and behave as expected, with a few exceptions. Results from both the current and flux simulations produced nearly identical results, indistinguish-

able at the scales needed to show the full start-up curve. The slight voltage difference at some points may be due to the fact that the flux calculations use the mutual and leakage inductance values from the previous iteration. Nevertheless, the hypersensitivity of these transient models to changes in stator frequency does not seem to agree with the steady state simulations. Plus, the effects of including the core resistance were surprising, and the excitation capacitance appears to have little effect on the steady state voltage and minimal impact on the buildup duration of the transient simulations. It seems likely that there is a problem with these simulations. If not, it will be extremely difficult to maintain precise enough frequency control using the six step inverter to control the generator voltage.

## 6.1 Simulation Equations

The Park's Transformation can be used to transform any balanced three phase variable (current, voltage, flux...) onto the corresponding two-axis representation. For synchronous machines, the direct d-axis is aligned with the field winding (i.e. with the field pole and flux from the field winding), and the quadrature q-axis leads the direct axis by 90 degrees. Things are a little more hazy with squirrel cage induction machines.

$$\begin{bmatrix} x_d \\ x_q \\ x_o \end{bmatrix} = \frac{2}{3} \begin{bmatrix} \cos\theta & \cos(\theta - \frac{2\pi}{3}) & \cos(\theta + \frac{2\pi}{3}) \\ -\sin\theta & -\sin(\theta - \frac{2\pi}{3}) & -\sin(\theta + \frac{2\pi}{3}) \\ \frac{1}{2} & \frac{1}{2} & \frac{1}{2} \end{bmatrix} \begin{bmatrix} x_a \\ x_b \\ x_c \end{bmatrix} \tag{6.1}$$

where $\theta = \omega t + \theta_o$ and $\theta_o$ is the initial angle between the d-axis and phase A at time zero.

The inverse transformation is:

$$\begin{bmatrix} x_a \\ x_b \\ x_c \end{bmatrix} = \frac{2}{3} \begin{bmatrix} \cos\theta & -\sin\theta & 1 \\ \cos(\theta - \frac{2\pi}{3}) & -\sin(\theta - \frac{2\pi}{3}) & 1 \\ \cos(\theta + \frac{2\pi}{3}) & -\sin(\theta + \frac{2\pi}{3}) & 1 \end{bmatrix} \begin{bmatrix} x_d \\ x_q \\ x_o \end{bmatrix} \tag{6.2}$$

The set of simulation equations using machine flux as state variables are given here.

$$\frac{d\psi_{ds}}{dt} = v_{ds} - R_s i_{ds} + \omega_e \psi_{qs} \tag{6.3}$$

$$\frac{d\psi_{qs}}{dt} = v_{qs} - R_s i_{qs} + \omega_e \psi_{ds} \tag{6.4}$$

$$\frac{d\psi_{dr}}{dt} = v_{dr} - R_r i_{dr} + (\omega_e - \omega_r)\psi_{qr} \tag{6.5}$$

$$\frac{d\psi_{qr}}{dt} = v_{qr} - R_r i_{qr} + (\omega_e - \omega_r)\psi_{dr} \tag{6.6}$$

$$\frac{dv_{qs}}{dt} = \frac{-i_{qs}}{C} - \frac{v_{qs}}{R_L C} \tag{6.7}$$

where

$$i_{ds} = \frac{\psi_{ds}L_R - \psi_{dr}L_m}{L_S L_R - L_m^2} \tag{6.8}$$

$$i_{qs} = \frac{\psi_{dr}L_S - \psi_{ds}L_m}{L_S L_R - L_m^2} \tag{6.9}$$

$$i_{dr} = \frac{\psi_{qs}L_S - \psi_{qr}L_m}{L_S L_R - L_m^2} \tag{6.10}$$

$$i_{qr} = \frac{\psi_{qr}L_R - \psi_{qs}L_m}{L_S L_R - L_m^2} \tag{6.11}$$

with $L_S = L_s + L_m$ and $L_R = L_r + L_m$

Similarly, the simulation equations with the machine currents as state variables are given below.

$$\frac{di_{ds}}{dt} = K(R_s L_R i_{ds} - \omega_s L_S L_R i_{qs} + (\omega_s - \omega_r)L_m^2 i_{qs} - R_r L_m i_{dr} + -\omega_r L_R L_m i_{qr}) \tag{6.12}$$

$$\frac{di_{qs}}{dt} = K(\omega_s L_S L_R i_{ds} - (\omega_s - \omega_r)L_m^2 i_{ds} + R_s L_R i_{qs} + \omega_r L_m L_R i_{dr} - R_r L_m i_{qr} - L_R v_{qs}) \tag{6.13}$$

$$\frac{di_{dr}}{dt} = K(-R_s L_m i_{ds} + \omega_r L_m L_S i_{qs} + R_r L_S i_{dr} + \omega_s L_m^2 i_{qr} - (\omega_s - \omega_r)L_S L_R i_{qr}) \tag{6.14}$$

$$\frac{di_{qr}}{dt} = K(-\omega_r L_S L_m i_{ds} - R_S L_m i_{qs} - \omega_s L_m^2 i_{dr} + (\omega_s - \omega_r)L_S L_R i_{dr} + R_r L_S i_{qr} + L_m v_{qs}) \tag{6.15}$$

$$\frac{dv_{qs}}{dt} = \frac{-i_{qs}}{C} - \frac{v_{qs}}{R_L C} \tag{6.16}$$

where K = $\frac{1}{L_m^2 - L_s L_r}$, $\omega_s$ is the stator frequency, and again, $L_S = L_s + L_m$ and $L_R = L_r + L_m$

The magnetizing inductance as a function of the magnetizing current was used in both the flux and current models. For the flux model, the zero voltage magnetizing inductance was used as an initial value and the calculated currents were used to determine the magnetizing inductance for the next step.

$$L_m = -6.7927^{-5} I_m^4 + 0.0017467 I_m^3 + -0.016119 I_m^2 + 0.049107 I_m + 0.055585 \quad (6.17)$$

where

$$i_m = \frac{\sqrt{(i_{ds} + i_{dr})^2 + (i_{qs} + i_{qr})^2}}{\sqrt{2}} \quad (6.18)$$

## 6.2 Conclusions and Recommendations for Future Work

Steady state simulations suggest that the generator output voltage can be maintained constant over the full range of load by adjusting the stator frequency. Variable reactive power can be circulated among the machine phases to maintain excitation by using a six step converter with the three switch pattern discussed in Chapter 4. Sufficient AC capacitance should be connected to the generator output to reduce the converter currents without exciting the machine, while the DC capacitor can be sized according to ripple requirements for the DC bus. Initial results from transient simulations indicate that a constant voltage output may depend on precise frequency control.

The transient models used here could be verified and extended to include the switching converter and DC capacitor.

The proposed control strategy could be experimentally verified on the low power generator. The next step is to see if a constant output voltage can be maintained for changing loads by adjusting the inverter frequency, as the theory suggests. The DC voltage could also be compared running under the two switch and three switch patterns.

Using a variable frequency source to investigate the frequency dependence of all of the machine parameters, particularly the mutual inductance, could improve the machine models as well as determine more precise operating limits of the control system.

One last missing piece of the puzzle is the torque-speed characteristic of the steam turbine used to drive the generator rotor. A detailed model for large steam turbines, as well as an understanding of reasonable variations in the turbine mechanical parameters and limits to existing speed controls, would be another important step in elaborating the existing model.

# *Appendix A*
# *Machine Testing Results*

---

The no-load test results include the approximate rotor mechanical speed in RPM, single-phase RMS stator input voltage and current, and single-phase RMS input real and reactive power.

# A.1 No Load Test Results

| No-Load Test Results | | | | |
|---|---|---|---|---|
| N (RPM) | V (V) | I (A) | P (W) | Q (VAR) |
| 1800 | 141.2 | 4.54 | 50 | 650 |
| 1800 | 135.4 | 4.12 | 50 | 560 |
| 1800 | 130.2 | 3.78 | 50 | 490 |
| 1800 | 125.2 | 3.52 | 33 | 434 |
| 1800 | 120.1 | 3.23 | 36 | 390 |
| 1800 | 114.7 | 3.07 | 29 | 351 |
| 1800 | 110.1 | 2.92 | 39 | 320 |
| 1800 | 104.8 | 2.72 | 29 | 284 |
| 1800 | 100.4 | 2.61 | 28 | 259 |
| 1800 | 94.9 | 2.39 | 23 | 224 |
| 1800 | 90.4 | 2.27 | 30 | 204 |
| 1800 | 85.0 | 2.09 | 24 | 180 |
| 1799 | 79.8 | 1.97 | 23 | 157 |
| 1798 | 75.0 | 1.84 | 27 | 138 |
| 1798 | 70.0 | 1.73 | 22 | 119 |
| 1798 | 65.2 | 1.56 | 21 | 102 |
| 1798 | 60.4 | 1.52 | 20 | 91 |
| 1797 | 55.1 | 1.35 | 18 | 74 |
| 1797 | 49.8 | 1.22 | 16 | 60 |
| 1796 | 44.9 | 1.08 | 16 | 48 |
| 1795 | 39.9 | 0.90 | 10 | 36 |
| 1793 | 34.8 | 0.84 | 9 | 29 |
| 1791 | 30.2 | 0.85 | 13 | 25 |
| 1785 | 25.1 | 0.95 | 16 | 24 |
| 1777 | 19.8 | 0.75 | 10 | 14 |
| 1744 | 14.8 | 1.16 | 12 | 16 |

The locked rotor test data include RMS stator input voltage and current as well as single-phase RMS input real and reactive power.

| Locked-Rotor Test Results | | | | |
|---|---|---|---|---|
| V (V) | I (A) | P (W) | Q (VAR) | Q/P |
| 26.3 | 8.11 | 90 | 192 | 2.13 |
| 26.3 | 8.04 | 86 | 192 | 2.23 |
| 23.7 | 7.13 | 67 | 154 | 2.30 |
| 21.7 | 6.07 | 51 | 122 | 2.39 |
| 18.5 | 5.06 | 35 | 86 | 2.46 |
| 18.5 | 5.03 | 35 | 86 | 2.46 |
| 15.8 | 4.14 | 23 | 60 | 2.61 |
| 15.8 | 3.98 | 21 | 58 | 2.76 |
| 13.3 | 3.17 | 14 | 39 | 2.79 |
| 13.3 | 3.11 | 14 | 38 | 2.71 |
| 10.0 | 2.01 | 6 | 18 | 3.00 |
| 9.8 | 2.00 | 5 | 18 | 3.60 |
| 8.4 | 1.16 | 2 | 9 | 4.50 |
| 7.0 | 0.92 | 1 | 6 | 6.00 |
| 5.6 | 0.42 | 0 | 2 | $\infty$ |

| 100 V, 60 Hz Generator Tests | | | | |
|---|---|---|---|---|
| N (RPM) | V (V) | I (A) | P (W) | Q (VAR) |
| 1810 | 99.0 | 2.62 | 100 | 240 |
| 1814 | 99.6 | 3.09 | 170 | 260 |
| 1818 | 99.6 | 3.40 | 210 | 270 |
| 1820 | 99.9 | 3.64 | 240 | 270 |
| 1825 | 100.1 | 4.29 | 310 | 300 |
| 1826 | 100.1 | 4.52 | 340 | 300 |
| 1829 | 99.9 | 4.98 | 380 | 320 |
| 1833 | 100.1 | 5.32 | 420 | 330 |
| 1834 | 100.0 | 5.58 | 450 | 340 |
| 1834 | 100.1 | 5.55 | 440 | 350 |
| 1835 | 100.1 | 5.62 | 450 | 340 |
| 1837 | 100.2 | 5.98 | 490 | 350 |
| 1839 | 100.3 | 6.10 | 500 | 360 |

| 80 $\mu$F, 52.5$\Omega$, Stand-Alone Generator Tests | | | | |
|---|---|---|---|---|
| N (RPM) | V (V) | f (Hz) | Icap (A) | Q |
| 1818 | 68.0 | 60.1 | 1.85 | 125 |
| 1818 | 68.0 | 60.2 | 2.07 | 155 |
| 1822 | 81.6 | 60.2 | 2.30 | 187 |
| 1823 | 83.4 | 60.3 | 2.30 | 190 |
| 1825 | 85.5 | 60.3 | 2.36 | 200 |
| 1827 | 89.4 | 60.4 | 2.47 | 220 |
| 1830 | 93.1 | 60.5 | 2.59 | 240 |
| 1833 | 96.4 | 60.6 | 2.68 | 257 |
| 1835 | 98.5 | 60.7 | 2.80 | 275 |
| 1842 | 105.3 | 61.0 | 2.95 | 309 |
| 1844 | 106.7 | 61.0 | 2.99 | 318 |
| 1845 | 107.9 | 61.0 | 3.09 | 330 |
| 1847 | 109.0 | 61.1 | 3.13 | 340 |
| 1850 | 111.0 | 61.2 | 3.13 | 347 |
| 1860 | 116.7 | 61.5 | 3.30 | 385 |
| 1863 | 118.4 | 61.6 | 3.36 | 397 |
| 1871 | 121.5 | 61.9 | 3.47 | 420 |
| 1878 | 124.6 | 62.1 | 3.65 | 452 |
| 1883 | 126.5 | 62.3 | 3.63 | 458 |
| 1896 | 130.4 | 62.7 | 3.78 | 490 |

*Appendix B*

# *Five Megawatt Induction Machine Design Specifications*

---

```
%Self-Excited Induction Generator Description

volt = 491;              % voltage is line-neutral, RMS
Nmech = 12016;           % stator frequency
r = 0.1605;              % rotor radius [m]
l = 0.3367;              % active length [m]
g = 0.001013;            % physical air gap length [m]
d = 0.0002194;           % rotor slot description: slice radial interval
lamr = 0.397;            % rotor slot fraction
hs = 0.0935;             % stator slot depth
lams = 0.427;            % slot fraction

nr = 24;                 % number of rotor slots = 3*nr3max
ns = 12;                 % total number of stator slots = 6*ns6max
cturn = 1;               % number of turns per coil

%Fixed Machine Parameters:

Prat = 5e6;              % machine rating  (watts)
qs = 3;                  % number of stator phases
qr = 3;                  % number of rotor phases
p = 2;                   % number of pole pairs
dw = 0.02;               % wire Diameter
ninh = 1;                % number of wires in hand
he = 0.02;               % end ring height
le = 0.01;               % end ring length
sk = 0.01;               % skew

siga = 5.88e7;           % stator conductor conductivity
sigr = 5.88e7;           % rotor material conductivity
sirb = 0;                % rotor steel conductivity, 0 if laminated
```

```
rhor = 8960;              % rotor conductor material density

db = 0.1;                 % core back iron depth
pb = 1.3;                 % core loss coefficient (Cogent N07)
omb = 100*pi;             % base frequency is 50 Hz
epps = 1.85;              % dissipation exponent (Cogent N07)
epf = 1.15;               % frequency exponent   (Cogent N07)
vaa1 = 1.58;              % core iron var base 1 (Cogent N07)
vaa2 = 0.04;              % core iron var base 2 (Cogent N07)
epa1 = 1.37;              % core iron var expon 1 (Cogent N07)
epa2 = 15.4;              % core iron var expon 2 (Cogent N07)

dtt = 10;                 % air temp rise for windage estimate
etf = 0.25;               % fan efficiency
rfan = 0.001;             % fan radius (for pressure rise)
bfend = 2;                % end winding adjustment factor
bfsurf = 0.1;             % adjustment for rotor flux variations

ds = 0;                   % depth of stator slot depression
us = 0;                   % width of stator slot depression
dr = 0;                   % depth of rotor slot depression
ur = 0;                   % width of rotor slot depression
```

# Bibliography


[1] P. L. Alger. *Induction Machines - Their Behavior and Uses.* Gordon and Breach Science Publishers, New York, NY, second edition, 1970.

[2] M.A. Al-Saffar, E. Nho, and T.A. Lipo. Controlled shunt capacitor self-excited induction generator. *The 1998 IEEE Thirty-Third Industry Applications Society Annual Meeting*, 2:1486–1490, October 1998.

[3] G. Bertotti, A. Boglietti, M. Chiampi, D. Chiarabaglio, F. Fiorillo, and M. Lazzari. An improved estimation of iron losses in rotating electrical machines. *IEEE Transactions on Magnetics*, 27(6):5007–5009, November 1991.

[4] S.N. Bhadra, K. Venkata Ratnam, and A. Manjunath. Study of voltage build up in a self-excited, variable speed induction generator / static inverter system with d.c. side capacitor. In *Proceedings of the 1996 International Conference on Power Electronics, Drives and Energy Systems for Industrial Growth*, volume 2, pages 964–970. IEEE, January 1996.

[5] M.B. Brennen and A. Abbondanti. Static exciters for induction generators. *IEEE Transactions on Industry Applications*, IA-13(5):422–428, September/October 1977.

[6] Y. Chen and P. Pillay. An improved formula for lamination and core loss calculations in machines operating with high frequency and high flux density excitation. *Conference Record of the 37th IEEE Industry Applications Society Annual Meeting*, 2:759–766, October 2002.

[7] J.B. Ekanayake and N. Jenkins. A three-level advanced static var compensator. *IEEE Transactions on Power Delivery*, 11(1):540–545, January 1996.

[8] H. Frank and B. Landstrom. Power-factor correction with thyristor-controlled capacitors. *ASEA Journal*, 44(6):180–184, 1971.

[9] L. Gyugyi. Reactive power generation and control by thyristor circuits. *IEEE Transactions on Industry Applications*, IA-15(5):521–532, September/October 1979.

[10] A.K. Al Jabri and A.I. Alolah. Capacitance requirement for the isolated self-excited induction generator. *IEE Proceedings Part B*, 137(3):154–159, May 1990.

[11] A.A. Jimoh and O. Ojo. Self-excitation in pwm inverter excited single-phase induction generator. *1999 IEEE AFRICON*, 2:871–876, September/October 1999.

[12] J.L. Kirtley. Induction generator design.

[13] S.C. Kuo and L. Wang. Analysis of voltage control for a self-excited induction generator using a current-controlled voltage source inverter (cc-vsi). *IEE Proceedings- Generation, Transmission and Distribution*, 148(5):431–438, September 2001.

[14] T.L. Maguire and A.M. Gole. Apparatus for supplying an isolated dc load from a variable-speed self-excited induction generator. *IEEE Transactions on Energy Conversion*, 8(3):468–475, September 1993.

[15] N. Mithulananthan, C.A. Canizares, J. Reeve, and G.J. Rogers. Comparison of pss, svc, and statcom controllers for damping power system oscillations. *IEEE Transactions on Power Systems*, 18(2):786–792, May 2003.

[16] E. Muljadi, J Sallan, M. Sanz, and C.P. Butterfield. Investigation of self-excited induction generators for wind turbine applications. *Conference Record of the 37th IEEE Industry Applications Society Annual Meeting*, 1(509-515), October 1999.

[17] D.W. Novotny, D.J. Gritter, and G.H. Studtmann. Self-excitation in inverter driven induction machines. *IEEE Transactions on Power Apparatus and Systems*, PAS-96(4):1117–1125, July/August 1977.

[18] D. Seyoum, C. Grantham, and M.F. Rahman. The dynamic characteristics of an isolated self-excited induction generator driven by a wind turbine. *IEEE Transactions on Industry Applications*, 39(4):936–944, July/August 2003.

[19] L. Shridhar, B. Singh, and C.S. Jha. A step towards improvements in the charachteristics of self excited induction generator. *IEEE Transactions on Energy Conversion*, 8(1):40–46, March 1993.

[20] M.G. Simoes and F.A. Farret. *Renewable Energy Systems - Design and Analysis with Induction Generators.* Power Electronics and Applications Series. CRC Press, Boca Raton, Florida, 2004.

[21] B. Singh and L.B. Shilpakar. Analysis of a novel solid state voltage regulator for a self-excited induction generator. *IEE Proceedings- Generation, Transmission and Distribution*, 145(6):647–655, November 1998.

[22] S.P. Singh, B. Singh, and M.P. Jain. Performance characteristics and optimum utilization of a cage machine as capacitance excited induction generator. *IEEE Transactions on Energy Conversion*, 5(4):679–685, December 1990.

[23] J.R. Smith. *Response Analysis of A.C. Electrical Machines - computer models and simulation.* Research Studies Press LTD., Taunton, Somerset, England, 1990.

[24] D. Sutanto, C. Grantham, and F. Rahman. A regulated self-excited induction generator for use in a remote area power supply. *Sixth International Conference on Electrical Machines and Drives*, (IEEE Conf. Publ. No. 376):234–239, September 1993.

[25] A. M. Trzynadlowski. *Control of Induction Motors.* Academic Press, San Diego, CA, 2001.

[26] L. Wang and J. Su. Dynamic performance of an isolated self-excited induction generator under various loading conditions. *IEEE Transactions on Energy Conversion*, 14(1):93–100, 1999.

[27] C.H. Watanabe and A.N. Barreto. Self-excited induction generator/force-commutated rectifier system operating as a dc power supply. *IEE Proceedings Part B*, 134(5):255–260, September 1987.

[28] S. Wekhande and V. Agarwal. Wind driven self-excited induction generator with simple de-coupled excitation control. *Conference Record of the 1999 IEEE Thirty-Fourth Industry Applications Society Annual Meeting*, 3:2077–2083, October 1999.

[29] W. Wolfe, W.G. Hurley, and S. Arnold. Power factor correction for ac-dc converters with cost effective inductive filtering. *2000 IEEE 31st Annual Power Electronics Specialists Conference*, 1:332–337, June 2000.

[30] J.G. Zhu and V.S. Ramsden. Improved formulations for rotational core losses in rotating electrical machines. *IEEE Transactions on Magnetics*, 34(4):2234–2242, July 1998.

[31] IEEE Std 112-1996 Standard Test Procedure for Polyphase Induction Motors and Generators. Technical report, Institute of Electrical and Electronics Engineering, New York, NY, 1997.